

---

# Cladding Swelling and Rupture Models for LOCA Analysis

---

D. A. Powers, R. O. Meyer

Office of Nuclear Reactor Regulation

U.S. Nuclear Regulatory  
Commission



Available from

GPO Sales Program  
Division of Technical Information and Document Control  
U.S. Nuclear Regulatory Commission  
Washington, D.C. 20555

and

National Technical Information Service  
Springfield, Virginia 22161

---

---

# Cladding Swelling and Rupture Models for LOCA Analysis

---

---

Manuscript Completed: March 1980  
Date Published: April 1980

D. A. Powers, R. O. Meyer

**Division of Systems Safety  
Office of Nuclear Reactor Regulation  
U.S. Nuclear Regulatory Commission  
Washington, D.C. 20555**



## ABSTRACT

A description is given of fuel cladding behavior as it is modeled for emergency-core-cooling-system (ECCS) evaluations in the safety analysis of loss-of-coolant accidents (LOCAs). Data are tabulated from experiments that employed internally heated Zircaloy cladding that was ruptured in aqueous atmospheres, and new correlations based on these data are given for cladding rupture temperature, cladding burst strain, and fuel assembly flow blockage. Comparisons of these correlations with industry models that are used in current licensing analyses for commercial nuclear power plants reveal substantial differences. The correlations in this report are intended to be used as licensing standards for future LOCA analyses until such time that the continuing research programs would demonstrate a need for further revisions.

## CONTENTS

ABSTRACT . . . . .	iii
LIST OF FIGURES. . . . .	vii
PREFACE . . . . .	xiii
ACKNOWLEDGMENTS. . . . .	xv
NOMENCLATURE . . . . .	xvii
1. INTRODUCTION. . . . .	1
2. DATA BASE . . . . .	4
3. NEW CORRELATIONS. . . . .	6
3.1 Rupture Temperature . . . . .	6
3.2 Burst Strain. . . . .	12
3.3 Assembly Flow Blockage. . . . .	24
4. COMPARISON WITH PREVIOUS MODELS . . . . .	38
4.1 Early AEC Model . . . . .	38
4.2 Babcock & Wilcox. . . . .	38
4.3 Combustion Engineering. . . . .	51
4.4 Westinghouse. . . . .	61
4.5 General Electric. . . . .	61
4.6 Exxon . . . . .	71
4.7 Yankee Atomic Electric. . . . .	71
5. CONCLUSIONS . . . . .	86
6. REFERENCES. . . . .	89
APPENDIX A -- FUEL CLADDING BURST DATA . . . . .	93
APPENDIX B -- TABULATION OF CLADDING CORRELATIONS. . . . .	111
APPENDIX C -- FORMAL COMMENTS ON DRAFT NUREG-0630 . . . . .	113

## LIST OF FIGURES

<u>Figure</u>		<u>Page</u>
1	Rupture temperature as a function of engineering hoop stress for internally heated Zircaloy cladding in aqueous atmospheres . . . . .	8
2	Rupture temperature as a function of engineering hoop stress for ORNL internally heated, single rods tested in aqueous atmospheres at a heating rate of 28°C/s . . . . .	11
3	ORNL correlation of rupture temperature as a function of engineering hoop stress and temperature-ramp rate with data from internally heated Zircaloy cladding in aqueous atmospheres. . . . .	13
4	Maximum circumferential strain as a function of rupture temperature for internally heated Zircaloy cladding in aqueous atmospheres . . . . .	14
5	Maximum circumferential strain as a function of rupture temperature for ANL directly heated, single rods tested in aqueous atmospheres . . . . .	16
6	Maximum circumferential strain as a function of rupture temperature for internally heated Zircaloy cladding in aqueous atmospheres at heating rates less than or equal to 10°C/s . . . . .	18
7	Maximum circumferential strain as a function of rupture temperature for internally heated Zircaloy cladding in aqueous atmospheres at heating rates greater than or equal to 25°C/s. . . . .	20
8	Maximum circumferential strain as a function of rupture temperature for internally heated Zircaloy cladding in aqueous atmospheres for all heating rates. . . . .	23
9	Reduction in local flow area as a function of rupture temperature for internally heated Zircaloy clad bundles in aqueous atmospheres. . . . .	25
10	Outline of flow blockage model . . . . .	26
11	Computer drawn profile from digitized data of ORNL bundle B-1 section at 76.5-cm elevation . . . . .	27

<u>Figure</u>		<u>Page</u>
12	Coolant channel flow area restriction as a function of elevation in ORNL bundle B-1 . . . . .	30
13	Reduction in local flow area as a function of average coplanar rod strain . . . . .	31
14	Reduction in local flow area as a function of rupture temperature for internally heated Zircaloy clad bundles in aqueous atmospheres at heating rates less than or equal to 10°C/s . . . . .	33
15	Reduction in local flow area as a function of rupture temperature for internally heated Zircaloy clad bundles in aqueous atmospheres at heating rates greater than or equal to 25°C/s. . . . .	34
16	Reduction in PWR assembly flow area as a function of rupture temperature and ramp rate. . . . .	37
17	WREM model and ORNL correlation of rupture temperature as a function of engineering hoop stress and ramp rate . .	39
18	WREM model and slow-ramp correlation of circumferential burst strain as a function of rupture temperature. . . . .	40
19	WREM model and fast-ramp correlation of circumferential burst strain as a function of rupture temperature. . . . .	41
20	WREM model and slow-ramp correlation of reduction in assembly flow area as a function of rupture temperature. .	42
21	WREM model and fast-ramp correlation of reduction in assembly flow area as a function of rupture temperature. .	43
22	B&W model and ORNL correlation of rupture temperature as a function of engineering hoop stress and ramp rate . .	44
23	B&W THETA model and slow-ramp correlation of circumferential burst strain as a function of rupture temperature . . . . .	45
24	B&W THETA model and fast-ramp correlation of circumferential burst strain as a function of rupture temperature . . . . .	46
25	B&W CRAFT model and slow-ramp correlation of circumferential burst strain as a function of rupture temperature . . . . .	47

<u>Figure</u>		<u>Page</u>
26	B&W CRAFT model and fast-ramp correlation of circumferential burst strain as a function of rupture temperature . . . . .	48
27	B&W model and slow-ramp correlation of reduction in assembly flow area as a function of rupture temperature .	49
28	B&W model and fast-ramp correlation of reduction in assembly flow area as a function of rupture temperature .	50
29	C-E model and ORNL correlation of rupture temperature as a function of engineering hoop stress and ramp rate. .	52
30	C-E model and slow-ramp correlation of circumferential burst strain as a function of rupture temperature . . . .	53
31	C-E model and fast-ramp correlation of circumferential burst strain as a function of rupture temperature . . . .	54
32	C-E model and slow-ramp correlation of reduction in assembly flow area as a function of rupture temperature .	55
33	C-E model and fast-ramp correlation of reduction in assembly flow area as a function of rupture temperature .	56
34	C-E proposed model and slow-ramp correlation of circumferential burst strain as a function of rupture temperature . . . . .	57
35	C-E proposed model and fast-ramp correlation of circumferential burst strain as a function of rupture temperature . . . . .	58
36	C-E proposed model and slow-ramp correlation of reduction in assembly flow area as a function of rupture temperature . . . . .	59
37	C-E proposed model and fast-ramp correlation of reduction in assembly flow area as a function of rupture temperature . . . . .	60
38	W small-break model and ORNL correlation of rupture temperature as a function of engineering hoop stress and ramp rate . . . . .	62
39	W large-break model and ORNL correlation of rupture temperature as a function of engineering hoop stress and ramp rate . . . . .	63



<u>Figure</u>		<u>Page</u>
40	W model and slow-ramp correlation of circumferential burst strain as a function of rupture temperature . . . . .	64
41	W model and fast-ramp correlation of circumferential burst strain as a function of rupture temperature . . . . .	65
42	W model and slow-ramp correlation of reduction in assembly flow area as a function of rupture temperature . . . . .	66
43	W model and fast-ramp correlation of reduction in assembly flow area as a function of rupture temperature . . . . .	67
44	GE model and ORNL correlation of rupture temperature as a function of engineering hoop stress and ramp rate . . . . .	68
45	GE model and slow-ramp correlation of circumferential burst strain as a function of rupture temperature . . . . .	69
46	GE model and fast-ramp correlation of circumferential burst strain as a function of rupture temperature . . . . .	70
47	ENC PWR model and ORNL correlation of rupture temperature as a function of engineering hoop stress and ramp rate. . . . .	72
48	ENC PWR model and slow-ramp correlation of circumferential burst strain as a function of rupture temperature . . . . .	73
49	ENC PWR model and fast-ramp correlation of circumferential burst strain as a function of rupture temperature . . . . .	74
50	ENC model and slow-ramp correlation of reduction in assembly flow area as a function of rupture temperature . . . . .	75
51	ENC model and fast-ramp correlation of reduction in assembly flow area as a function of rupture temperature . . . . .	76

<u>Figure</u>		<u>Page</u>
52	ENC BWR model and ORNL correlation of rupture temperature as a function of engineering hoop stress and ramp rate . . . . .	77
53	ENC BWR model and slow-ramp correlation of circumferential burst strain as a function of rupture temperature . . . . .	78
54	ENC BWR model and fast-ramp correlation of circumferential burst strain as a function of rupture temperature . . . . .	79
55	YR model and ORNL correlation of rupture temperature as a function of engineering hoop stress and ramp rate . . . . .	81
56	YR model and slow-ramp correlation of circumferential burst strain as a function of rupture temperature. . . . .	82
57	YR model and fast-ramp correlation of circumferential burst strain as a function of rupture temperature. . . . .	83
58	YR model and slow-ramp correlation of reduction in assembly flow area as a function of rupture temperature. . . . .	84
59	YR model and fast-ramp correlation of reduction in assembly flow area as a function of rupture temperature. . . . .	85

## PREFACE

This report was first issued as a draft in November 1979 and was circulated for review by the technical community for the purpose of obtaining a technical critique. In addition to several informal comments, formal comments were received, and those comments are listed in Appendix C and have been placed in the NRC Public Document Room.

Based on the comments and some new data, which were also received during the comment period, some of the cladding correlations have been revised. In general, the burst strain correlation exhibits slightly larger strains, the assembly flow blockage correlation exhibits slightly smaller blockages, and most of the strain and blockage peaks are shifted toward higher temperatures by about 25°C compared with the correlations presented in the draft report. The rupture temperature correlation is unchanged.

## ACKNOWLEDGMENTS

The authors would like to express their appreciation for technical contributions that were made by members of the NRC Fuel Behavior Research Branch and by NRC contractors, R. H. Chapman (ORNL), H. M. Chung (ANL), and T. F. Kassner (ANL). We are also grateful to F. J. Erbacher (KfK, Germany), S. Kawasaki (JAERI, Japan), and many others for their comments on the draft manuscript and contributions to the final report.

## NOMENCLATURE

AEC	Atomic Energy Commission
ANL	Argonne National Laboratory
ASTM	American Society for Testing and Materials
BCL	Battelle Columbus Laboratories
BWR	boiling water reactor
B&W	Babcock and Wilcox Company
CRNL	Chalk River National Laboratory
CSNI	Committee on the Safety of Nuclear Installations
C-E	Combustion Engineering Company
ECCS	emergency core cooling system
ENC	Exxon Nuclear Company
FABIOLA	Facility for Burst Testing of Zircaloy-4 Cladding Tubes Under Fuel Interaction, Steam Oxidation, and LOCA Conditions.
FRF	Fuel Rod Failure experiment
FRG	Federal Republic of Germany
FR-2	Forschungszentrum Reaktor-2
GE	General Electric Company
KfK	Kernforschungszentrum Karlsruhe
JAERI	Japan Atomic Energy Research Institute
LOCA	loss-of-coolant accident
MRBT	Multirod Burst Test Program
NRC	Nuclear Regulatory Commission
ORNL	Oak Ridge National Laboratory
PWR	pressurized water reactor

REBEKA	Reflood Blockage Experiments
TREAT	Transient Reactor Test
W	Westinghouse Electric Company
WREM	Water Reactor Evaluation Model
YAEC	Yankee Atomic Electric Company
YR	Yankee Rowe

## 1. INTRODUCTION

During a postulated loss-of-coolant accident (LOCA), the reactor coolant pressure may drop below the internal fuel rod gas pressure causing the fuel cladding to swell (balloon) and, under some conditions, rupture. Core behavior during a LOCA would depend on the type of accident, the time at which swelling and rupture occurred, the magnitude of swelling, and the resulting coolant flow blockage (i.e., reduction in flow area).

Such phenomena were among the many reactor safety issues discussed during the 1972-1973 rule-making hearing on Acceptance Criteria for Emergency Core Cooling Systems (ECCS). The adopted acceptance criteria (Ref. 1) limited predicted (calculated) reactor performance such that if certain oxidation and temperature limits were not exceeded, then core cooling would be assured. It was required that each licensee use a safety evaluation model to analytically demonstrate compliance with the acceptance criteria.

Appendix K (Ref. 2) gives requirements for some features of evaluation models, and, in particular, states that to be acceptable the swelling and rupture calculations shall be based on applicable data in such a way that the degree of swelling and incidence of rupture are not underestimated. The degree of swelling and incidence of rupture are then used to calculate other core variables including gap conductance, cladding temperature, oxidation, embrittlement, and hydrogen generation. After the conclusion of the ECCS hearing, the NRC reviewed and approved

cladding behavior models (Refs. 3-18) for each U.S. fuel manufacturer (and for Yankee Atomic Electric Company) for their use in ECCS analyses.

During the ECCS hearing, uncertainties were apparent in the prediction of fuel behavior during a LOCA. Therefore, in the Commission's concluding opinion (Ref. 19), the Commission directed the AEC's research office (now the NRC Office of Nuclear Regulatory Research) to undertake a major confirmatory research program on cladding behavior under LOCA conditions. The resulting multi-million dollar program includes simple bench-type Zircaloy tests, single- and multi-rod burst tests that simulate some in-reactor conditions, and actual in-reactor tests ranging in size up to small-bundle tests.

The research programs are not all finished, but with the completion of many out-of-reactor and a few in-reactor tests, we are at a plateau of understanding that exceeds our understanding in 1974 and suggests that improvements should be made in the licensing models. The trend of these recent data shows the likelihood of more ruptures, larger burst strains, and greater flow blockages than predicted by some of the licensing models. Consequently, we see the need to reevaluate all cladding models used for LOCA analyses to assure that licensing analyses are performed in accordance with Appendix K.

In the following sections we will display the relevant body of data, describe our evaluation of these data to arrive at useable correlations (curves), and compare these correlations with those currently used in



licensing analyses. Since the data show strong heating-rate effects,\* we have derived different correlations for different ramp rates. The rupture temperature correlation explicitly accounts for ramp rate; the rates for which the slow-ramp and fast-ramp strain and flow blockage correlations apply will be defined, and correlations for intermediate rates can be obtained by linear interpolation.

---

\* Both heating rate and strain rate are important factors in determining cladding burst pressure and strain. However, most burst experiments are not designed to distinguish between heating-rate effects and strain-rate effects. For the purposes of this report, the actual differences are probably unimportant. Therefore to avoid confusion, in the remainder of this report we will refer to both effects simply as heating-rate effects.

## 2. DATA BASE

The ballooning and rupture behavior of Zircaloy are fairly complex phenomena in part because (a) the stresses are biaxial and the material is anisotropic in the temperature range of most interest, (b) the crystal structure changes in the temperature range of interest, (c) the properties of zirconium-base alloys are susceptible to strain-rate effects, (d) axial and circumferential temperature variations in the cladding strongly influence strain localization, (e) oxygen embrittlement increases yield and failure strengths, (f) the cracking of oxide coatings results in failure sites that can localize stresses, and (g) aggressive fission products can reduce the threshold stress at which crack propagation will proceed. Consequently the behavior of Zircaloy cladding depends strongly on environment and hence on test conditions (Refs. 20-21).

In-reactor tests are difficult to interpret and are too expensive to be used for investigating all of these variables, while some out-of-reactor tests lack sufficient realism. Therefore, for final calibration of the data correlations, we have selected only those data from experiments employing pressurized rods in aqueous atmospheres and either internal fuel-pellet simulators (i.e., indirect cladding heaters) or actual fuel pellets (in-reactor). This selection emphasizes the more recent prototypical test data and deemphasizes much of the earlier data. The data we have selected come from independent programs at four major laboratories: (1) Oak Ridge National Laboratory, (2) Battelle Columbus Laboratories, (3) Kernforschungszentrum Karlsruhe (Germany), and (4) Japan Atomic Energy

Research Institute. Appendix A provides a tabulation of all of the data we have used, their references, and a legend of symbols that are used in the later figures.

There are gaps in this data base, however, particularly with regard to the absence of large bundle tests, and we have utilized the results from simpler less typical tests to bridge the gaps. While these more pristine tests are atypical in a sense, they do reveal fundamental features of Zircaloy behavior, they are valid for determining relative effects, and they allow one to interpret the sparser prototypical data more accurately.

### 3. NEW CORRELATIONS

#### 3.1 Rupture Temperature

The incidence of rupture depends on the differential pressure across the cladding wall, the cladding temperature, and on the length of time those conditions are maintained. Time duration under conditions of plastic deformation manifests itself as a heating-ramp-rate effect, and this effect will be treated explicitly. Truly isothermal conditions will not be treated exactly, but will be treated the same as very slow ramps. To eliminate design-specific dimensional effects, we have converted differential pressures to hoop stresses. The conversion was made using a thin-shell formula,

$$\sigma = (d/2t)\Delta P, \quad (3-1)$$

where  $\sigma$  is engineering hoop stress,  $d$  is the undeformed cladding mid-wall diameter,  $t$  is the undeformed cladding thickness, and  $\Delta P$  is differential pressure across the cladding wall at the time of rupture. Table 1 shows some computed values of hoop stress in terms of differential pressure for some common commercial fuel designs.

Figure 1 shows rupture temperature data as a function of hoop stress for a wide range of test conditions. While this figure shows the general trend -- rupture temperature decreases with increasing wall stress -- the data are scattered primarily because

TABLE 1

Engineering Hoop Stress as a Function of Internal Fuel Rod  
Gas Pressure and Fuel Vendor Design

---

Design	Hoop Stress (psi) for a 600 psi Differential Across the Cladding Wall
B&W 15x15	4570
B&W 17x17	4540
C-E 16x16	4280
W 15x15	4910
W 17x17	4690
GE 8x8	4050
ENC 15x15*	3940
ENC 8x8**	3880

---

\* D. C. Cook, Unit 1

\*\* Oyster Creek

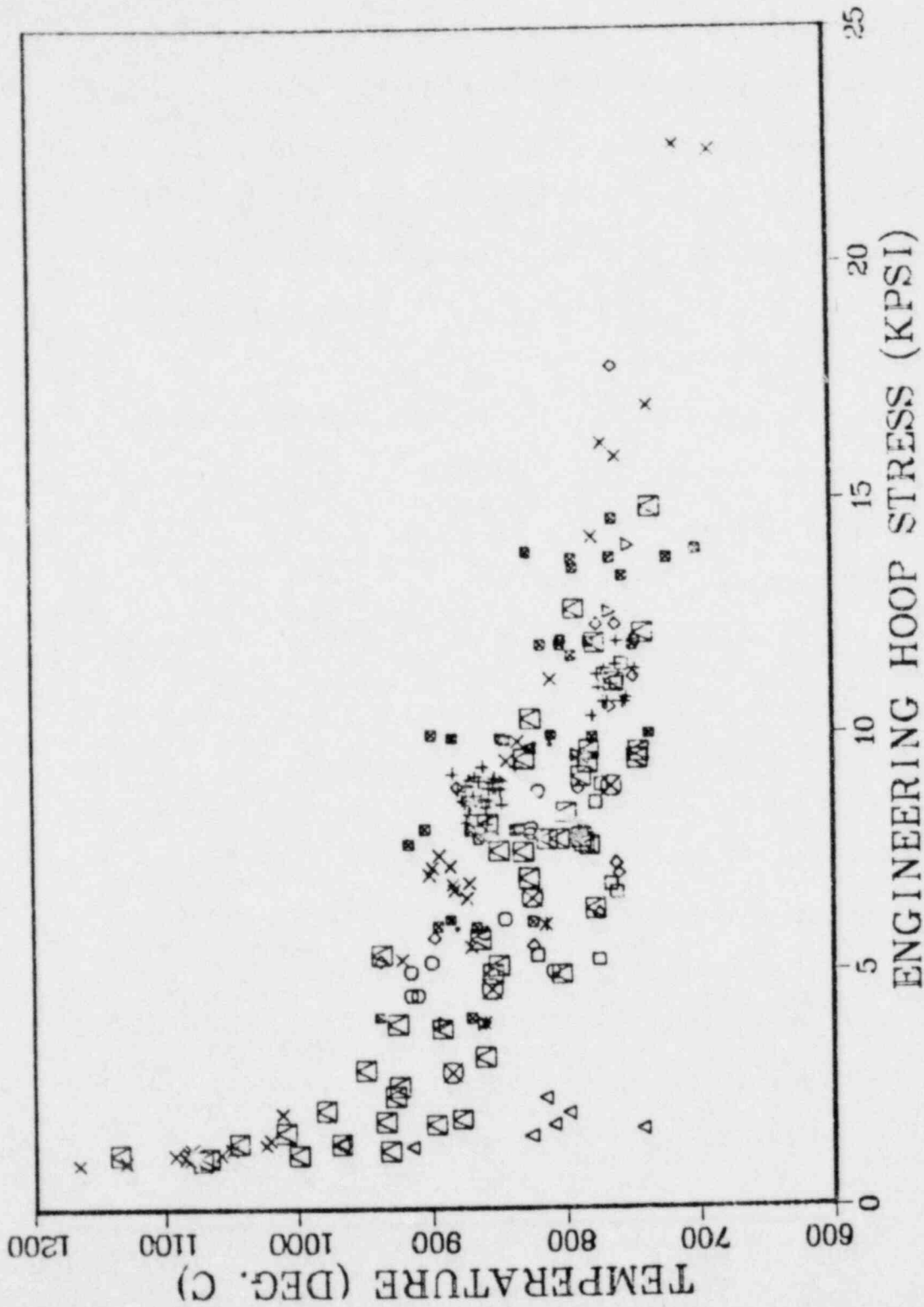


Fig. 1 Rupture temperature as a function of engineering hoop stress for internally heated Zircaloy cladding in aqueous atmospheres.

of ramp-rate effects and experimental uncertainties in determining rupture temperatures and effective ramp rates.

The uncertainty in determining the true rupture temperature arises mainly for two reasons. First, temperature measurements with thermocouples may result in a local perturbation of the true material temperature, and second, thermocouples are usually not located at the exact rupture locations. Therefore true rupture temperatures are likely to be higher than those experimentally measured.

These effects are minimized in the ORNL experiments because, first, the temperature profiles of the ORNL internal heaters are well known allowing placement of thermocouples very near to rupture sites (hot spots), and second, the combination of thin-external thermocouple wires with low steam flow rates results in small temperature perturbations (Ref. 22).

The uncertainty in determining the effective ramp rate arises from imprecision in the definition of ramp rate. For example, experimentalists most frequently report ramp rate as the increment in cladding temperature divided by the time duration where these values are taken from the start of the transient to the occurrence of rupture. However, the effective ramp rate may be limited only to the time interval over which plastic deformation occurs.

Unfortunately, the measurement of an effective ramp rate during this time of swelling is very difficult and has not been rigorously

assessed for the data compiled in Appendix A. Nevertheless, for those experiments conducted with a constant temperature-ramp rate, such as some of the ORNL experiments, the uncertainty in determining the effective ramp rate should be smaller than for experiments conducted with a constant power-ramp rate.

We have thus chosen a set of ORNL data that were all taken under similar conditions and were all determined with thermocouples attached to the external cladding surfaces. Figure 2 shows these ORNL single rod test data at 28°C/s (a common ramp rate used in the ORNL experiments) and the basic correlation we will adopt as developed by Chapman (Ref. 23) using numerical regression techniques. It is clear that most of the apparent data scatter has been eliminated by restricting the data to a single ramp rate.

Using rupture data taken with slower ramp rates (i.e., rates down to creep rupture conditions with up to a maximum 100-s hold time), Chapman has developed a ramp-rate correlation (Ref. 24),

$$T_R = 3960 - \frac{20.4\sigma}{1 + H} - \frac{8,510,000\sigma}{100(1+H) + 2790\sigma}, \quad (3-2)$$

where  $T_R$  is the rupture temperature in °C,  $\sigma$  is the engineering hoop stress in kpsi, and  $H$  is the ratio of the heating rate in °C/s to 28°C/s ( $H$  varies from 0 to 1). This correlation can be used to produce a family of rupture-temperature curves. The correlation assumes that ramp-rate effects on the rupture temperature saturate at 28°C/s.



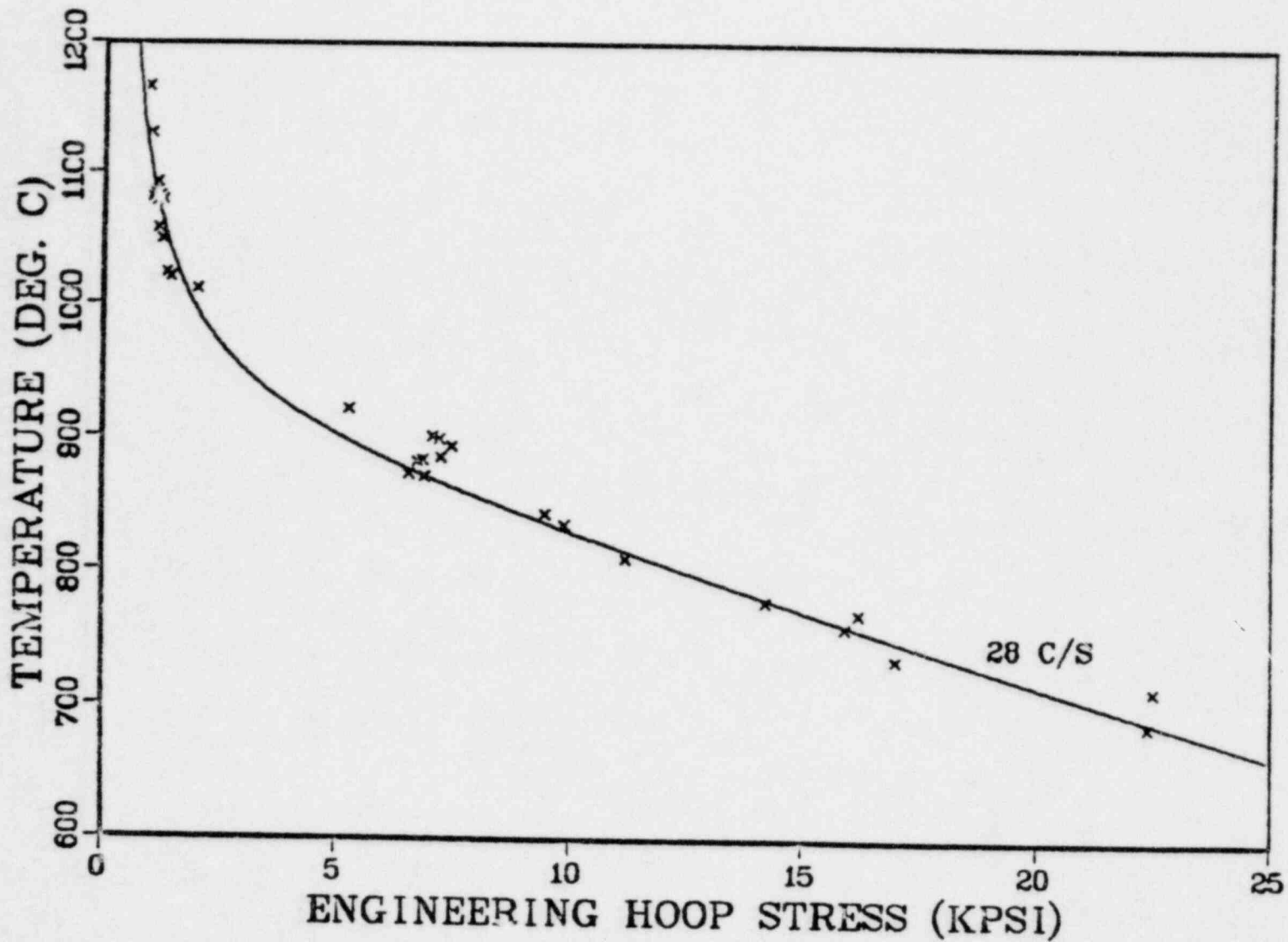


Fig. 2 Rupture temperature as a function of engineering hoop stress for ORNL internally heated, single rods tested in aqueous atmospheres at a heating rate of 28°C/s.

The curves that span the more frequently calculated ramp rates are shown in Fig. 3 along with the data of Fig. 1. Chapman has shown that most of the original scatter is attributable to ramp-rate effects, and the curves in Fig. 3 are seen to span most of the data. The up-right triangles still deviate from the correlations and the major body of data. Difficulties in temperature measurement for these TREAT in-reactor data (Refs. 25-26) are believed to be responsible for this deviation, and such discrepancies will be seen in later displays as well.

The closed squares are recent data from KfK by Erbacher and, in general, are seen to lie above the correlation. These differences probably result from the use of isobaric testing conditions rather than the more realistic constant-gas-inventory testing conditions, which were used at ORNL.

### 3.2 Burst Strain

Deformation (burst strain) at the location of a rupture depends on temperature, differential pressure (which is related to temperature by the correlation in Eq. 3-2), ramp rate, and several other variables such as local temperature variations and metallurgical conditions. These effects have been discussed previously (Refs. 20-21,27). Figure 4 shows burst strain\* as a function of one of these variables,

---

\*Occasionally it has been observed that the maximum measured circumferential strain on a test rod will not coincide with the burst location. For infrequent instances such as these, we have used (and tabulated in Appendix A) the maximum circumferential strain as the burst strain, provided that this information was published by the originating authors.

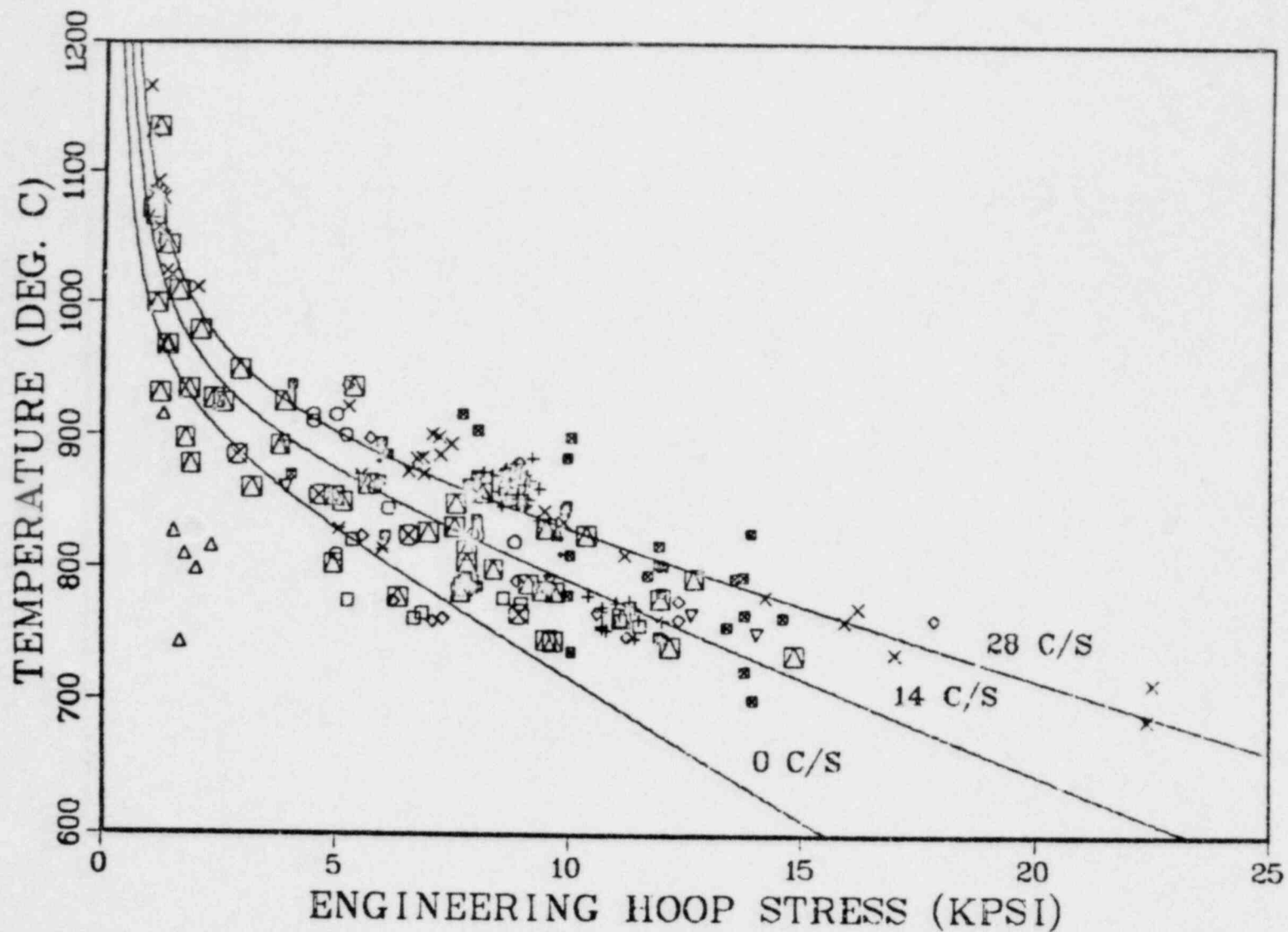


Fig. 3 ORNL correlation of rupture temperature as a function of engineering hoop stress and temperature-ramp rate with data from internally heated Zircaloy cladding in aqueous atmospheres.

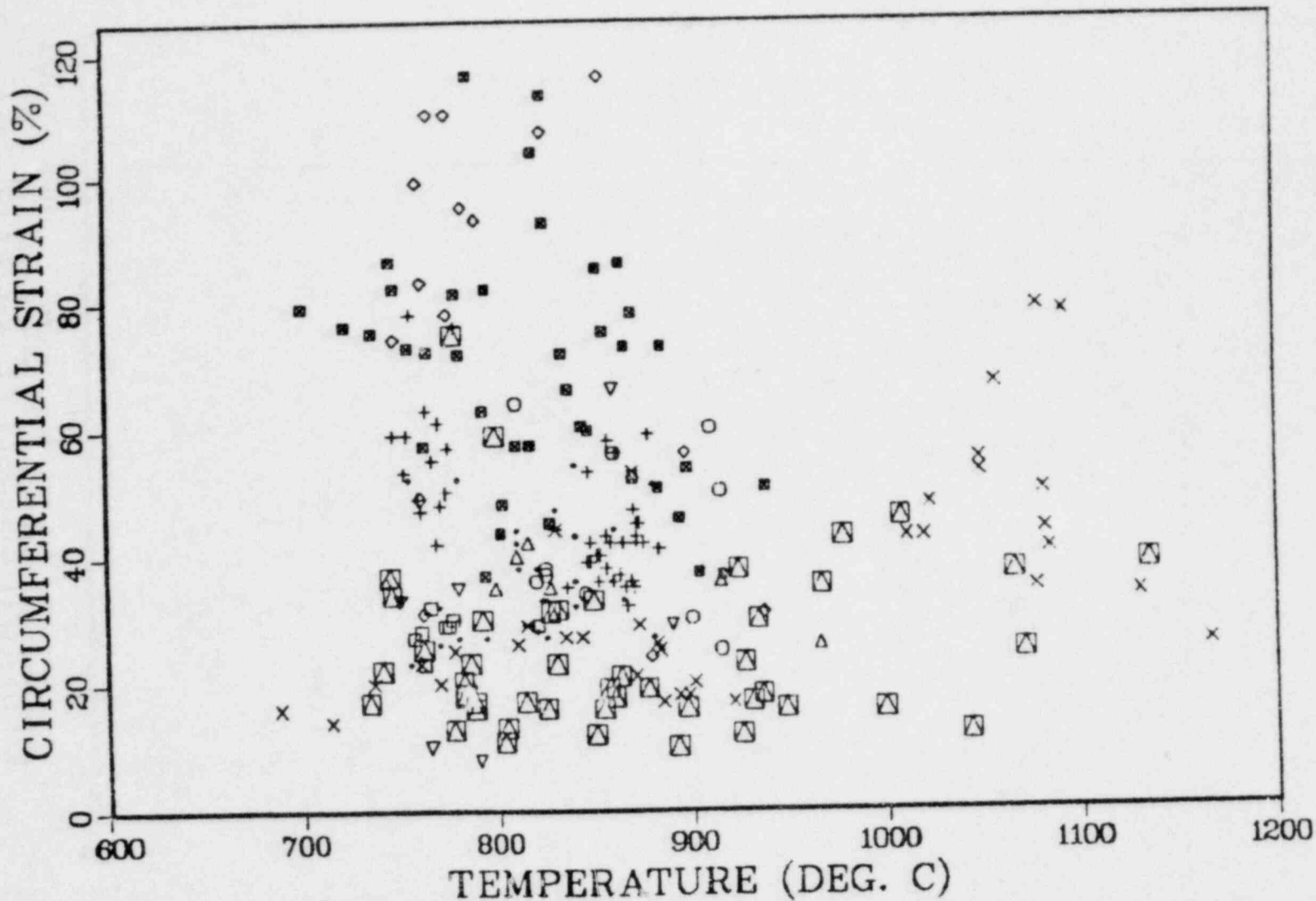


Fig. 4 Maximum circumferential strain as a function of rupture temperature for internally heated Zircaloy cladding in aqueous atmospheres.

rupture temperature, and the data scatter is therefore due to temperature measurement difficulties and the other variables mentioned above.

The scatter in Fig. 4 is bewildering, so we have used results from less prototypical (but more controlled) tests to help resolve basic characteristics of Zircaloy and isolate the effects of certain variables. Figure 5 shows burst strain versus rupture temperature from Chung and Kassner's work (Ref. 21) with short Zircaloy tubes heated by passing an electrical current directly through the Zircaloy. This figure is one of many similar figures in Reference 21 and was chosen because it illustrates several fundamental features. There are three superplastic peaks\* -- one in the low-temperature alpha phase around 800°C and two in the high-temperature beta phase around 1050°C and 1250°C. The very important valley at about 925°C is a consequence of mixed alpha-plus-beta-phase material, which exhibits low ductility. Heating-rate effects are also visible. Slow-ramp rates produce large strains in the temperature regime below about 950°C, but slow-ramp rates produce very small strains at temperatures greater than about 950°C because the Zircaloy has time to oxidize and

---

\*Superplasticity has been observed in zirconium alloys (Refs. 21,28-29). There is general agreement that the superplastic effect results in unusually large tensile extensibility that can occur in alloys of small grain size when strained at temperatures above approximately 40% of the absolute melting point at strain rates where the flow stress is highly strain-rate sensitive. Though there is not universal agreement that the superplastic deformation mechanism is responsible for generating all three of the peaks in Figure 5, it is sufficient for our purposes to state that the material appears to behave superplastically inasmuch as it resists necking and large strains can occur.

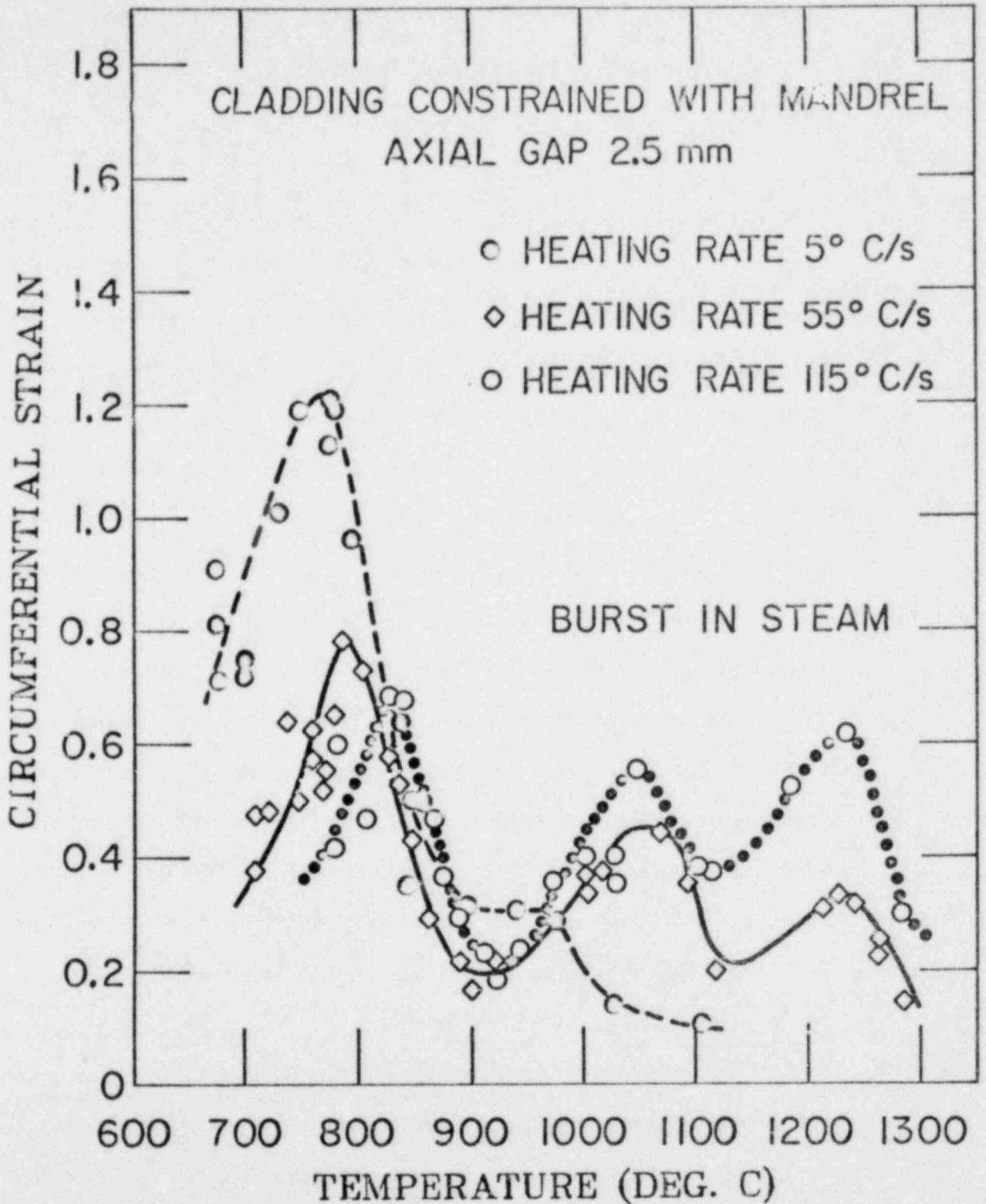


Fig. 5 Maximum circumferential strain as a function of rupture temperature for ANL directly heated, single rods tested in aqueous atmospheres.

embrittle before significant ballooning can occur. Fast-ramp rates produce the opposite effects in both temperature regimes by allowing local temperature gradients and precluding significant oxidation prior to rupture. In the region of phase transition, the burst strain appears to be relatively insensitive to ramp rate.

To derive the slow-ramp correlation (applicable to ramp rates  $\leq 10^\circ\text{C/s}$ ), which is shown in Fig. 6, we have retained the shape of Chung and Kassner's curves and positioned the peaks and valleys according to the 0-10°C/s data in our prototypical data base.

The alpha-phase peak was located at 800°C and assigned the value of 90% based on the data in Figure 6. Selection of 90% strain for this alpha-phase peak height was influenced by several factors. First, most of the data below the curve were discounted because they are from tests with features that are known to reduce strain (e.g., non-uniform heaters, corrosion fission products, cold shrouds) but might not be present in a real LOCA. Second, Chapman (Ref. 30) recommends 100% for this peak, but bases that recommendation in part on Chung and Kassner's data, which come from directly heated cladding specimens; direct or external heating methods are capable of exaggerating burst strains by maintaining artificially small local temperature variations (see Ref. 20), and such experiments were excluded from our data base. Third, Erbacher's recent data (Ref. 31) in the vicinity of 800°C have a mean value of about 90% (90.5% within 25°C of the peak).

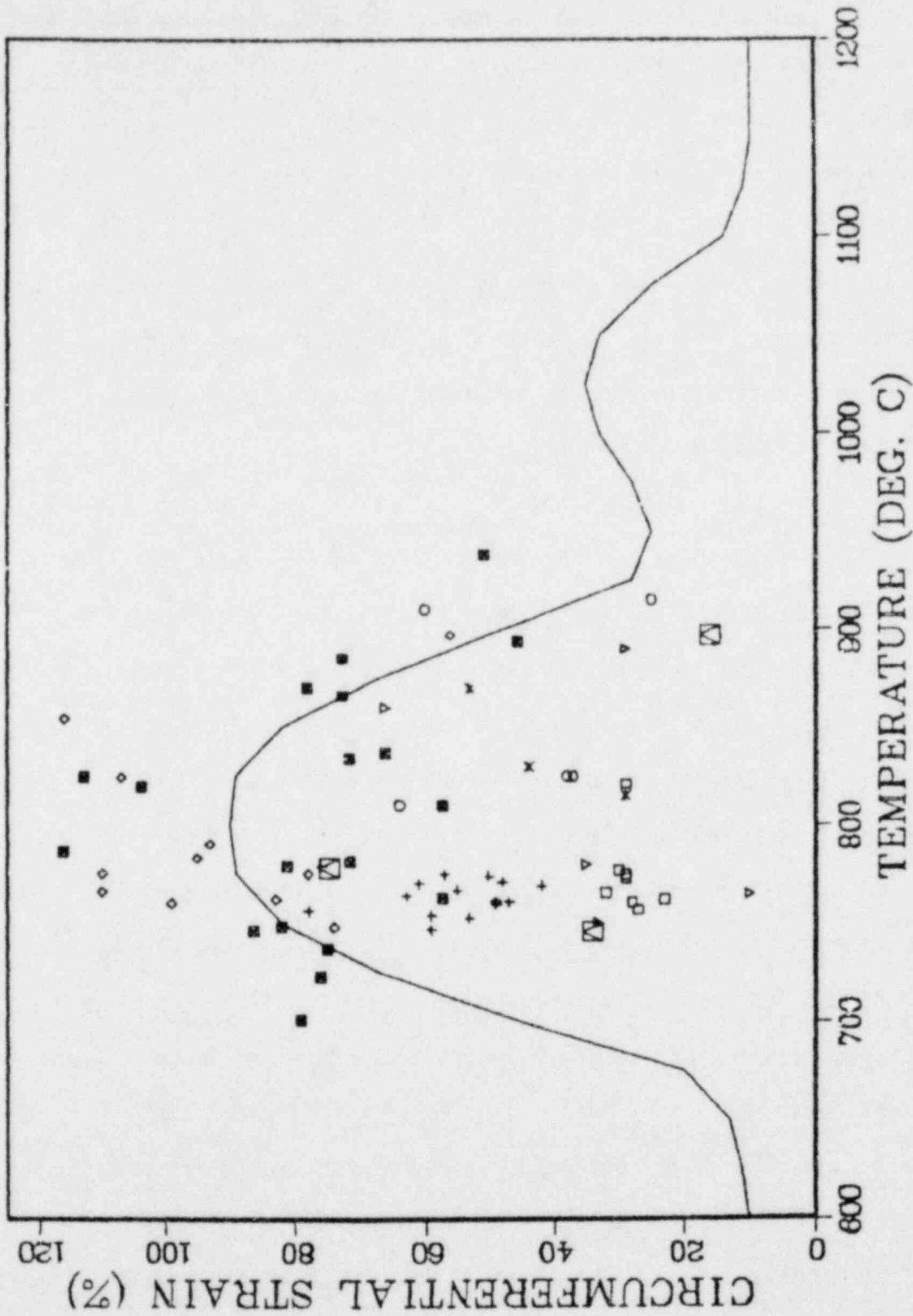


Fig. 6 Maximum circumferential strain as a function of rupture temperature for internally heated Zircaloy cladding in aqueous atmospheres at heating rates less than or equal to 10°C/s.



Erbacher speculates (Ref. 32) that the temperatures might be more uniform than would occur under reactor accident conditions (azimuthal temperature variations in these tests were measured to be up to 70°C in magnitude at the time of rupture). We believe that prototypical testing is currently the best way of estimating temperature uniformity and we find no reason to discount Erbacher's results. Finally, Chapman's single-rod heated-shroud data in the vicinity of 800°C had a mean value of about 90% (93.3% within 25°C of the peak). Two of Chapman's 0°C/s test results were eliminated from this averaging because the heater power was so low (about 3W) that these tubes may have ruptured as if they were in a muffle furnace (the heated shrouds) and that would be equivalent to external heating (not included in our data base).

The strain in the alpha-plus-beta-phase valley is the same in the slow-ramp and the fast-ramp correlations, and the data that influenced the valley floor can be seen in Fig. 7.

A beta-phase peak was included in Fig. 6 at 1025°C even though our data base contains no data in that temperature range and Fig. 5 does not exhibit such a peak, although other figures in Reference 21 do exhibit the peak. At high temperatures strains should be limited for slow-ramp rates because of the opportunity for oxidization and embrittlement prior to rupture. We have estimated the amount of oxidation for a slow ramp (1°C/s in this case) terminating at 1025°C and concluded that the amount of oxidation is too small to eliminate this strain peak due to embrittlement of the cladding wall; however, the strain

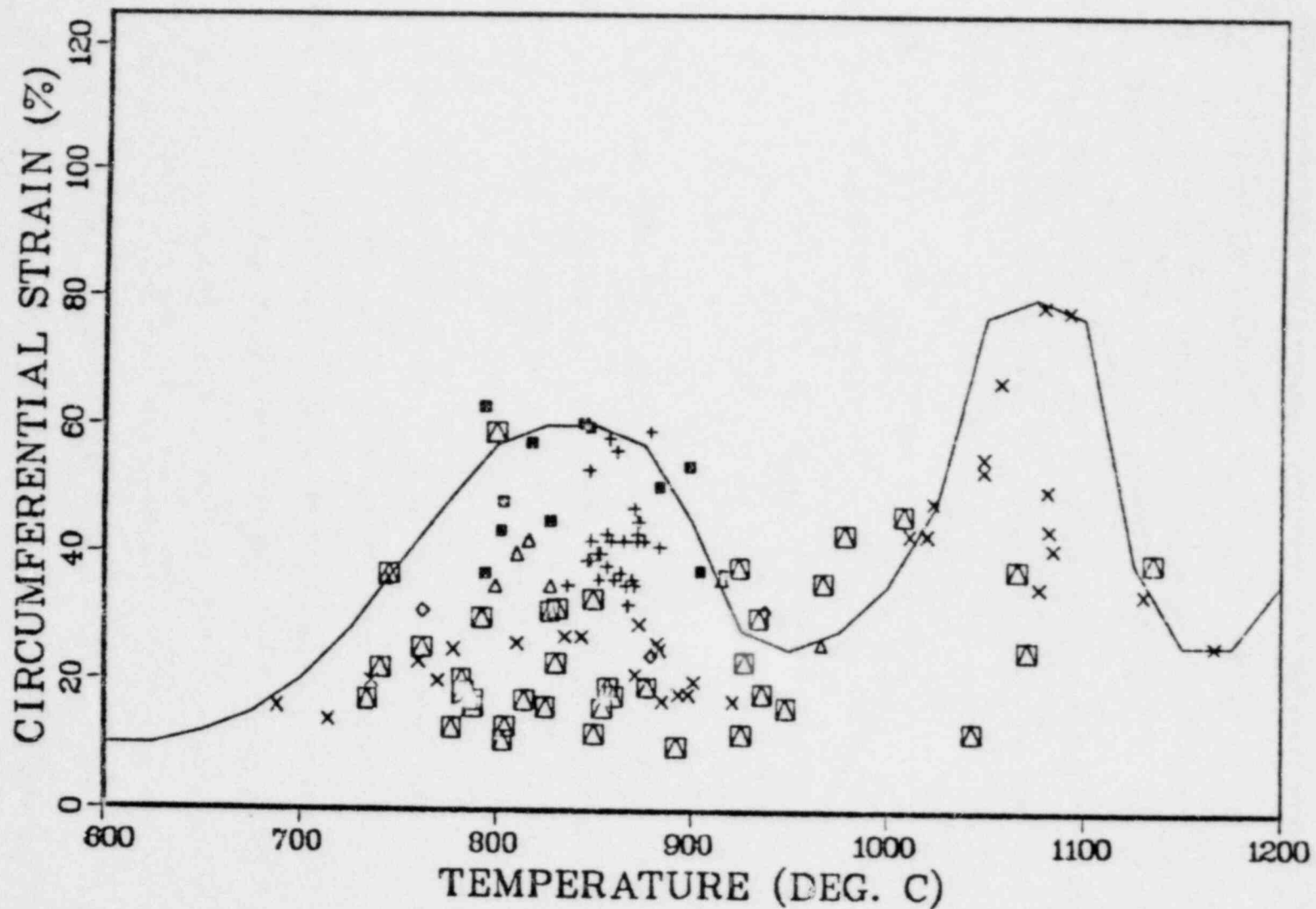


Fig. 7 Maximum circumferential strain as a function of rupture temperature for internally heated Zircaloy cladding in aqueous atmospheres at heating rates greater than or equal to 25°C/s.

peak should be attenuated because of oxide cracking, which exposes bare metal surfaces to further oxidation and thus localizes the hoop stress. Furthermore, because of the temperature dependence of oxidation, the symmetric peak for fast ramps (or in vacuum) will be skewed to the left with an apparent lowering of the temperature at which the peak occurs. Chung and Kassner's work shows a peak shift on the order of 50°C. Based on these considerations and other rod burst data not displayed here, we have located the peak at 1025°C and chosen 35% strain as the peak value.

To derive the fast-ramp correlation (applicable to ramp rates  $\geq$  25°C/s), which is shown in Fig. 7, we have again retained the shape of Chung and Kassner's curves and positioned the peaks and valleys according to our data base for ramp rates greater than or equal to 25°C/s. As with the slow-ramp correlation, we have bounded most of the data because there are experimental limitations that can explain most of the low-lying data.

For the alpha-phase peak, there is less uncertainty in the fast-ramp data than for slow-ramp data, and the peak was set at 60% strain from 825 to 850°C. For the beta-phase peak, we have bounded the high-ramp-rate ORNL data, and the peak was placed at 1075°C with 30% strain. There is some concern (Ref. 30 and 33) that the ORNL high-temperature fast-ramp data may not be best characterized as fast-ramp data. This is because during the course of some of these experiments, the ramp rate, which was initially set at about 40°C/s, decreased below 25°C/s before rupture occurred. Since (a) such

conditions are plausible during a real LOCA and (b) the fast-ramp data were taken with the older-version heaters and unheated shrouds such that straining was inhibited, we believe that downward adjustments to the fast-ramp correlation are not warranted. The strain in this temperature regime does not presently affect licensing analyses, so these uncertainties are relatively unimportant.

We have structured the fast-ramp curve to predict increasing strain at 1175°C to reflect a second high-temperature beta-phase peak at about 1250°C. The strain magnitude in this off-scale temperature region is scaled to correspond to the average burst strain obtained in the second TREAT experiment, FRF-2. Although peak heights for the slow-ramp and fast-ramp correlations were determined primarily from the prototypical data base, they bear approximately the same relation to each other as found in Chung and Kassner's work.

Figure 8 shows the composite (i.e., envelope) of the curves in Figs. 6 and 7 along with all of the data from Fig. 4 (including intermediate-rate data not shown in Figs. 6 and 7). The composite curve gives a good representation of the data, provided that the causes of small strains are kept in mind. Since we have bounded most of the data and approximated the data for conditions that could cause large strains in real LOCAs, we believe these correlations satisfy the intention of Appendix K not to underestimate the degree of swelling.

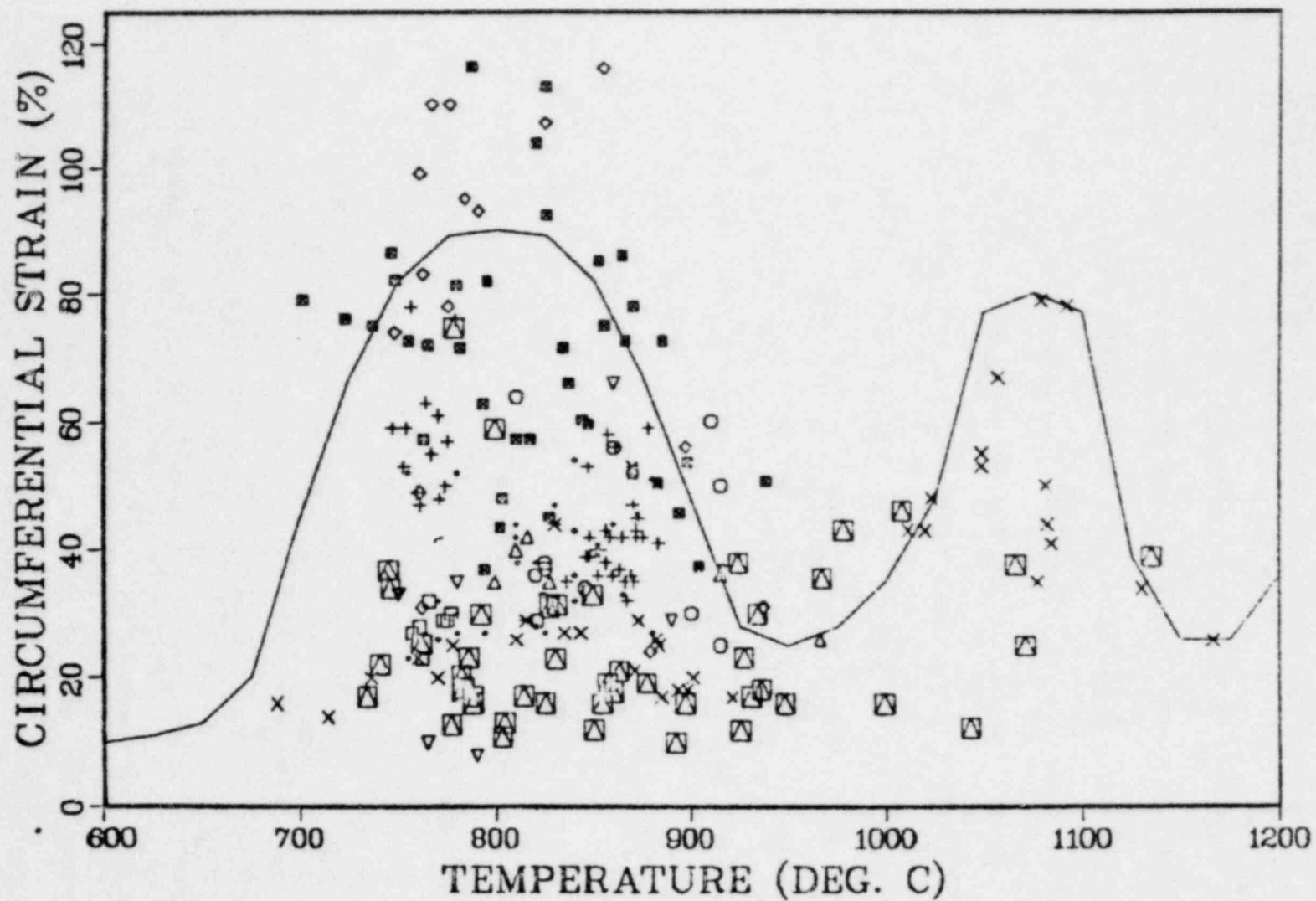


Fig. 8 Maximum circumferential strain as a function of rupture temperature for internally heated Zircaloy cladding in aqueous atmospheres for all heating rates.

### 3.3 Assembly Flow Blockage

Flow blockage is defined as the percent reduction in cross-sectional flow area of a bundle. Very few direct measurements of bundle blockage have been made under prototypical conditions and the best attempts are shown in Fig. 9. Because of the scarcity of the blockage data, it is necessary to derive bundle blockage from single-rod burst strains and then to compare results with bundle data for verification rather than to rely solely on the bundle data. The derivation is not straight forward, however, since actual flow around a burst node is complex and since test results have shown that bursts in a bundle are not coplanar. To accomplish this derivation, therefore, we will determine an empirical relation between burst strain and bundle blockage from the three ORNL MRBT experiments.

The diagram in Fig. 10 outlines the steps in deriving flow blockage. An empirical (non-mechanistic) relation is first found between burst strain and average rod strain in the plane of blockage; it will be seen that the average coplanar rod strain is only about half of the burst strain. Figure 11 illustrates this step.

Figure 11 shows the plane of maximum blockage in Chapman's bundle B-1 (Ref. 34-35). Only 4 rods ruptured in this plane; the other 12 rods ruptured at other elevations (rod number 3 leaked and has been excluded from some of the analysis). The average rod strain in this plane is seen to be 25%. The average burst strain for these 15 rods was measured to be 42% with a standard deviation of 7% strain.

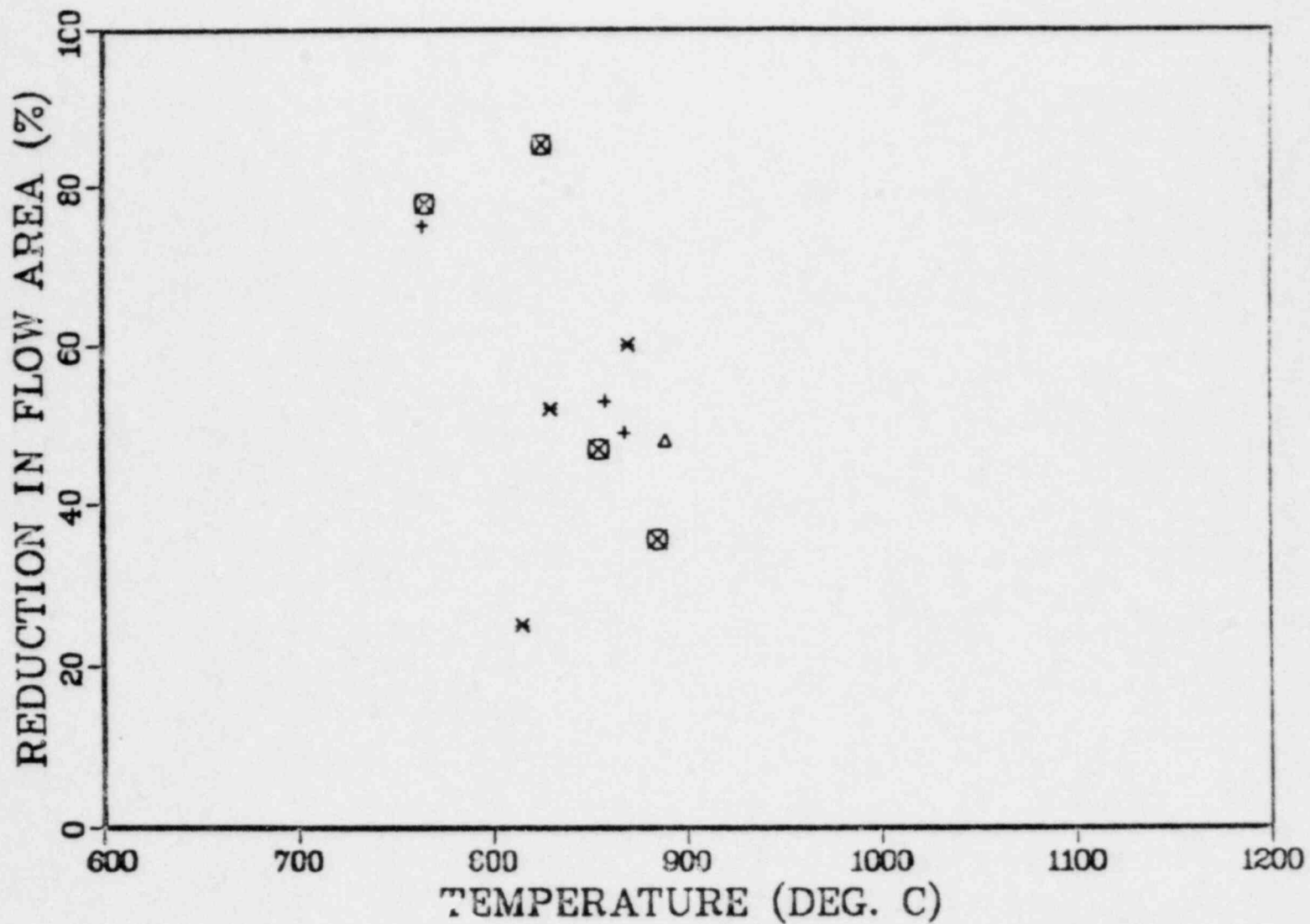


Fig. 9 Reduction in local flow area as a function of rupture temperature for internally heated Zircaloy clad bundles in aqueous atmospheres.

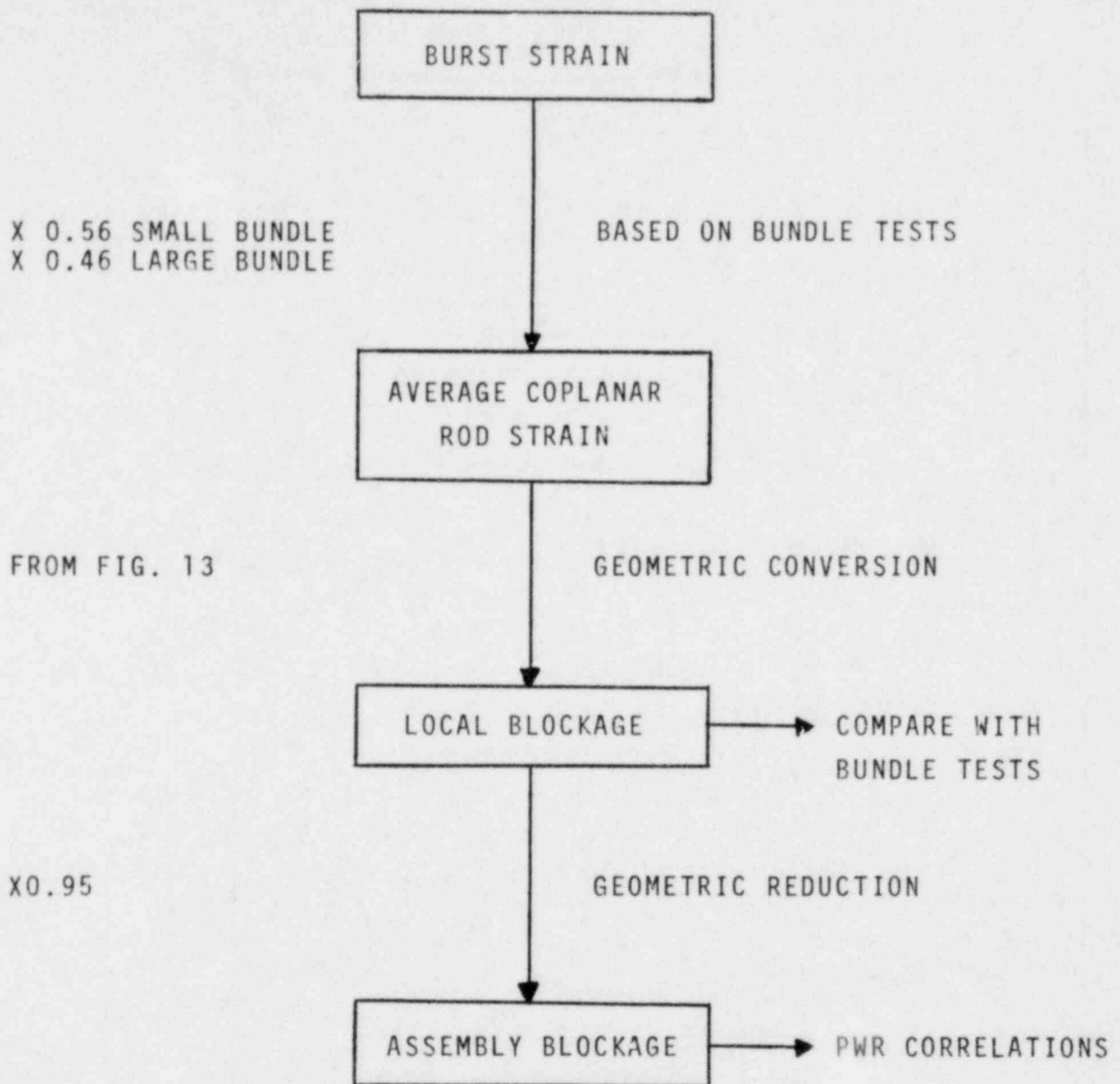


Fig. 10 Outline of flow blockage model.



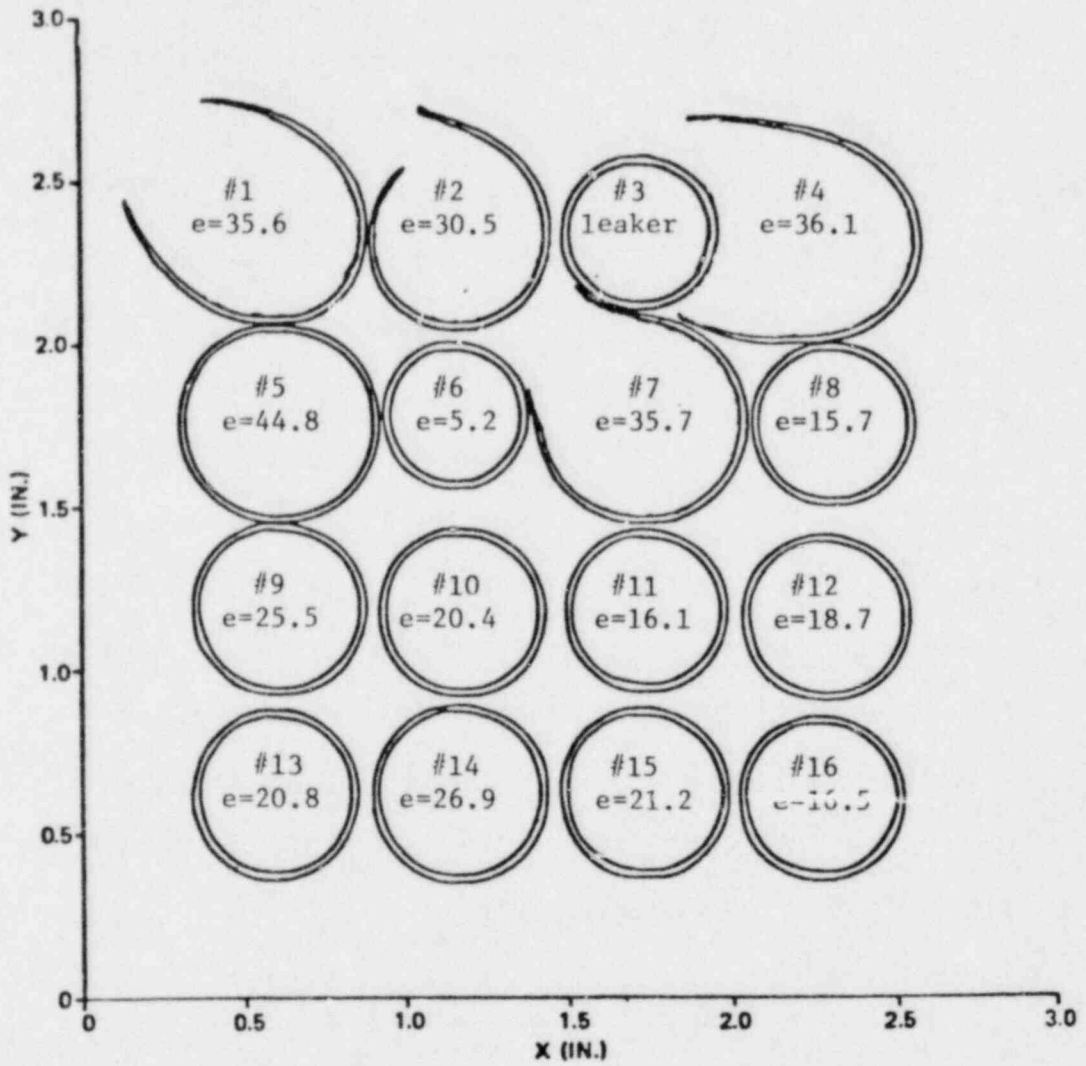


Fig. 11 Computer drawn profile from digitized data of ORNL bundle B-1 section at 76.5-cm elevation.

For this bundle the ratio of the average coplanar rod strain (25%) to the one-sigma conservatively biased\* burst strain (49%) is 0.51. Repeating this procedure for bundles B-2 and B-3 gives ratios of 0.57 and 0.59. Thus the overall average ratio is 0.56, which is the relationship to be used for small bundles.

To obtain flow blockage for large commercial-size fuel assemblies, a small modification is needed in the derivation. First, it must be recognized that maximum planar bundle blockage, which is desired, is a function of bundle size. This can be seen by envisioning an 8x8 test bundle that is analyzed quadrant by quadrant. If each 4x4 quadrant is viewed as a small bundle, the planes of maximum blockage for the quadrants would be expected to occur at different elevations because of some randomness in the rupture process. One would therefore expect to find the plane of maximum blockage in each quadrant to have greater flow restriction than the plane of maximum blockage in the bundle taken as a whole. That is, the large bundle size introduces an averaging effect.

---

\*A conservatively biased burst strain is used here to reduce the calculated blockage when Figs. 6 and 7 are utilized. Initially we believed that Figs. 6 and 7 were conservative. In that case, using a conservative bias in the derivation would be appropriate. We now believe that the strain curves in Figs. 6 and 7 are best-estimate correlations for LOCA conditions that are conducive to large strains. Nevertheless, since retaining this bias in the derivation improves the agreement between measured and predicted flow blockages, we have retained the bias.

To account for this averaging effect for commercial PWR fuel assemblies ranging from 14x14 to 17x17, we have used an axially averaged blockage from Chapman's bundle tests rather than the maximum blockage value used above for small bundles. For bundle B-1 (Fig. 12), the average (41%) of the blockages was found between the 23-cm and 47-cm locations where the suppressing effect of spacer grids at 10-cm and 66-cm has dissipated. Similar averages were found for bundles B-2 and B-3. Using these average values in deriving the ratio of average coplanar rod strain to one-sigma burst strain results in a smaller value, and the ratio to be used to derive large assembly blockages from burst strain data is thus 0.46 (compared with 0.56 for small arrays).

The remaining steps in deriving flow blockage involve simple geometric calculations. Given the average rod strain in the plane of blockage, the percent local flow blockage (i.e., blockage with no credit for non-swelling guide tubes) can be found from Fig. 13.

Figure 13 relates average coplanar rod strain to flow area reduction in such a way that the rods retain their circular cross section until they first touch (at 32% strain), and for larger strains the cross sections become square. Complete blockage (100%) results when average coplanar rod strain reaches about 70%. Since current PWR fuel designs have equivalent pitch-to-rod-diameter ratios, Fig. 13 applies to all PWR fuel designs.

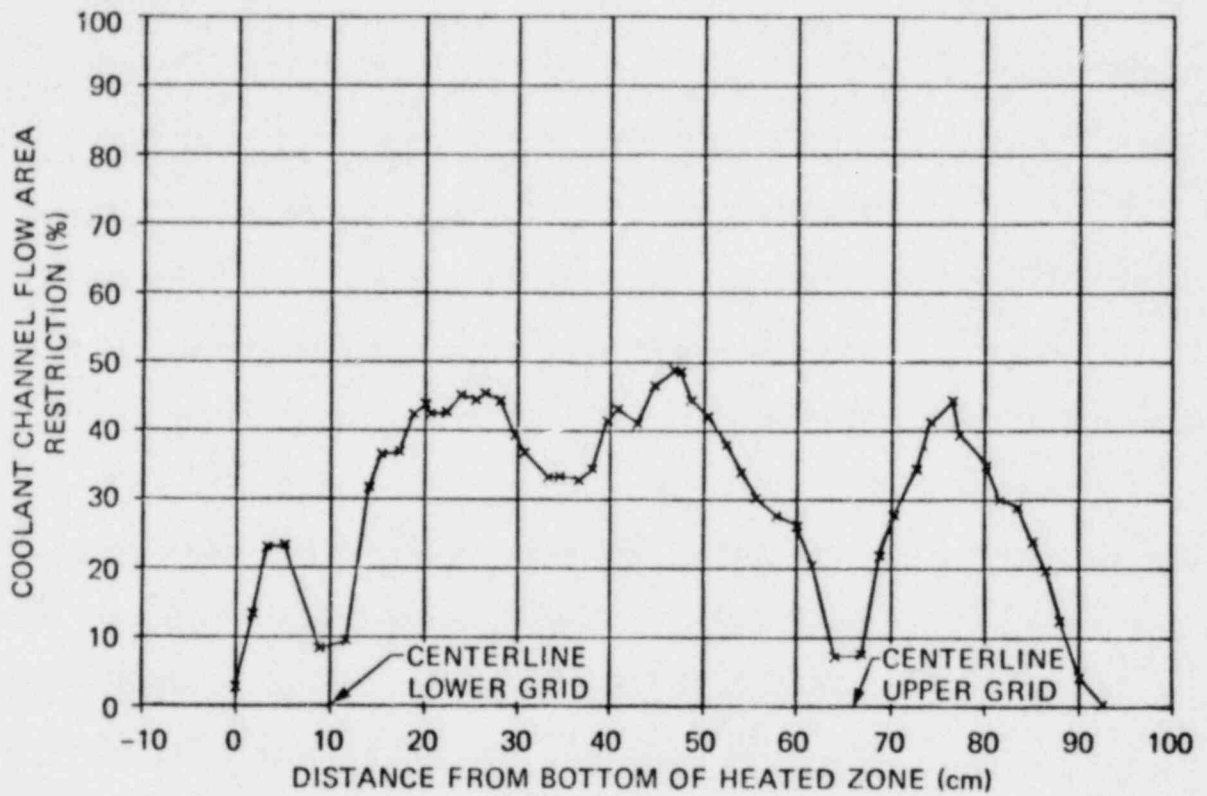


Fig. 12 Coolant channel flow area restriction as a function of elevation in ORNL bundle B-1.

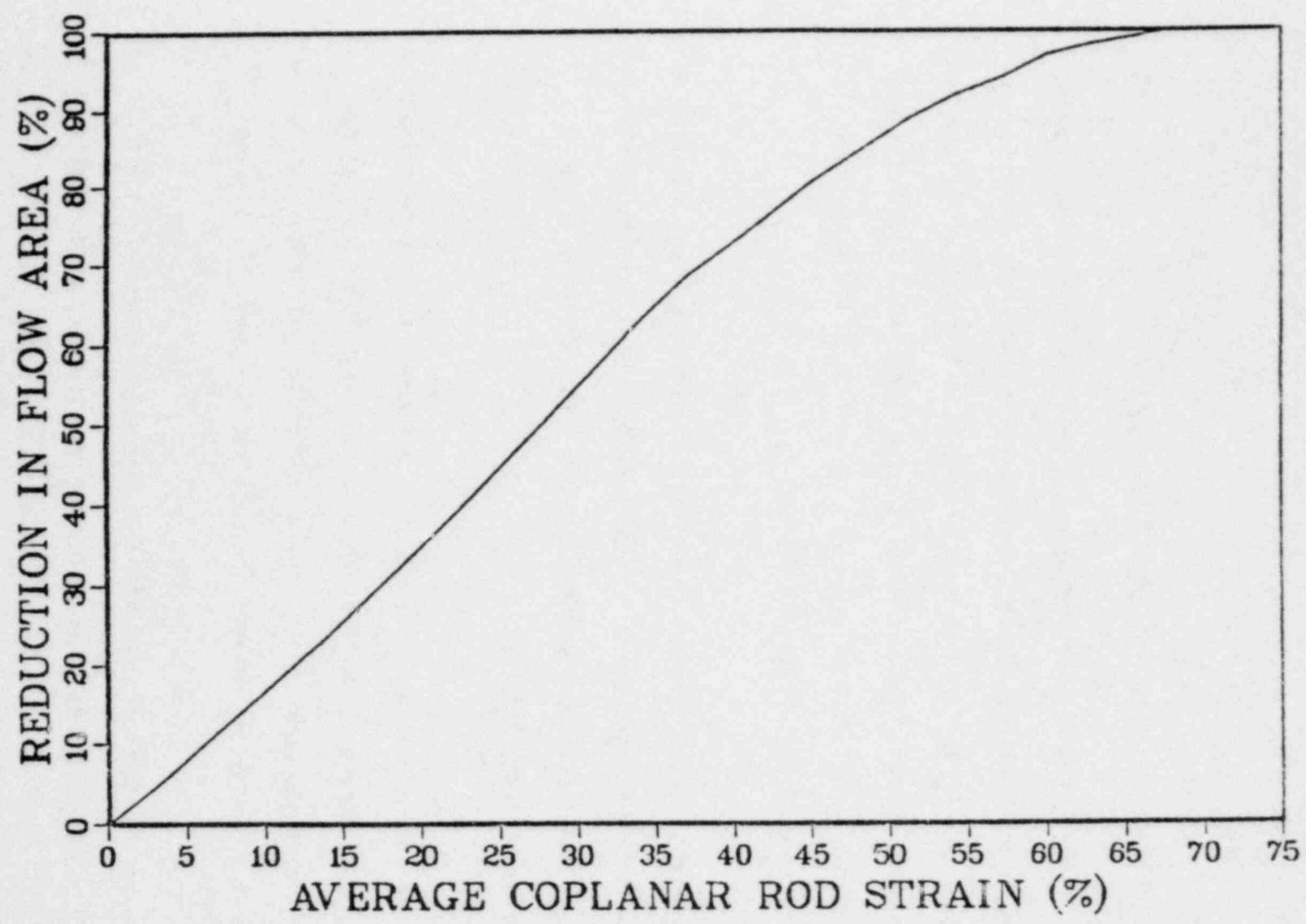


Fig. 13 Reduction in local flow area as a function of average coplanar rod strain.

The final step in deriving assembly blockage involves a reduction of 5% to account for instrument tubes and guide tubes that would not balloon. The exact scaling factor depends on the fuel design and is given by

$$\text{Scaling factor} = N_r A_r / (N_r A_r + N_g A_g), \quad (3-4)$$

where  $N_r$  is the number of fuel rods,  $A_r$  is the flow area around an undeformed fuel rod,  $N_g$  is the number of guide tubes or instrument tubes, and  $A_g$  is the flow area around an undeformed guide tube or instrument tube. The differences in scaling factors of different commercial fuel designs are small so we have used the approximate reduction of 5% for all PMR designs.

Figures 14 and 15 compare the flow blockage data with correlations derived from Figs. 6 and 7. The curves in Figs. 14 and 15 are for small bundles without guide tubes and are, therefore, directly comparable with the data.

Although the data are sparse and do not cover the entire temperature range of interest, we think that Figs. 14 and 15 provide good verification of the correlation. This is especially true when the reasons for the deviations between the data and the curve are examined.

The most significant deviation is the asterisk symbol in Fig. 14 at 25% blockage. This datum point represents a 3x3 bundle test (Rebeka 1)

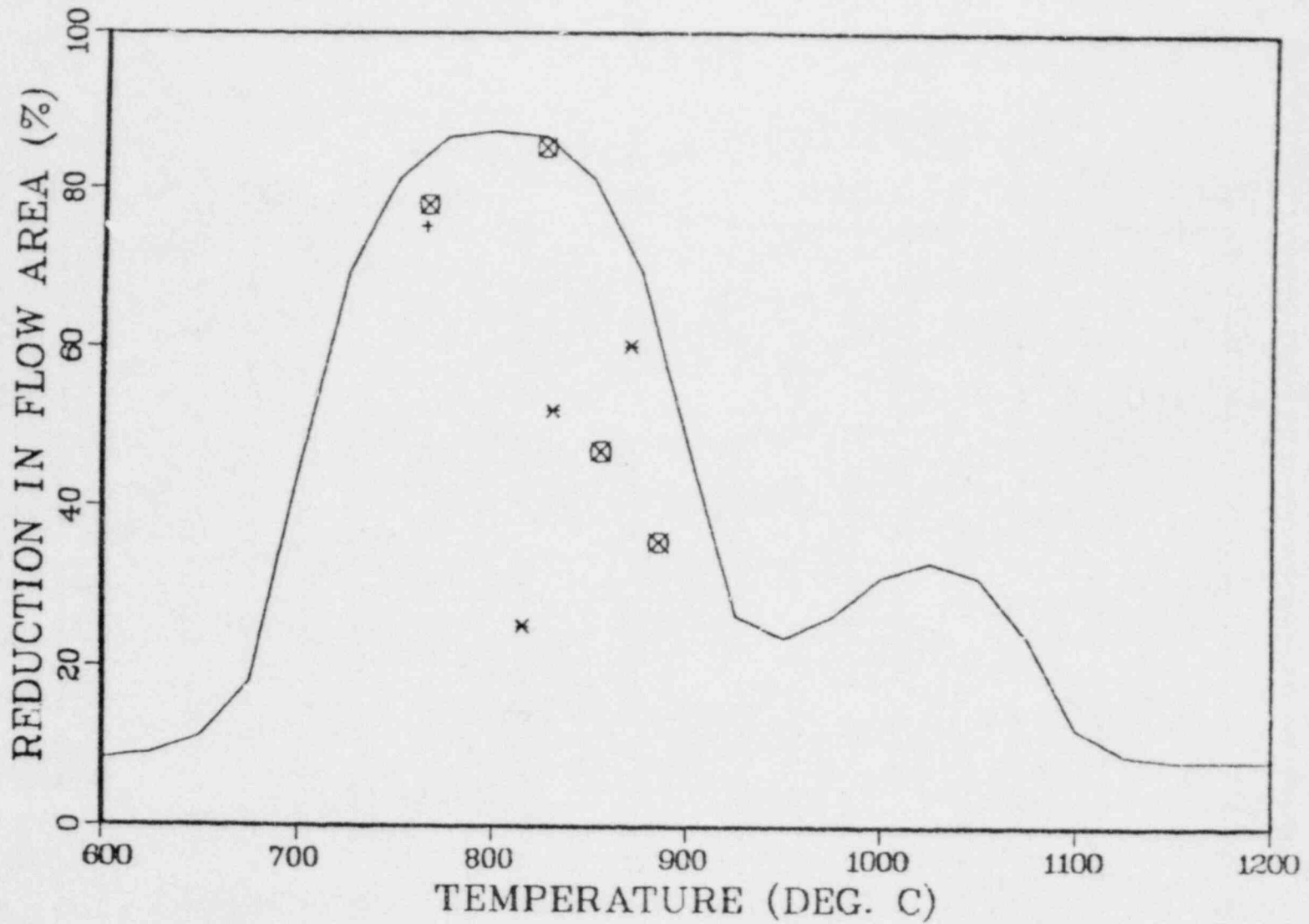


Fig. 14 Reduction in local flow area as a function of rupture temperature for internally heated Zircaloy clad bundles in aqueous atmospheres at heating rates less than or equal to 10°C/s.

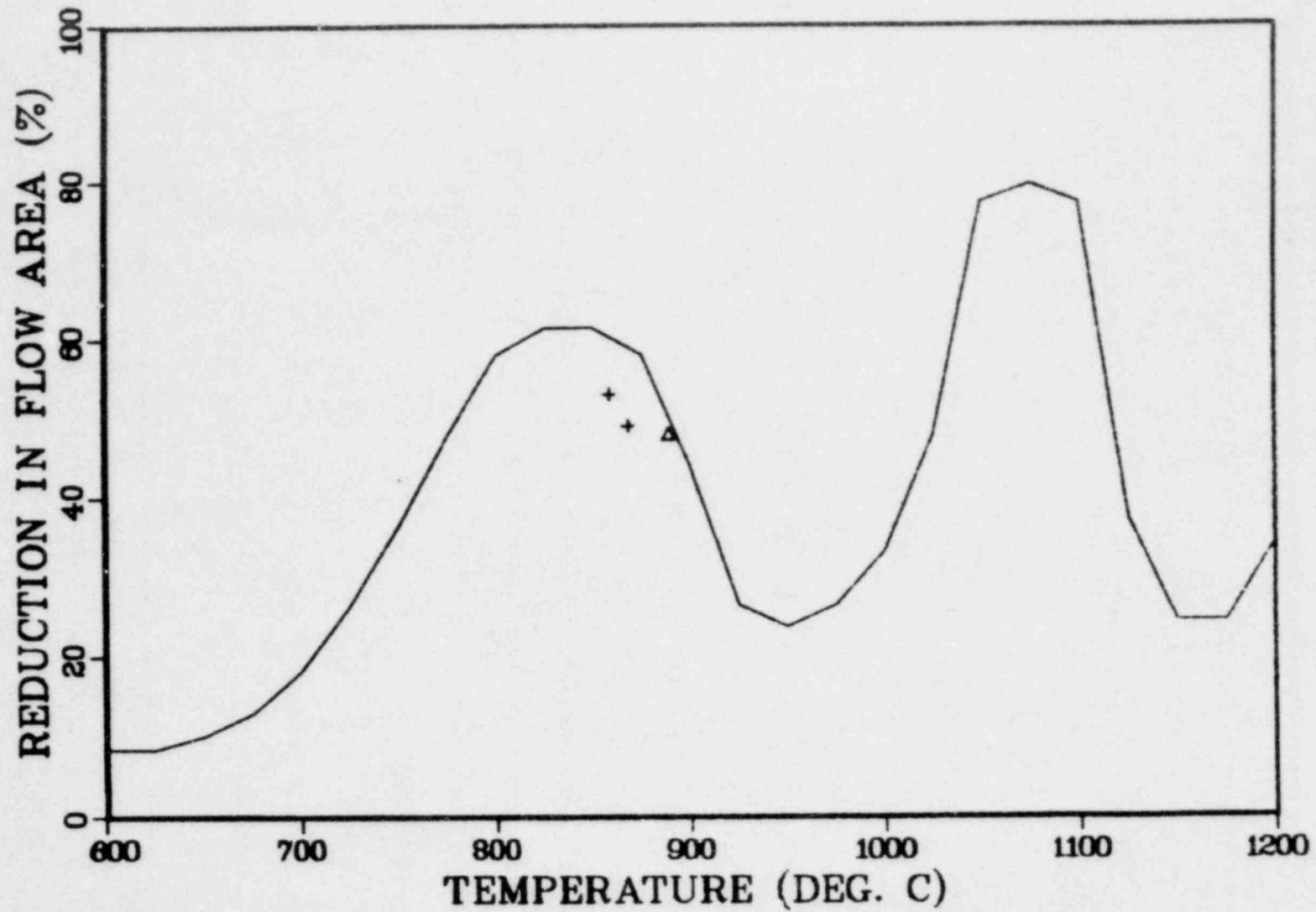


Fig. 15 Reduction in local flow area as a function of rupture temperature for internally heated Zircaloy clad bundles in aqueous atmospheres at heating rates greater than or equal to 25°C/s.



in which only 2 of the 9 rods ruptured. Had the cladding temperatures in this bundle test been high enough to perforate all 9 rods (as they should have if their temperatures are to be interpreted as rupture temperatures), then more blockage would have resulted and this datum point on Fig. 14 would have appeared at a higher rupture temperature and a higher degree of blockage -- in closer agreement with the correlation.

The three plus symbols represent Chapman's bundle tests on which we have based one step in the blockage model. The blockages shown here utilize Chapman's "minimum blockage" definition. These points fall below the blockage curves because the individual burst strains fall below the strain curves (Figs. 6 and 7). Bundle B-2 had an unheated shroud, while B-1 and B-3 had heated shrouds, but the shroud temperatures lagged the cladding temperatures too much to have provided a uniform temperature environment. Using more effectively heated shrouds and new internal heaters, Chapman finds larger strains in single rod tests; we would therefore expect the same increases for these bundles.

The upright triangle symbol on Fig. 15 represents the only\* in-pile bundle experiment, FRF-1, which was conducted in the TREAT reactor.

---

\*FRF-2 was also an in-reactor bundle experiment, and it produced a maximum flow blockage of 91%; however the FRF-2 cladding rupture temperatures were about 50°C greater than the current licensing peak cladding temperature limit of 1204°C (2200°F) and fall well outside the range of allowable conditions. Data for FRF-2 are also compiled in Appendix A.

It has been suggested (Ref. 36) that the reported coolant channel blockages in the TREAT experiment were atypically high because the bundle design employed a hexagonal fuel array with triangular coolant subchannels that were smaller than square subchannels of the same pitch. This objection would be justified had the blockages reported in Refs. 25-26 and 37 been obtained by a direct measurement of the coolant subchannel areas. However, this method was not used; rather, the individual rod cross-sectional areas were determined, summed, and subtracted from the total area encompassed by the sleeve (shroud). For this experiment, the ratio of the area inside the sleeve to the total undeformed fuel rod cross-sectional area was 2.16, which is approximately equal to that ratio for a PWR (2.24). Therefore, we believe that the TREAT blockage is directly applicable to our blockage analysis.

We have reviewed the experimental conditions of all of the out-of-reactor tests and found that none of the tests included all of the features of a PWR that enhance strain and blockage. We therefore believe that the correlations in Figs. 14 and 15 are best estimates for the conditions that are conducive to blockage even though those correlations bound the available data.

For large-size PWR assemblies, the flow blockage correlations are shown in Fig. 16, and the coordinates for these curves are tabulated in Appendix B. Boiling water reactors, with shrouded fuel assemblies and upper core sprays, are sufficiently different from PWRs that assembly flow blockage correlations are not used in ERS analysis.

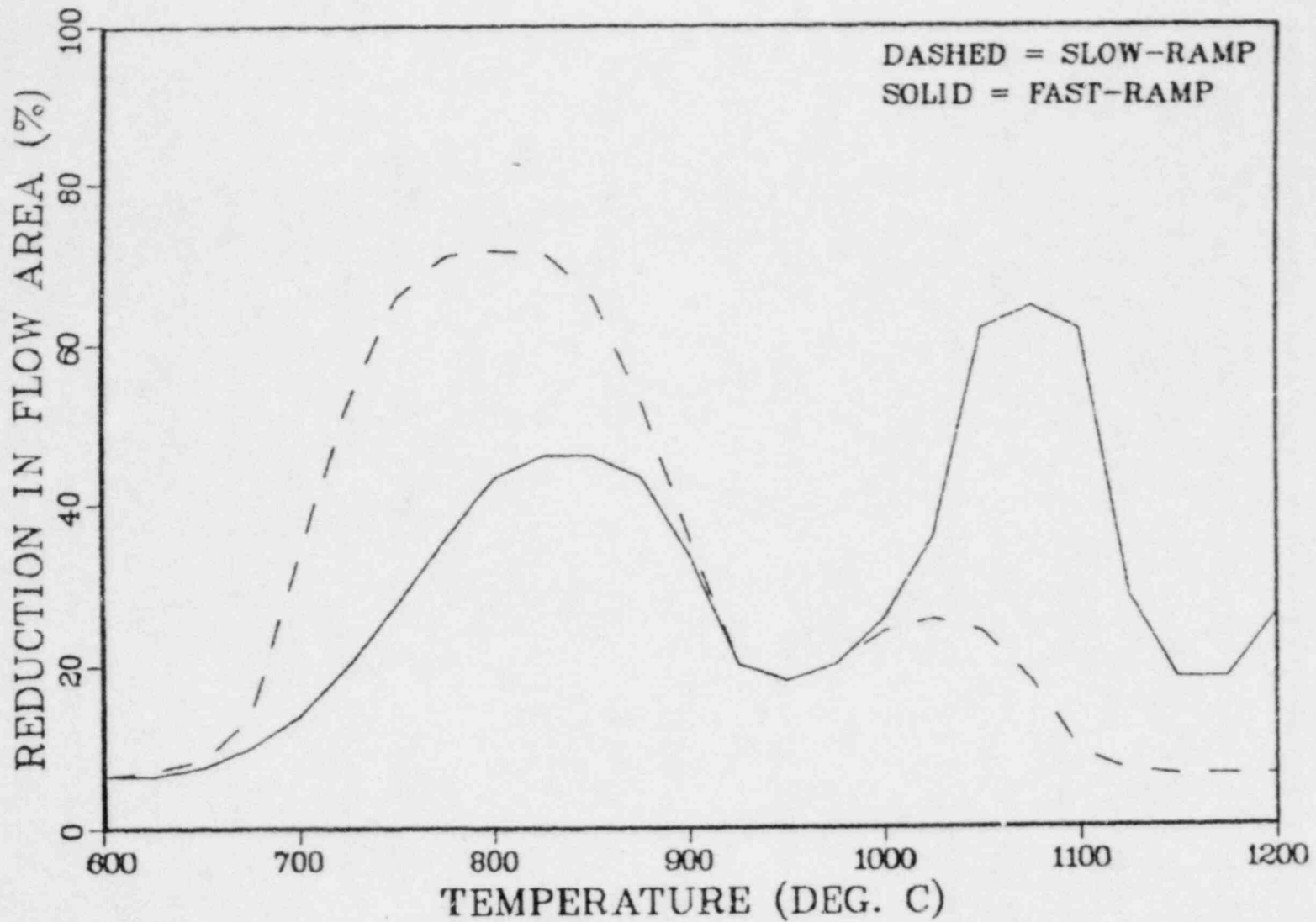


Fig. 16 Reduction in PWR assembly flow area as a function of rupture temperature and ramp rate.

#### 4. COMPARISON WITH PREVIOUS MODELS

##### 4.1 Early AEC Model

The Water Reactor Evaluation Model (WREM) (Ref. 38) was developed in 1975 as an audit model, but it was not used as a standard for acceptance of vendor licensing models. Figures 17-21 show the WREM models compared with the present correlations. If it is kept in mind that fast heating rates were envisioned for WREM applications, agreement is good for rupture temperature (Fig. 17). The WREM burst strain model (Figs. 18-19) agrees well with our correlations at temperatures near 950°C, but does not exhibit the first beta-phase superplastic peak seen in the fast-ramp data (Fig. 19). The WREM assembly flow blockage model (Figs. 20-21) conservatively envelopes the present fast- and slow-ramp correlations, and it shows excellent agreement with the present slow-ramp alpha-phase peak.

##### 4.2 Babcock & Wilcox

Figures 22-28 show the B&W models compared with the present correlations. The B&W rupture temperature model (Fig. 22) agrees very well with the present correlation for slow-ramps and therefore conservatively predicts the incidence of rupture for higher ramp rates. Two sets of burst strain models are used by Babcock & Wilcox; the THETA model (Figs. 23-24) is used for single-rod analyses whereas the CRAFT model (Figs. 25-26) is used for blockage analyses. The B&W burst strains in general do not agree with our current understanding

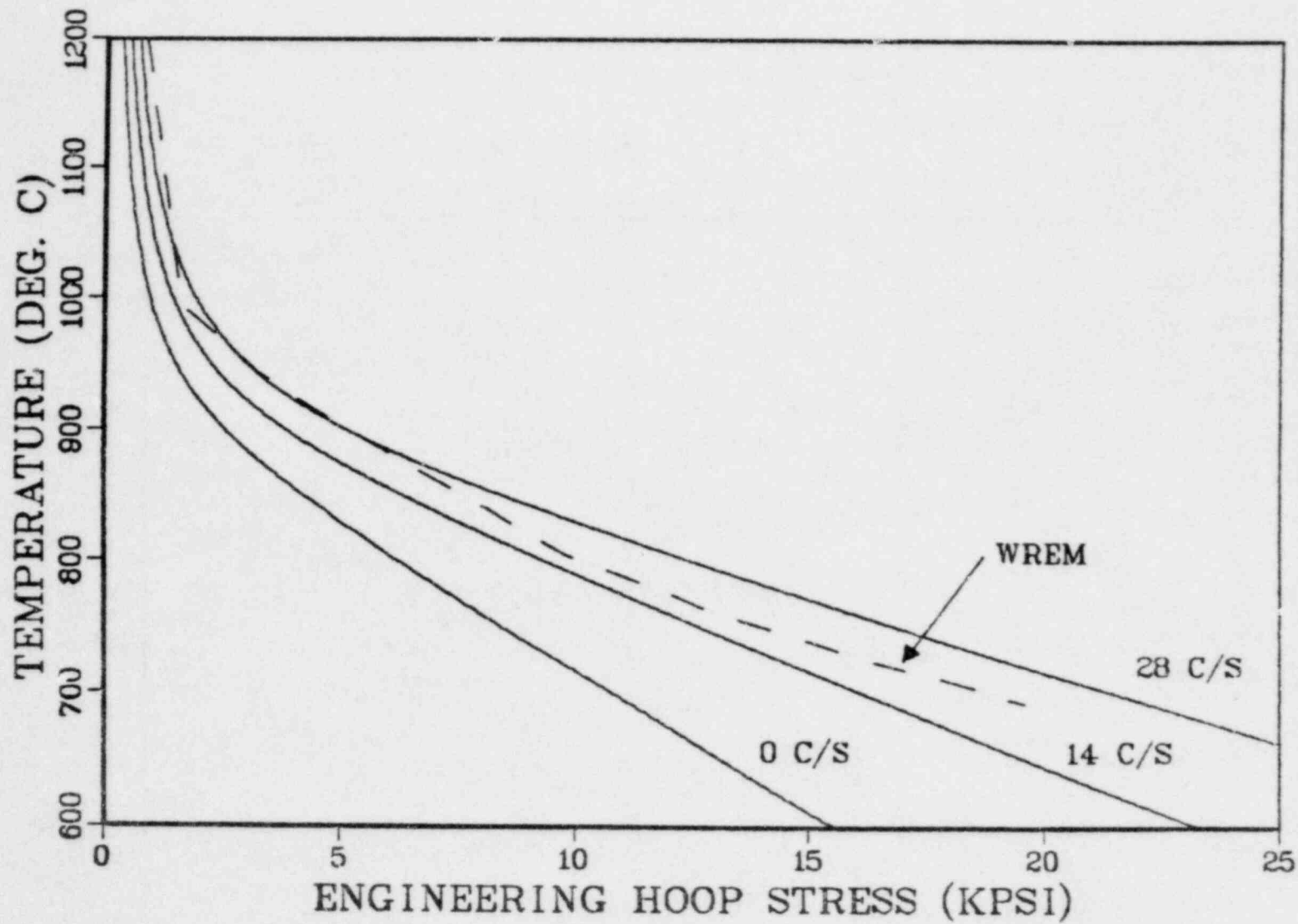


Fig. 17 WREM model and ORNL correlation of rupture temperature as a function of engineering hoop stress and ramp rate.

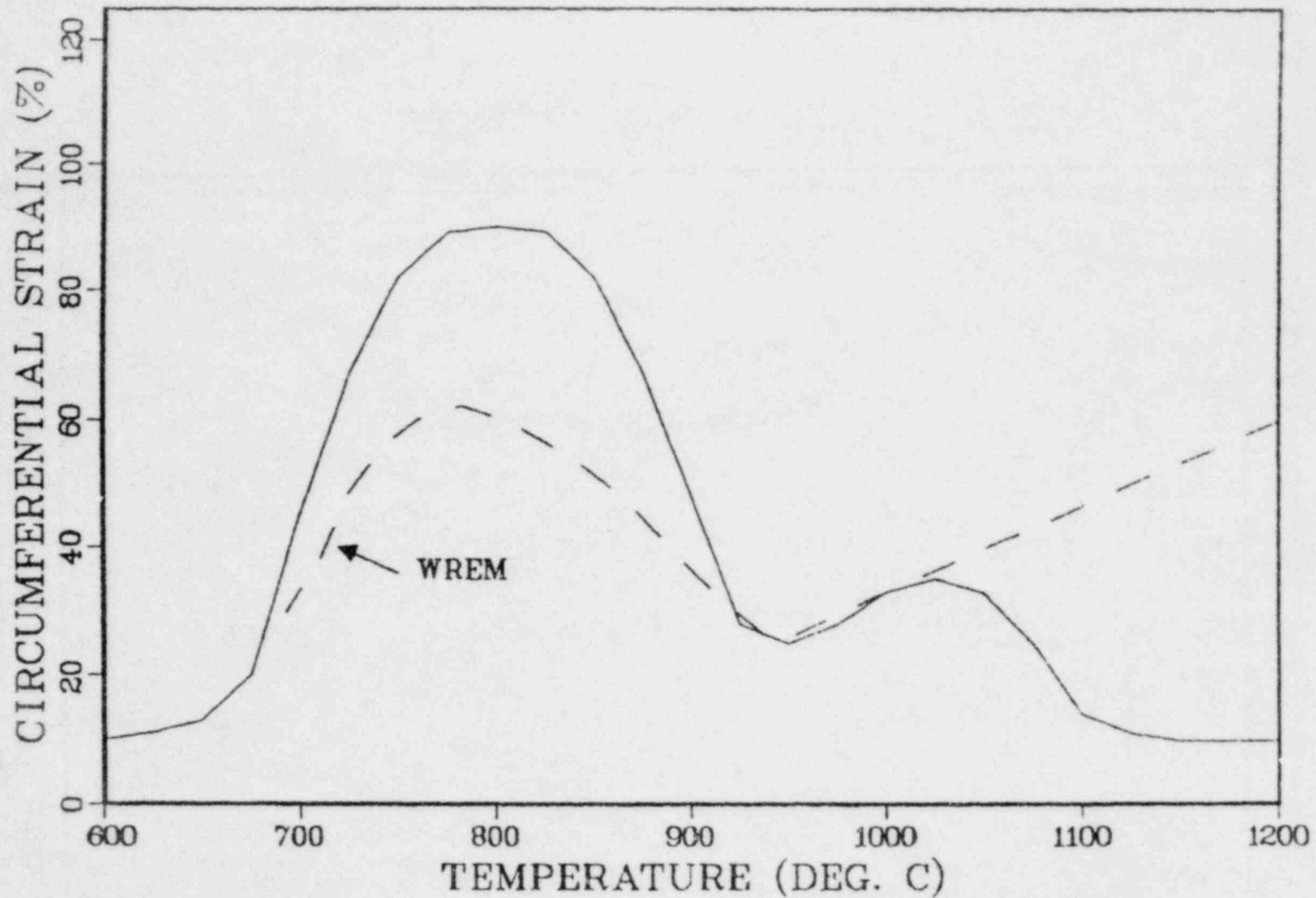


Fig. 18 WREM model and slow-ramp correlation of circumferential burst strain as a function of rupture temperature.

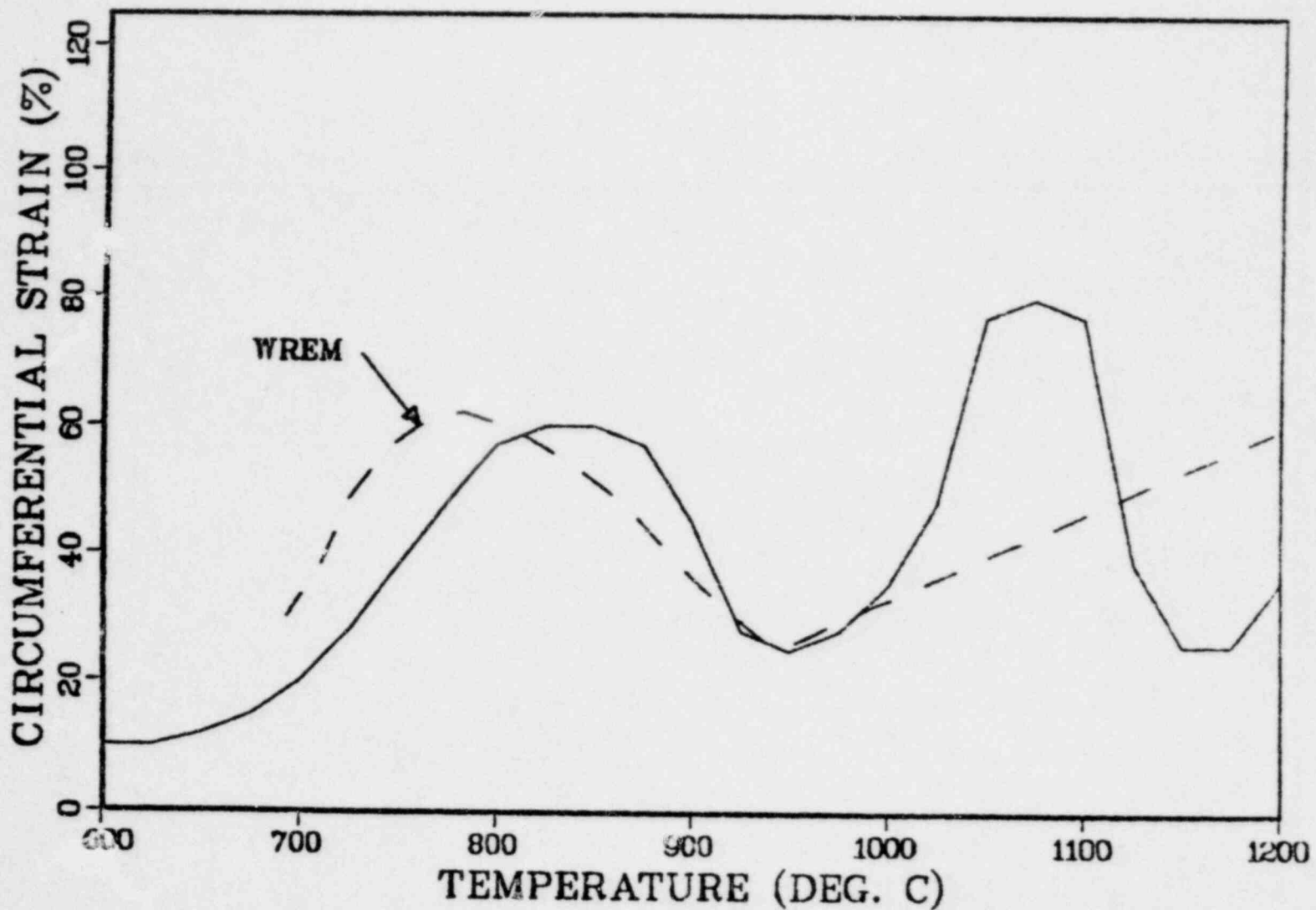


Fig. 19 WREM model and fast-ramp correlation of circumferential burst strain as a function of rupture temperature.

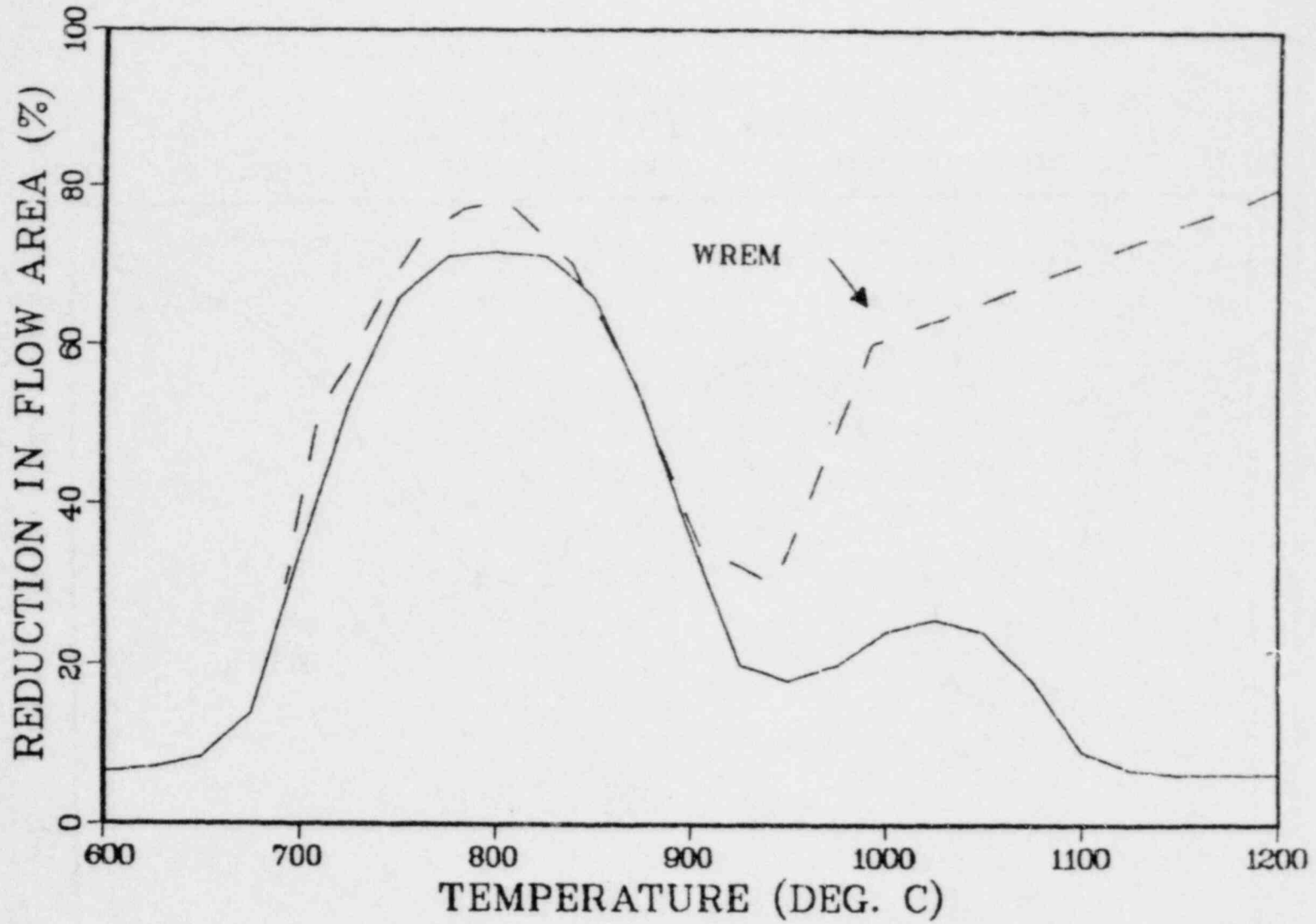


Fig. 20 WREM model and slow-ramp correlation of reduction in assembly flow area as a function of rupture temperature.



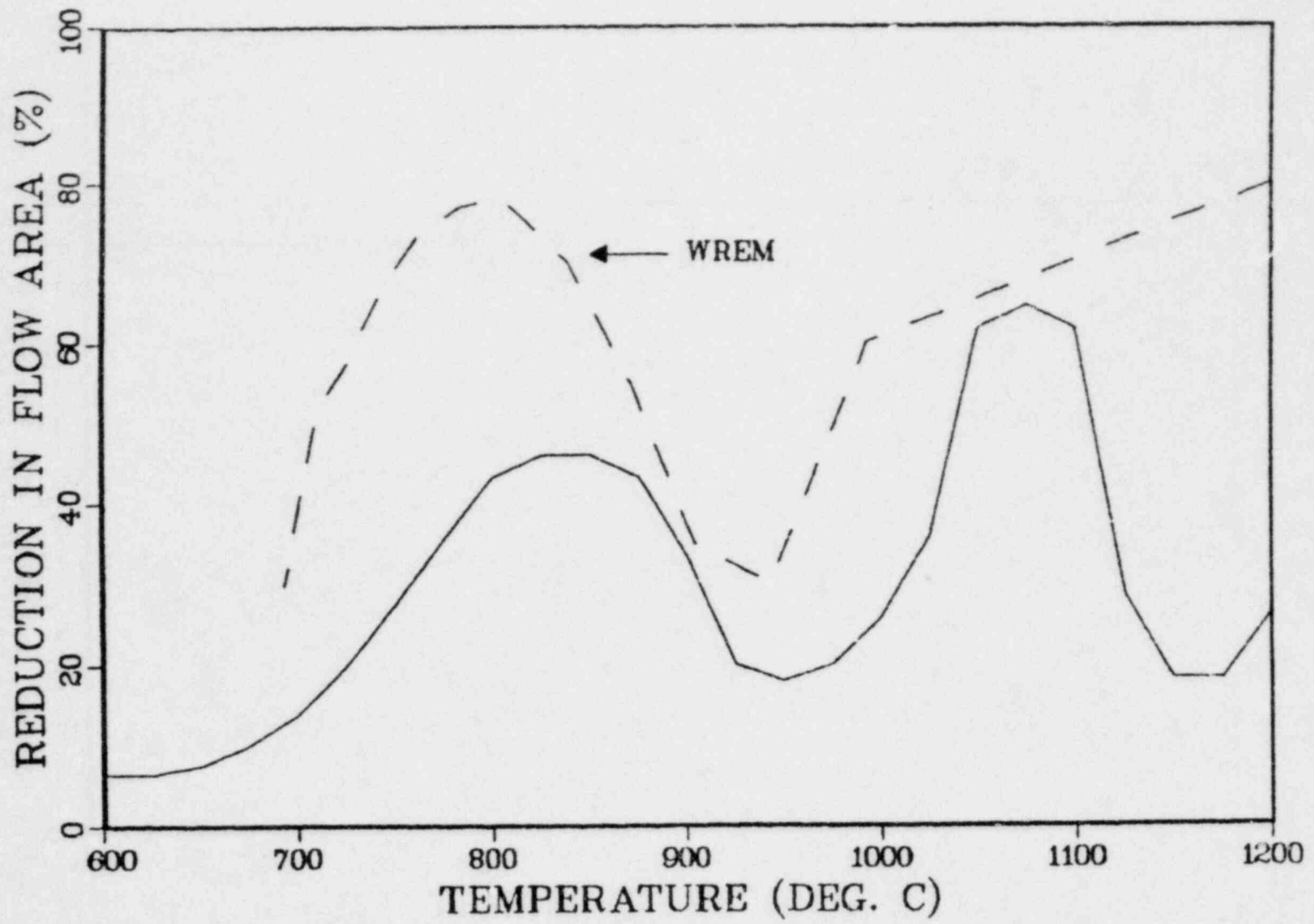


Fig. 21 WREM model and fast-ramp correlation of reduction in assembly flow area as a function of rupture temperature.

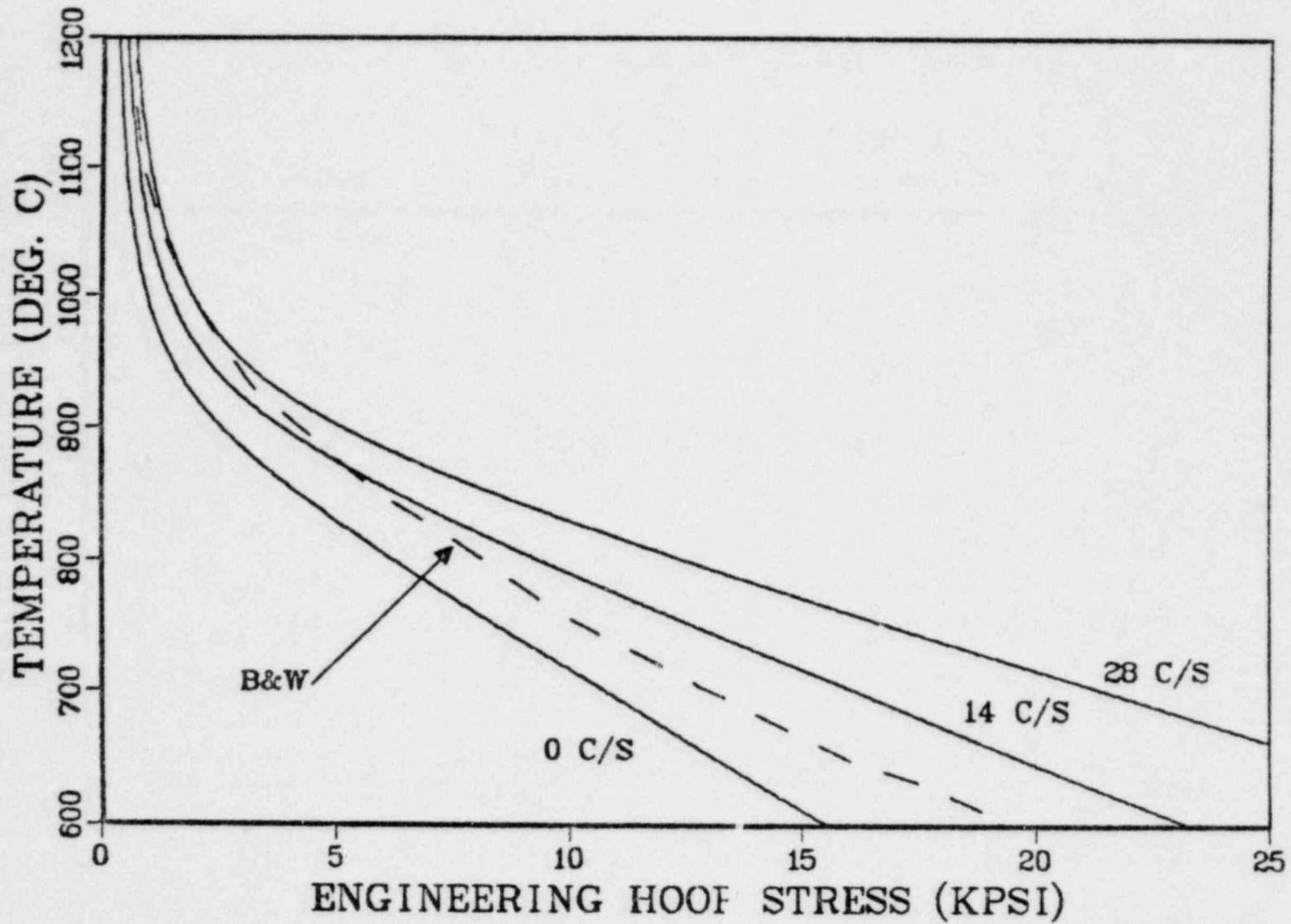


Fig. 22 B&W model and ORNL correlation of rupture temperature as a function of engineering hoop stress and ramp rate.

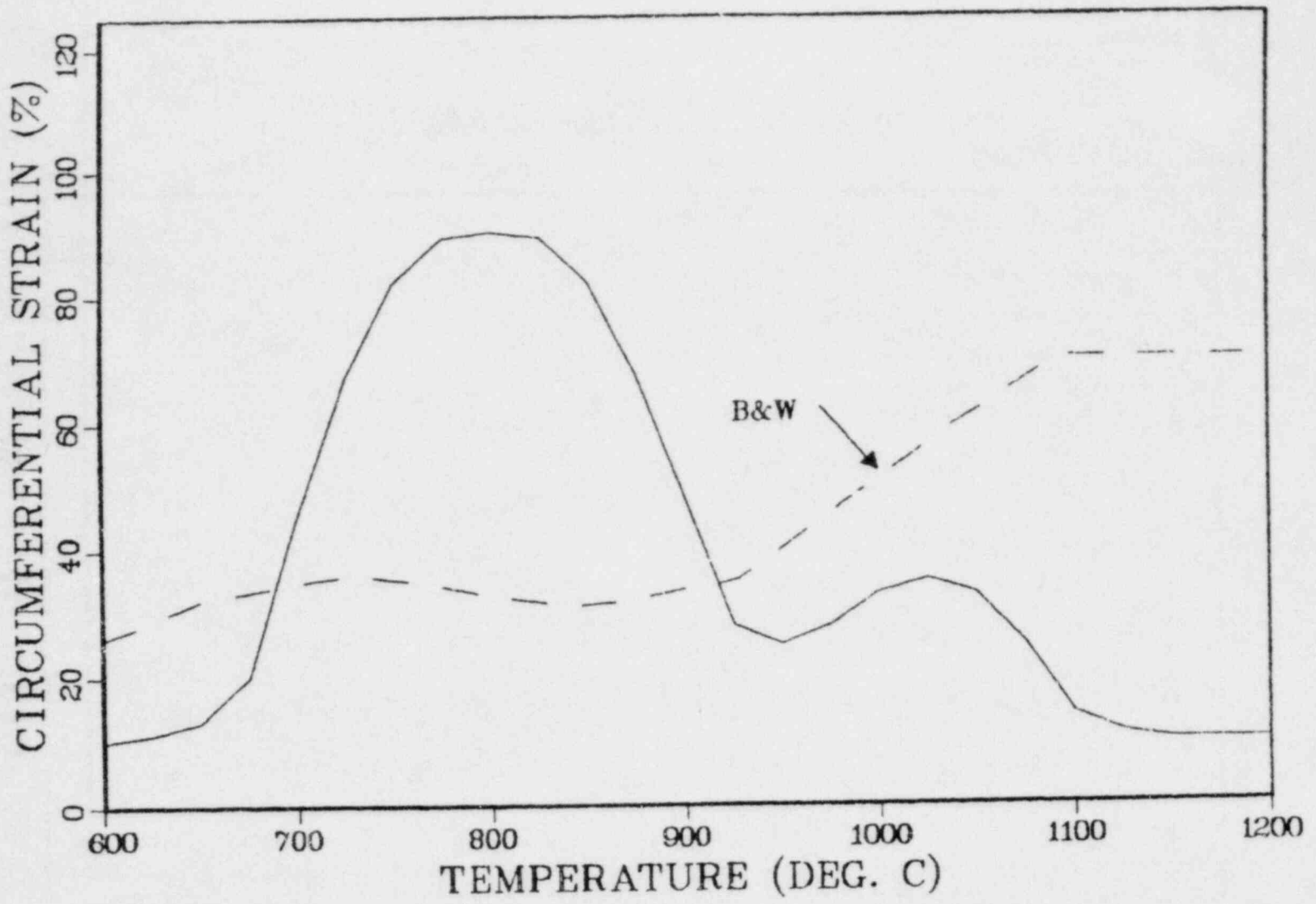


Fig. 23 B&W THETA model and slow-ramp correlation of circumferential burst strain as a function of rupture temperature.

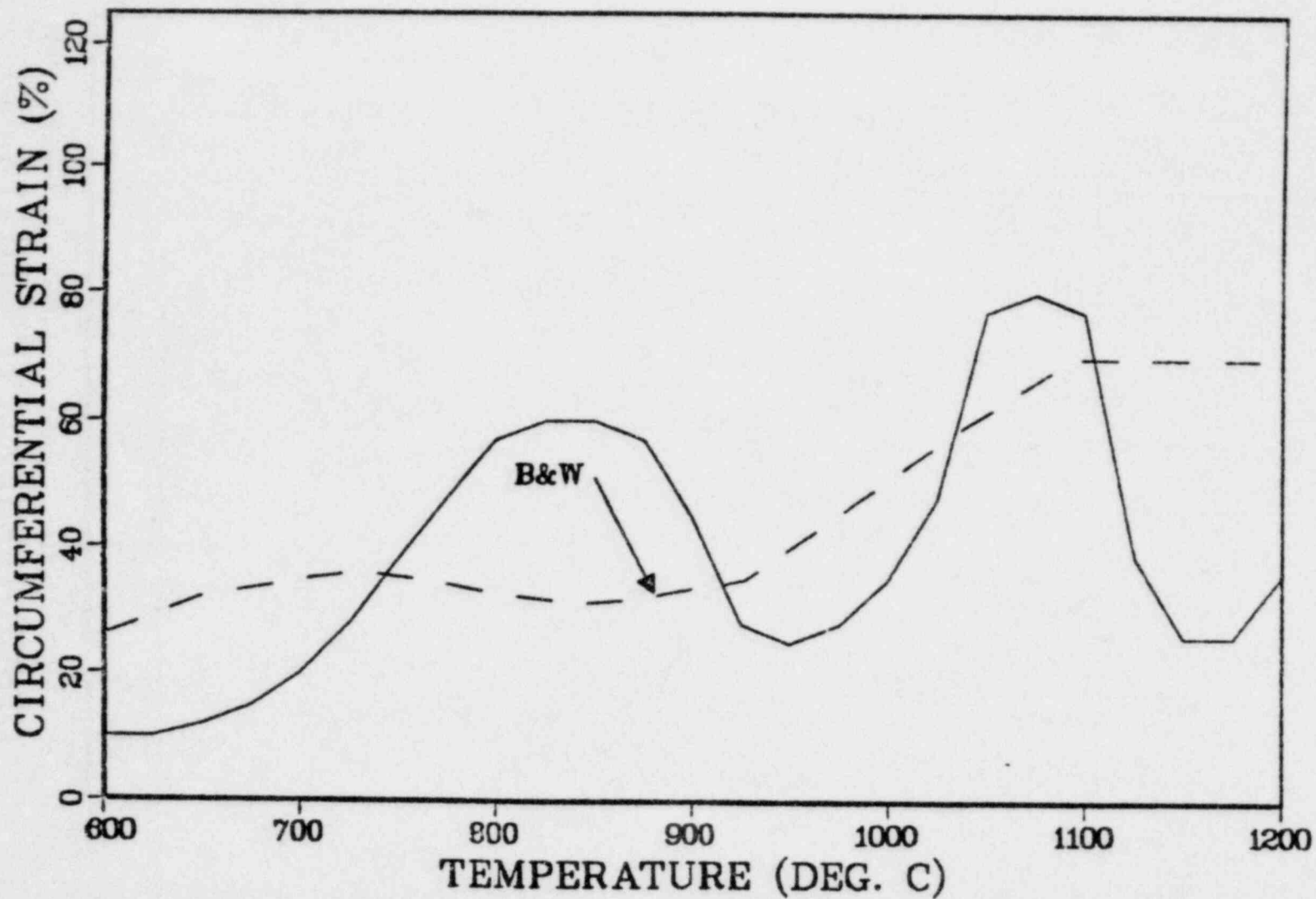


Fig. 24 B&W THETA model and fast-ramp correlation of circumferential burst strain as a function of rupture temperature.

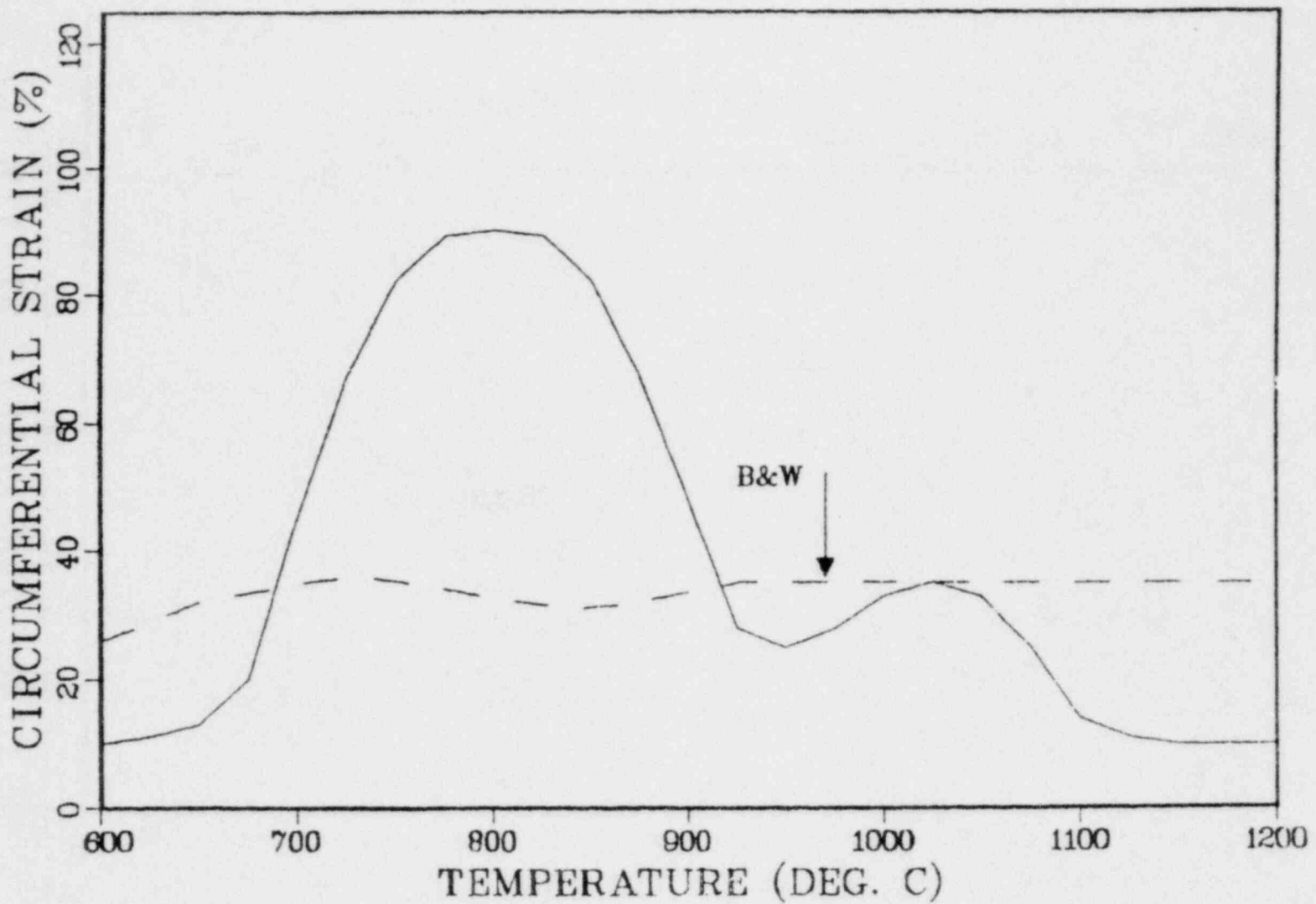


Fig. 25 B&W CRAFT model and slow-ramp correlation of circumferential burst strain as a function of rupture temperature.

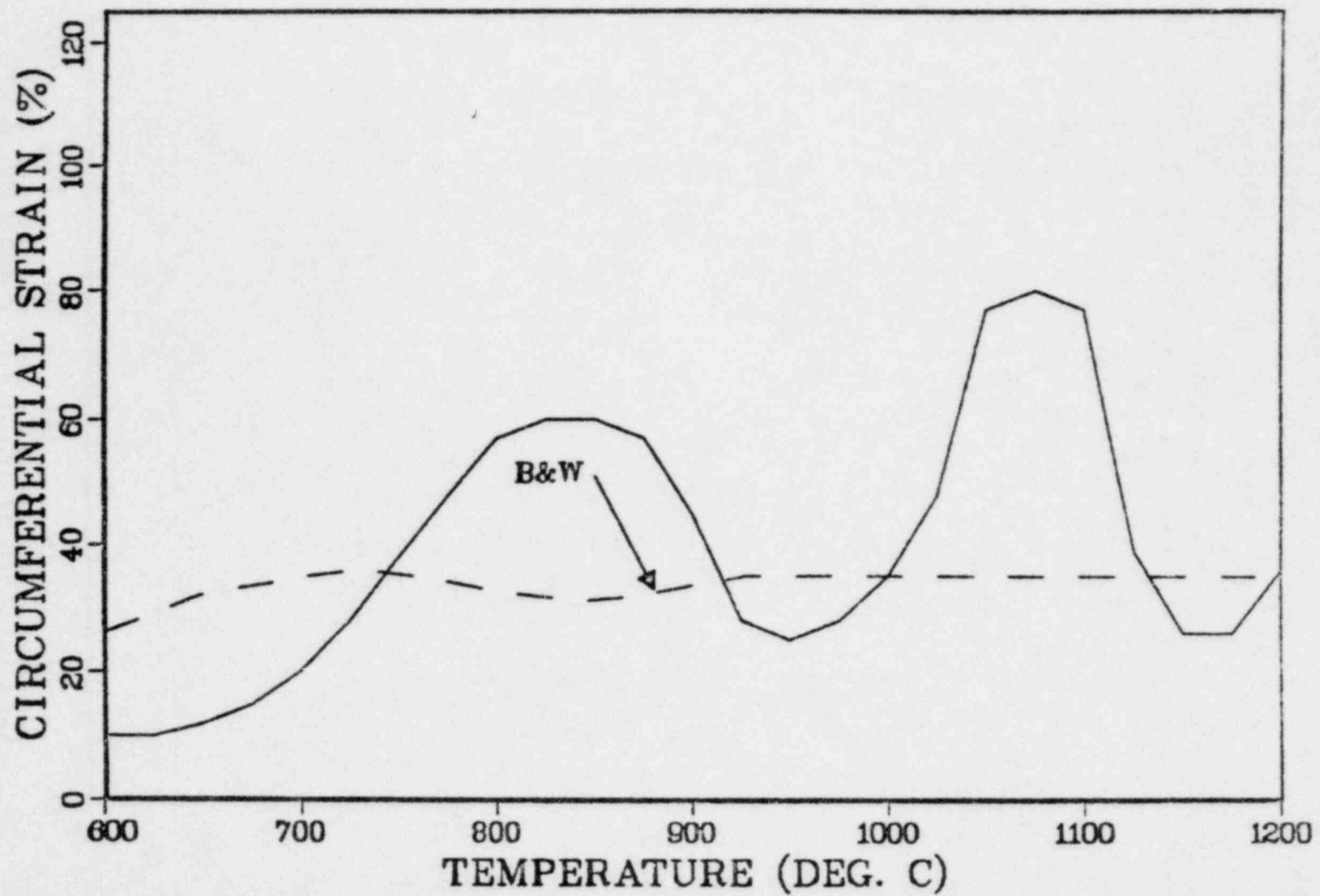


Fig. 26 B&W CRAFT model and fast-ramp correlation of circumferential burst strain as a function of rupture temperature.

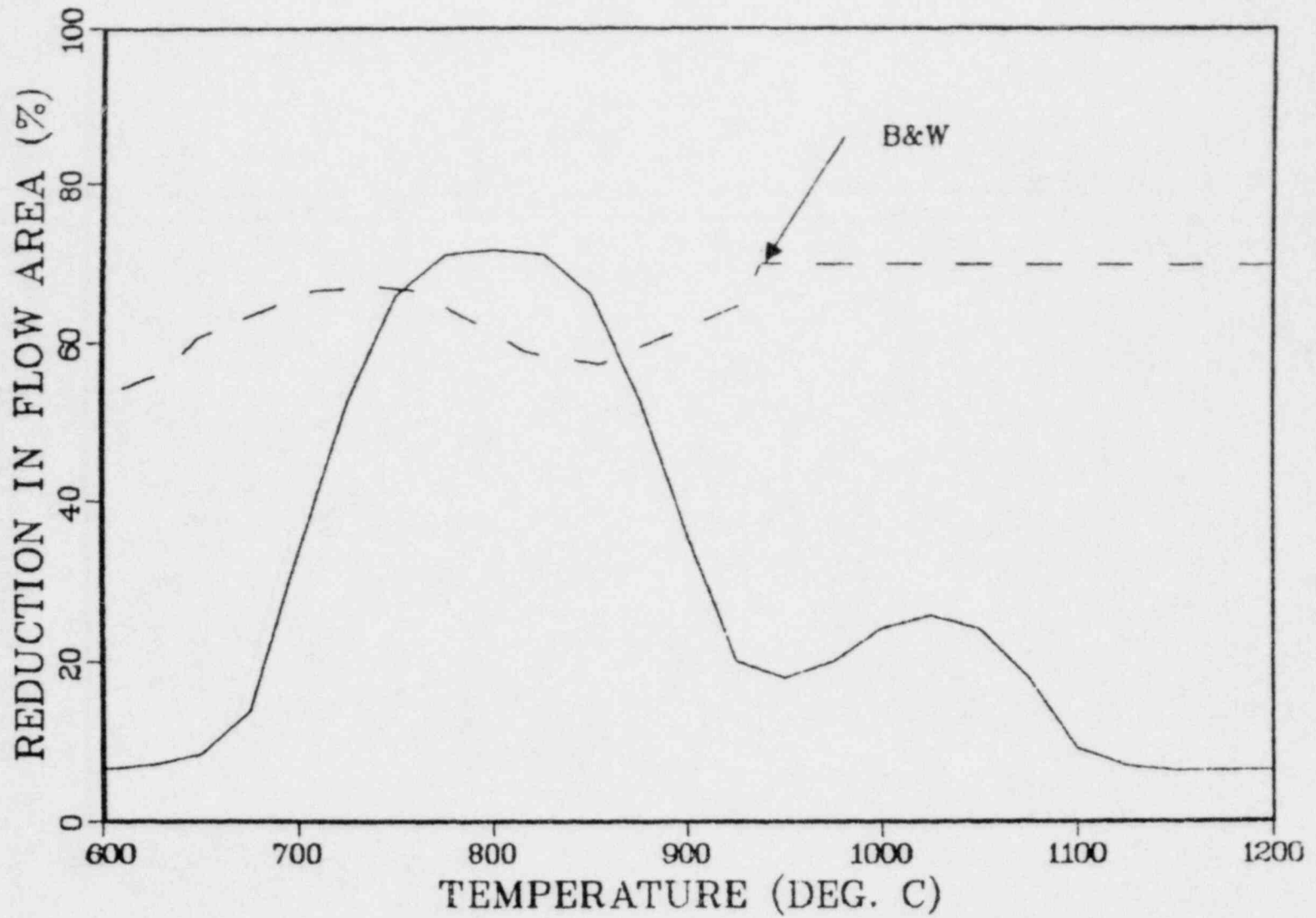


Fig. 27 B&W model and slow-ramp correlation of reduction in assembly flow area as a function of rupture temperature.

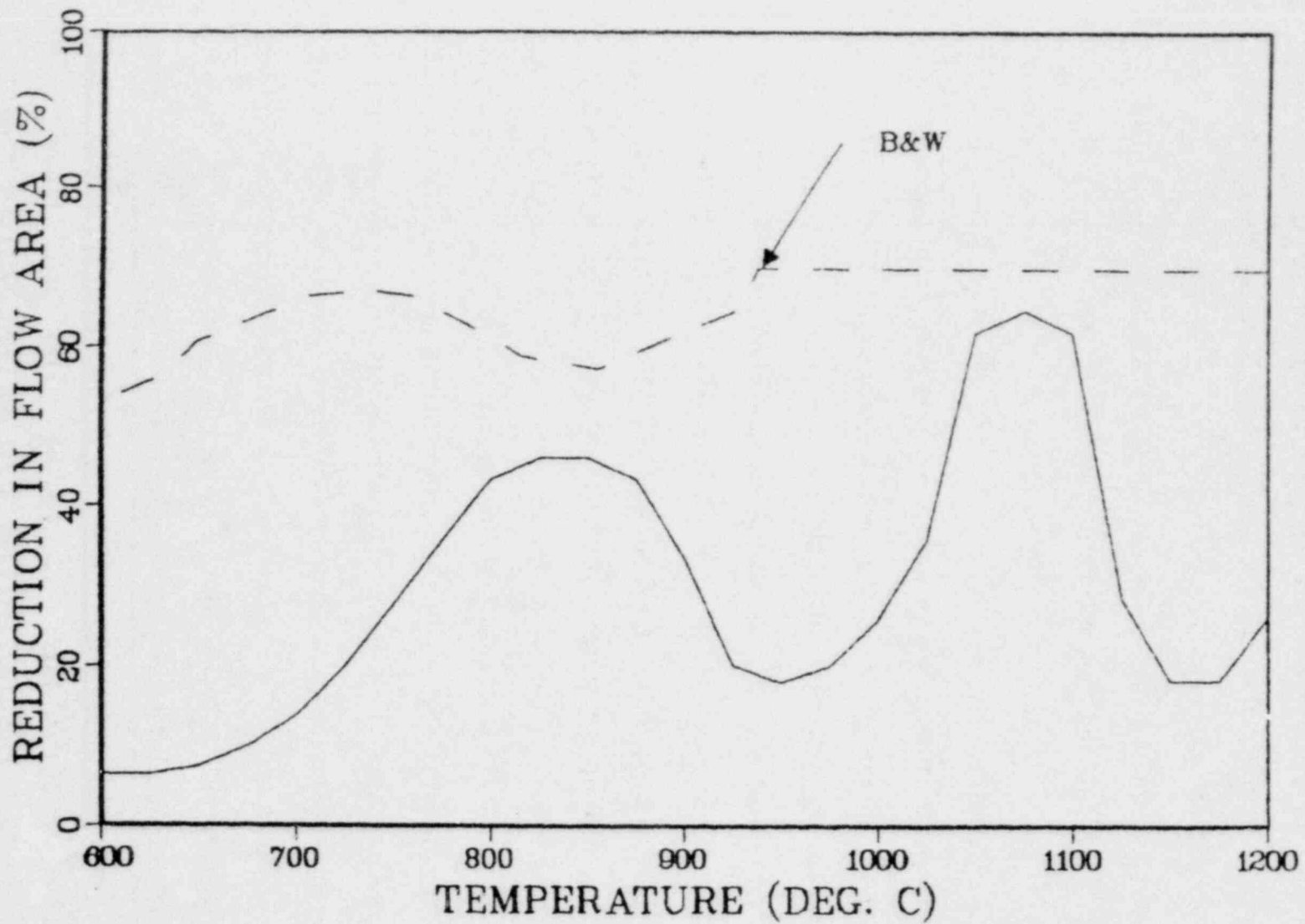


Fig. 28 R&W model and fast-ramp correlation of reduction in assembly flow area as a function of rupture temperature.



and significantly underpredict the degree of swelling at some temperatures. Although the B&W flow blockage model (Figs. 27-28) does not agree well with the current correlations, the B&W model overpredicts blockage for fast ramps over a wide range of temperatures and only modestly underpredicts blockage for slow ramps in the alpha-phase superplastic region.

#### 4.3 Combustion Engineering

Figures 29-33 show the presently approved Combustion Engineering models. Figure 29 shows the rupture temperature model, which is, in general, in only fair agreement with our present correlation. On the basis of the very low strains and blockages shown in Figs. 30-33, the NRC required C-E in March 1978 to reevaluate their ECCS analyses using larger burst strains and flow blockages (Ref. 39). Using some of the guidance that we provided for the strain and blockage models, C-E submitted the proposed models (Ref. 40) shown in Figs. 34-37 (the beta-phase region was not modeled in accordance with our guidelines). In that submittal C-E proposed that previously unused conservatisms in heat-transfer models compensated for the larger strains and blockages in their proposed models. The proposed C-E models are in fair agreement with the present correlations over wide temperature ranges (Figs. 35-36), but they underpredict the present correlations at low temperatures for slow ramps (Fig. 34) and over some temperature ranges for fast ramps (Fig. 35 and 37).

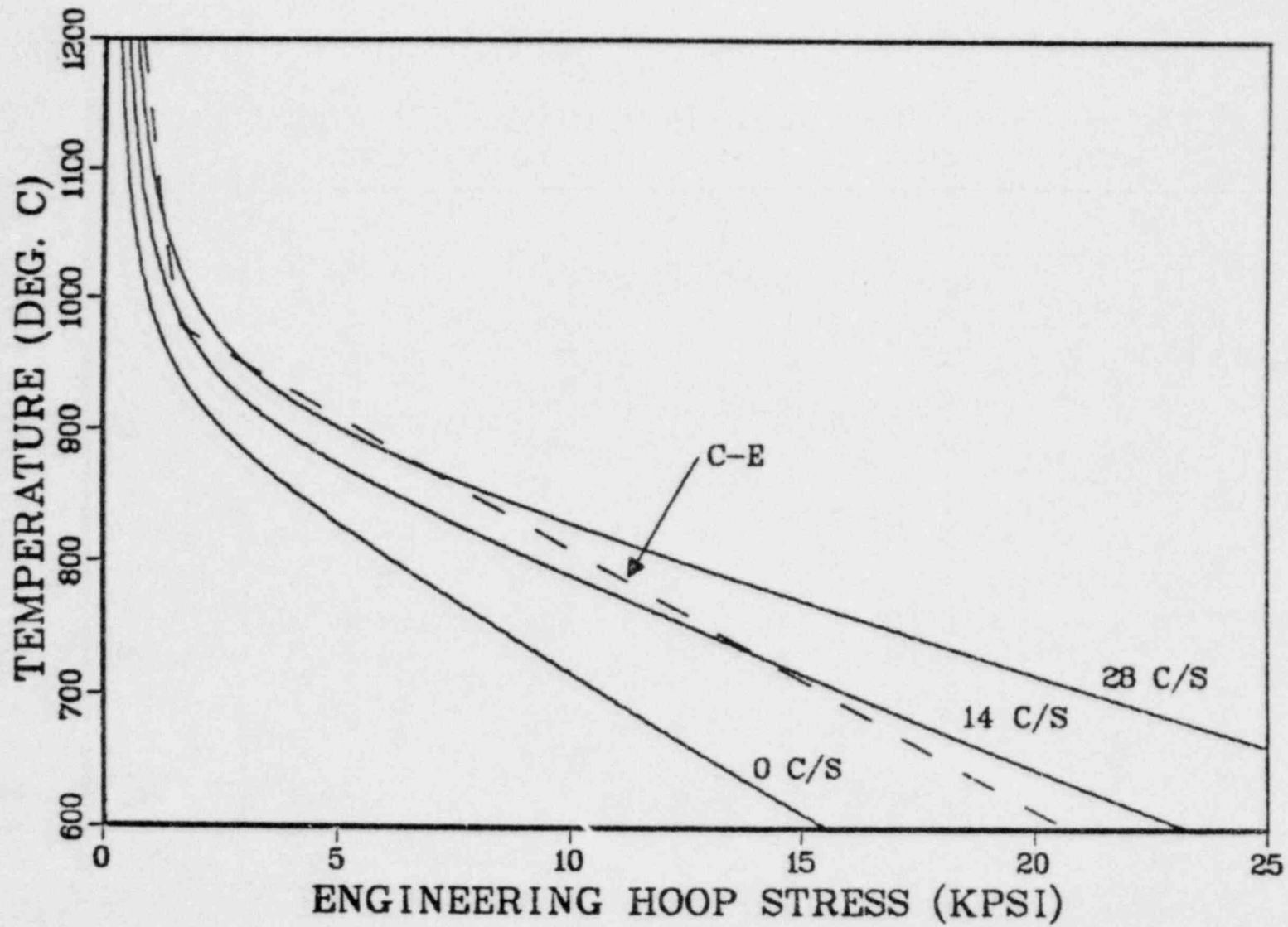


Fig. 29 C-E model and ORNL correlation of rupture temperature as a function of engineering hoop stress and ramp rate.

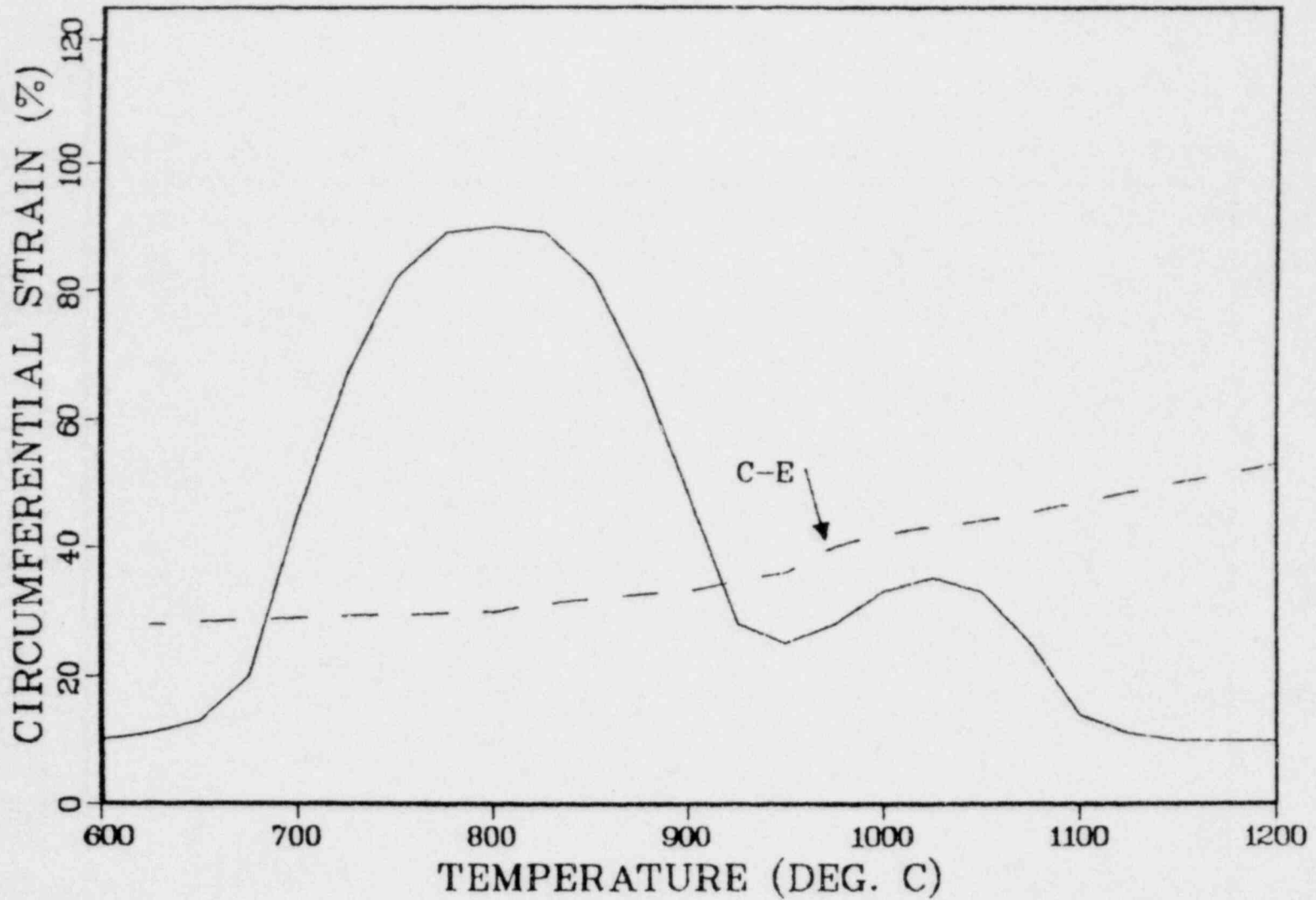


Fig. 30 C-E model and slow-ramp correlation of circumferential burst strain as a function of rupture temperature.

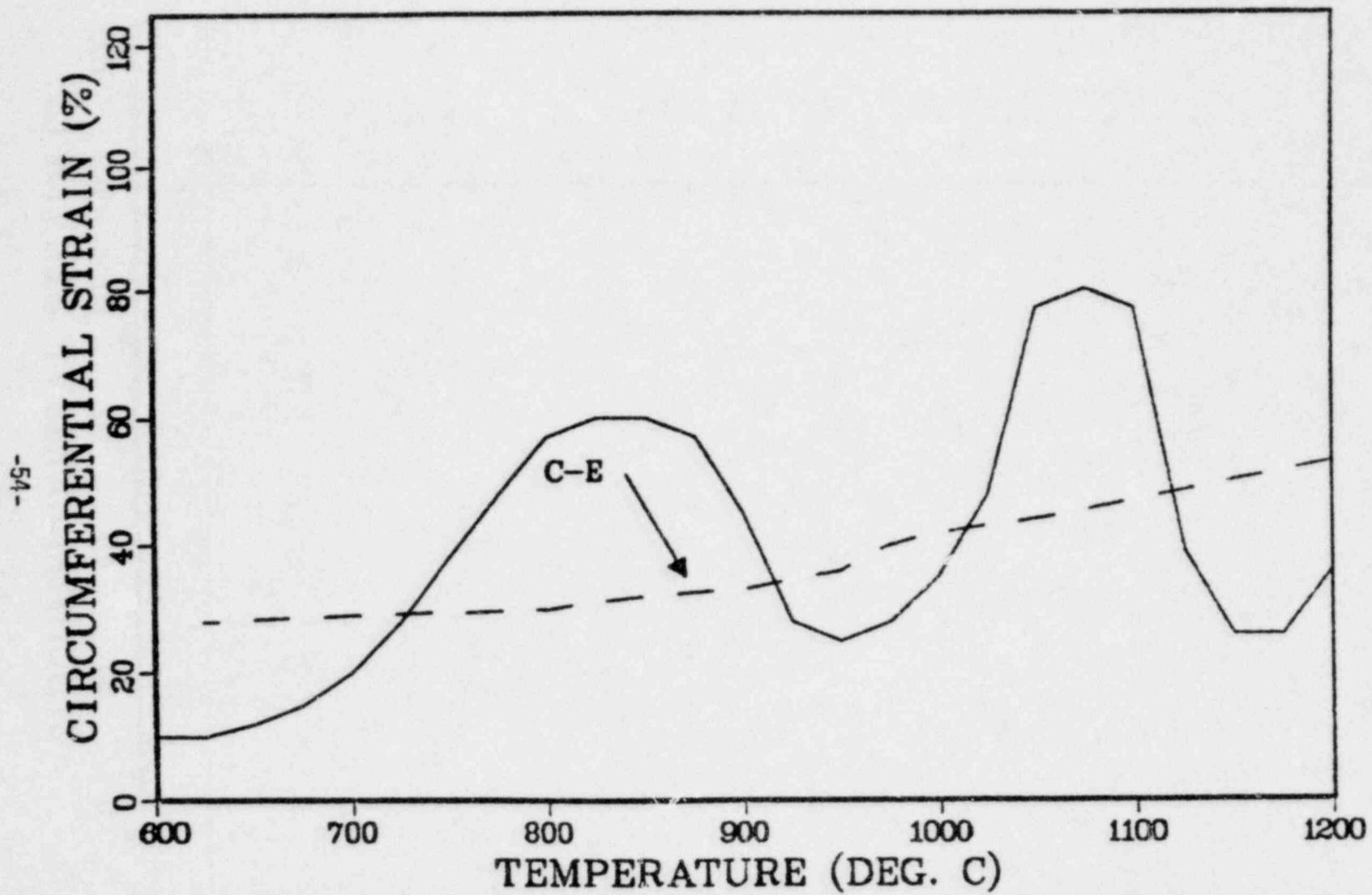


Fig. 31 C-E model and fast-ramp correlation of circumferential burst strain as a function of rupture temperature.

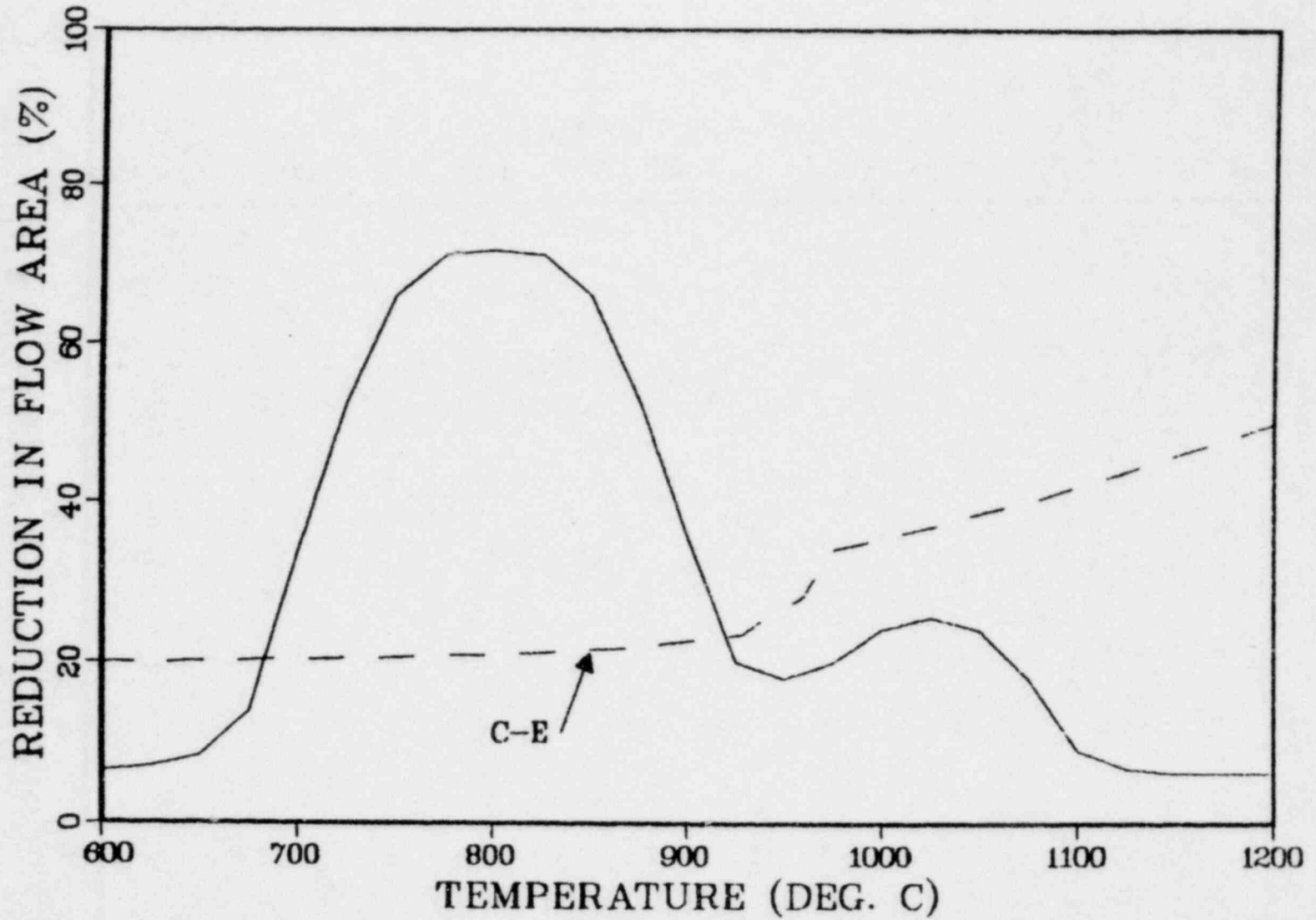


Fig. 32 C-E model and slow-ramp correlation of reduction in assembly flow area as a function of rupture temperature.

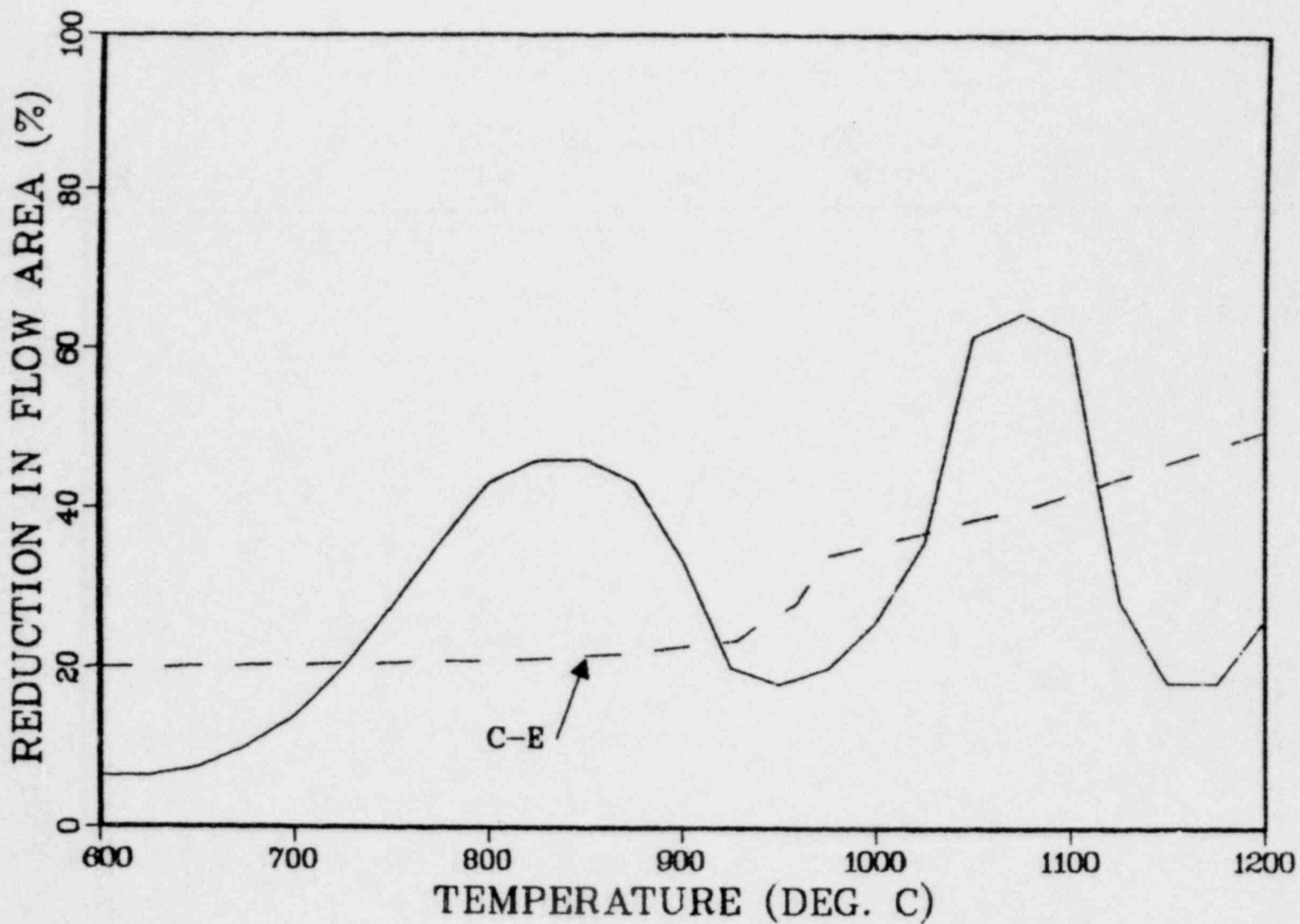


Fig. 33 C-E model and fast-ramp correlation of reduction in assembly flow area as a function of rupture temperature.

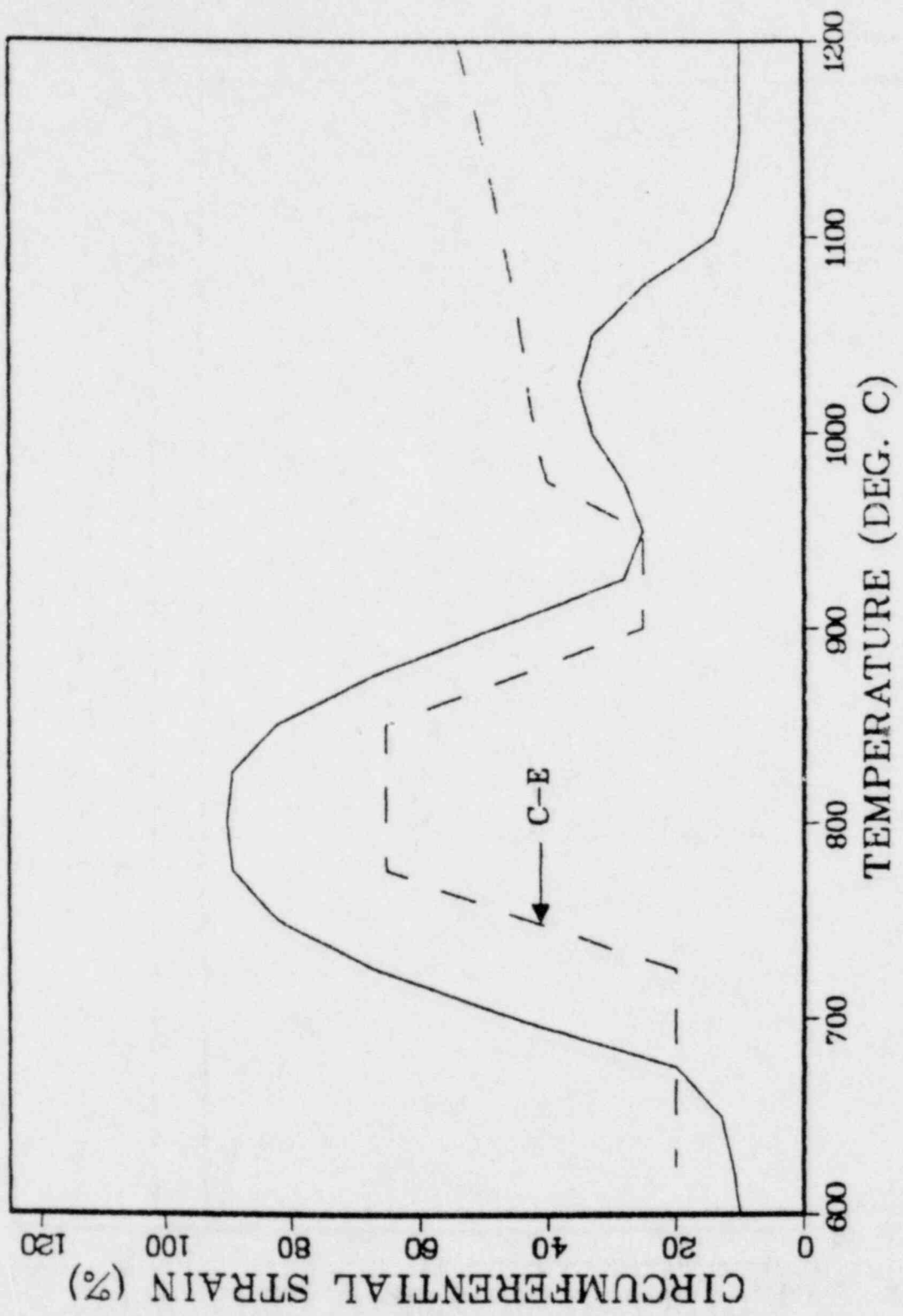


Fig. 34 C-E proposed model and slow-ramp correlation of circumferential burst strain as a function of rupture temperature.

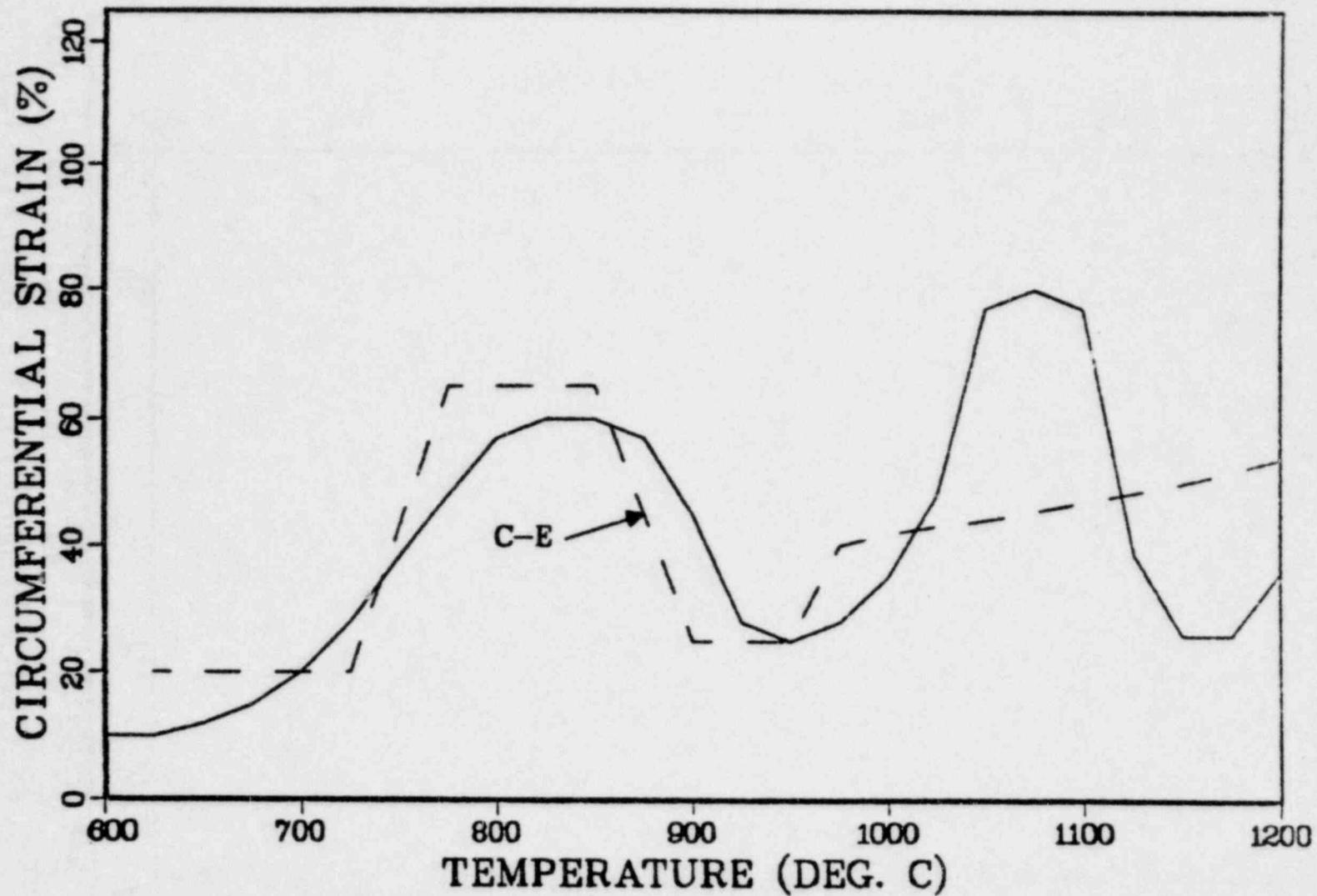


Fig. 35 C-E proposed model and fast-ramp correlation of circumferential burst strain as a function of rupture temperature.



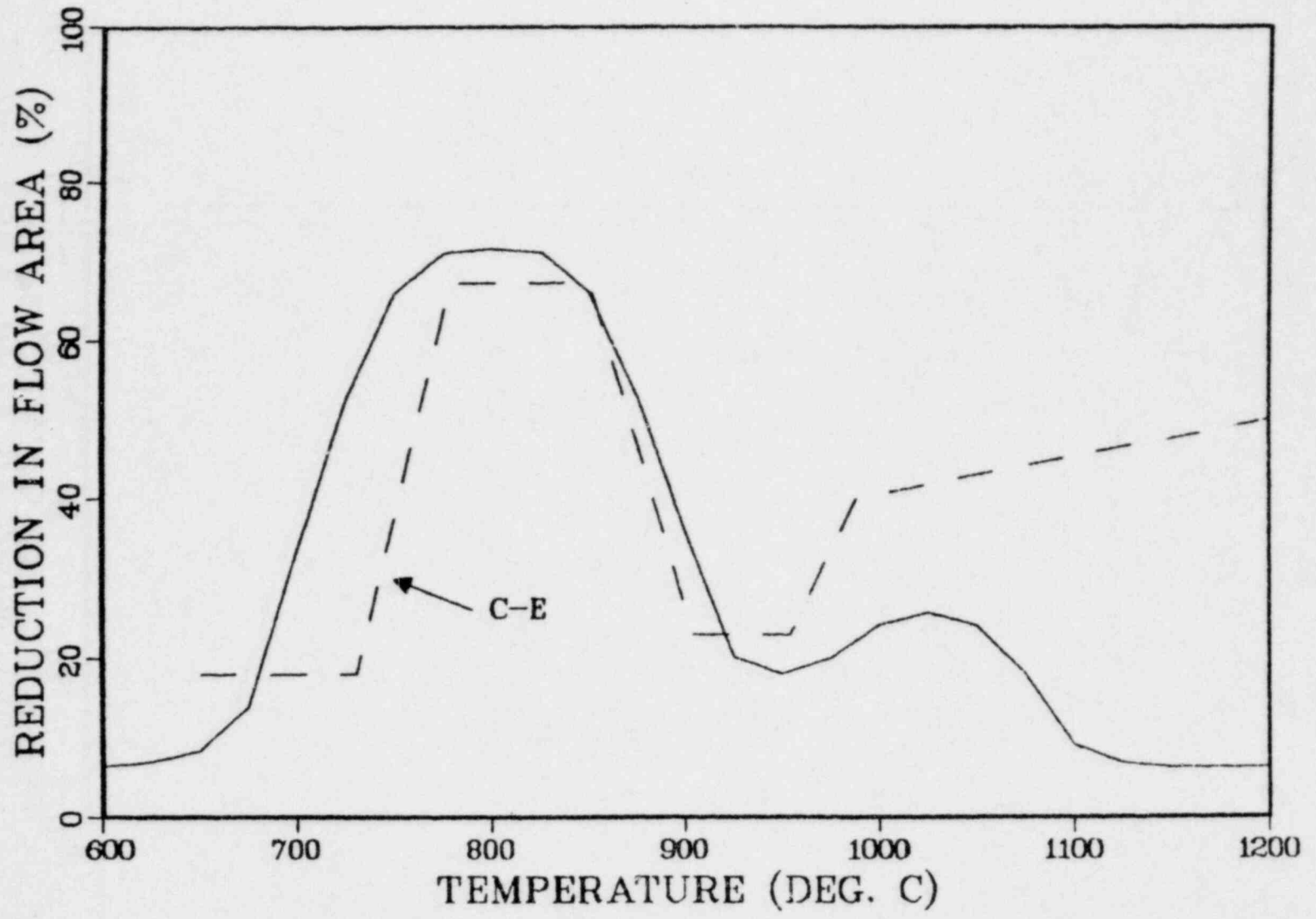


Fig. 36 C-E proposed model and slow-ramp correlation of reduction in assembly flow area as a function of rupture temperature.

-09-

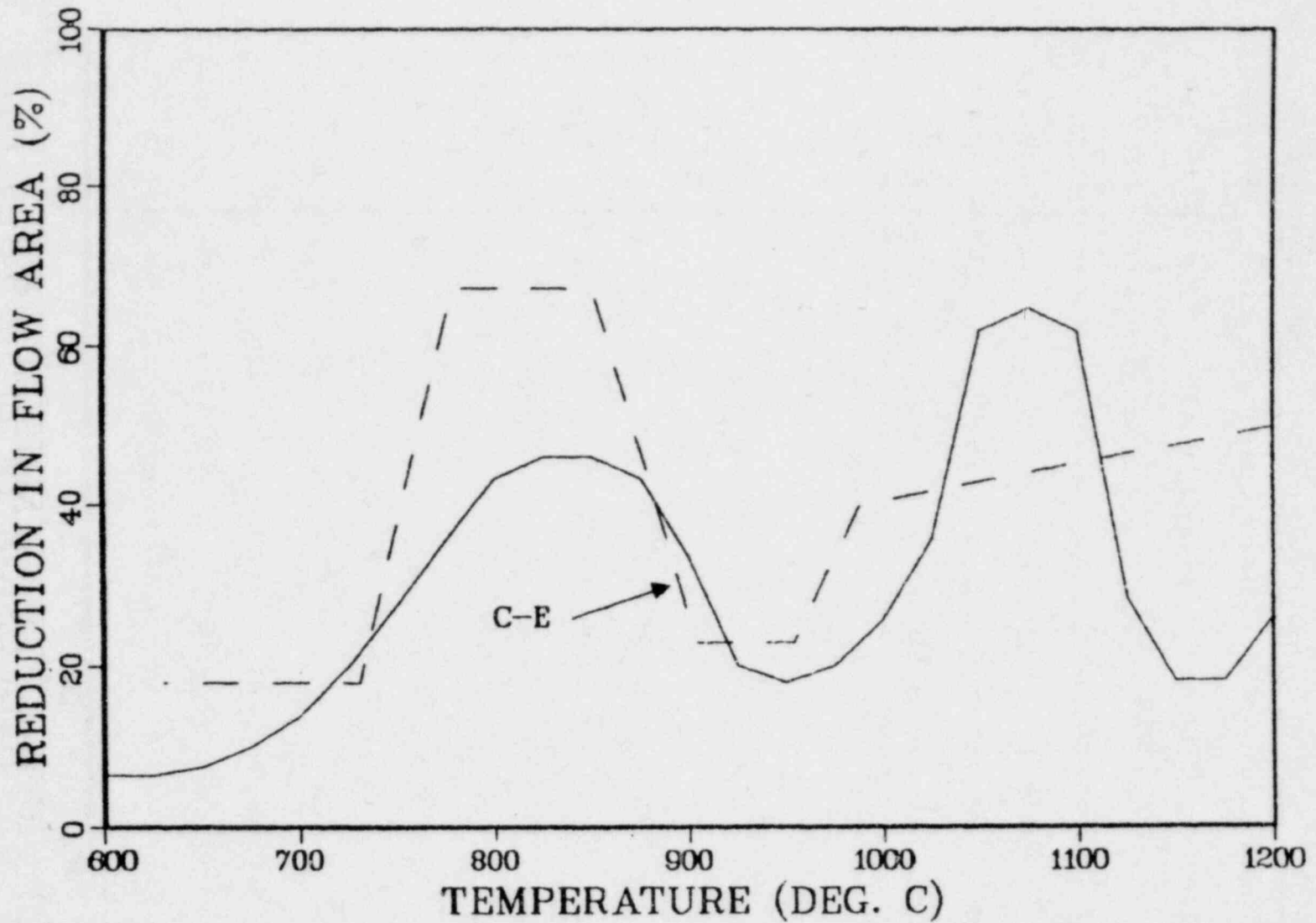


Fig. 37 C-E proposed model and fast-ramp correlation of reduction in assembly flow area as a function of rupture temperature.

#### 4.4 Westinghouse

Figures 38-43 show the Westinghouse models. For small-break analyses, Westinghouse accounts for ramp-rate effects on rupture temperature in a manner similar to our present correlation (Fig. 38); the large-break Westinghouse model is similar to the present fast-ramp correlation (Fig. 39). The Westinghouse burst-strain model (shown in Figs. 40-41) is similar to the WREM burst-strain model but approximates the present correlation only at temperatures near 950°C (Figs. 40-41). The Westinghouse flow blockage model (shown in Figs. 42-43) exhibits significantly smaller blockages than either WREM or the present correlation over large temperature ranges for both slow- and fast-ramp rates.

#### 4.5 General Electric

Figures 44-46 show the General Electric models. Figure 44 exhibits substantial underprediction of the incidence of rupture at high stresses (pressure differentials), but the high stress portion of this curve is not relevant for BWR fuel rods since they are pressurized to a much lesser extent than PWR fuel rods.

For temperatures above 925°C and for slow ramps, the conditions appropriate for BWRs, the GE burst strain model predicts strains as much as 10 to 15% lower than the present correlation (Fig. 45). The fast-ramp comparison in Fig. 46 is probably not relevant, but is shown for completeness.

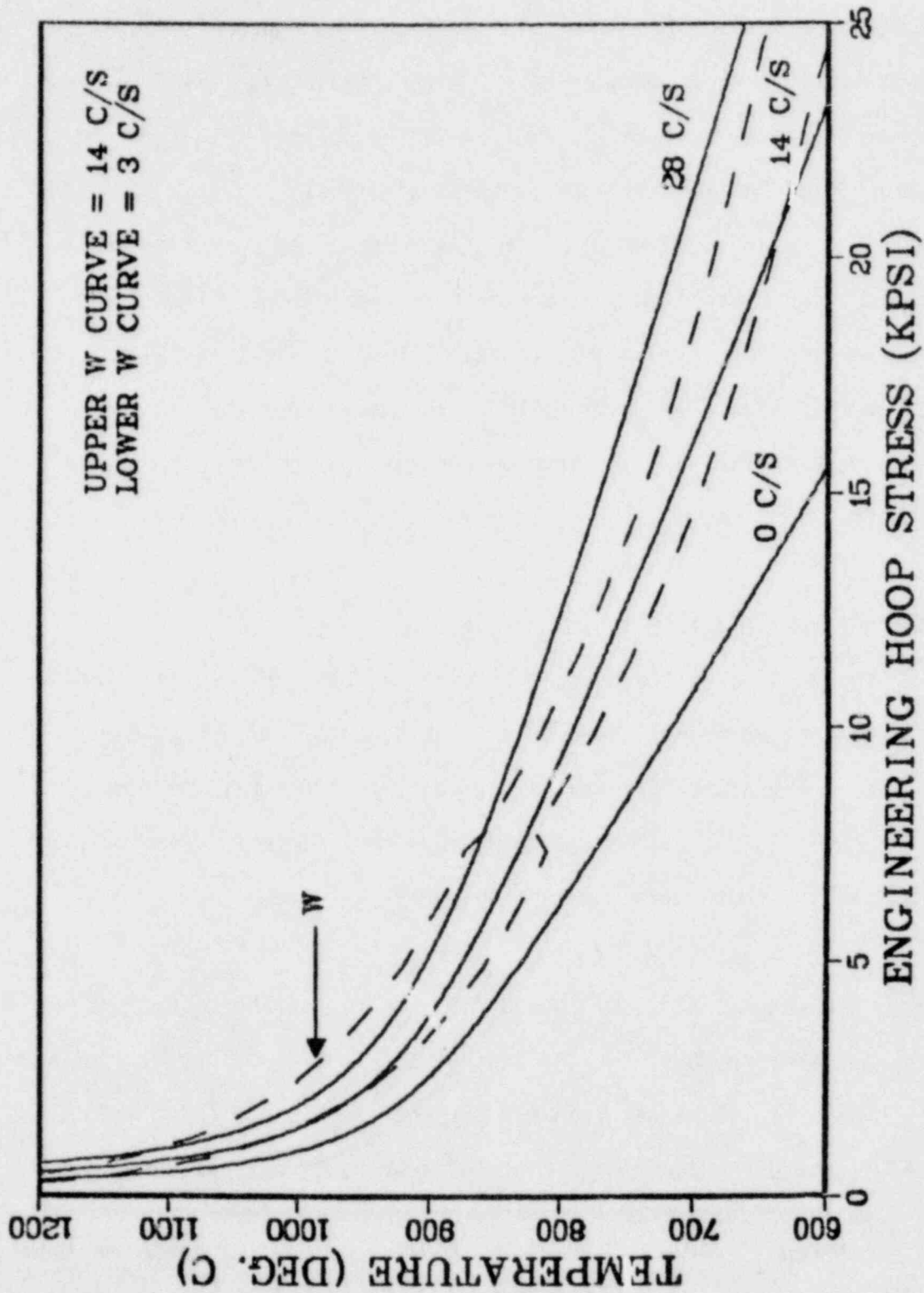


Fig. 38 W small-break model and ORNL correlation of rupture temperature as a function of engineering hoop stress and ramp rate.

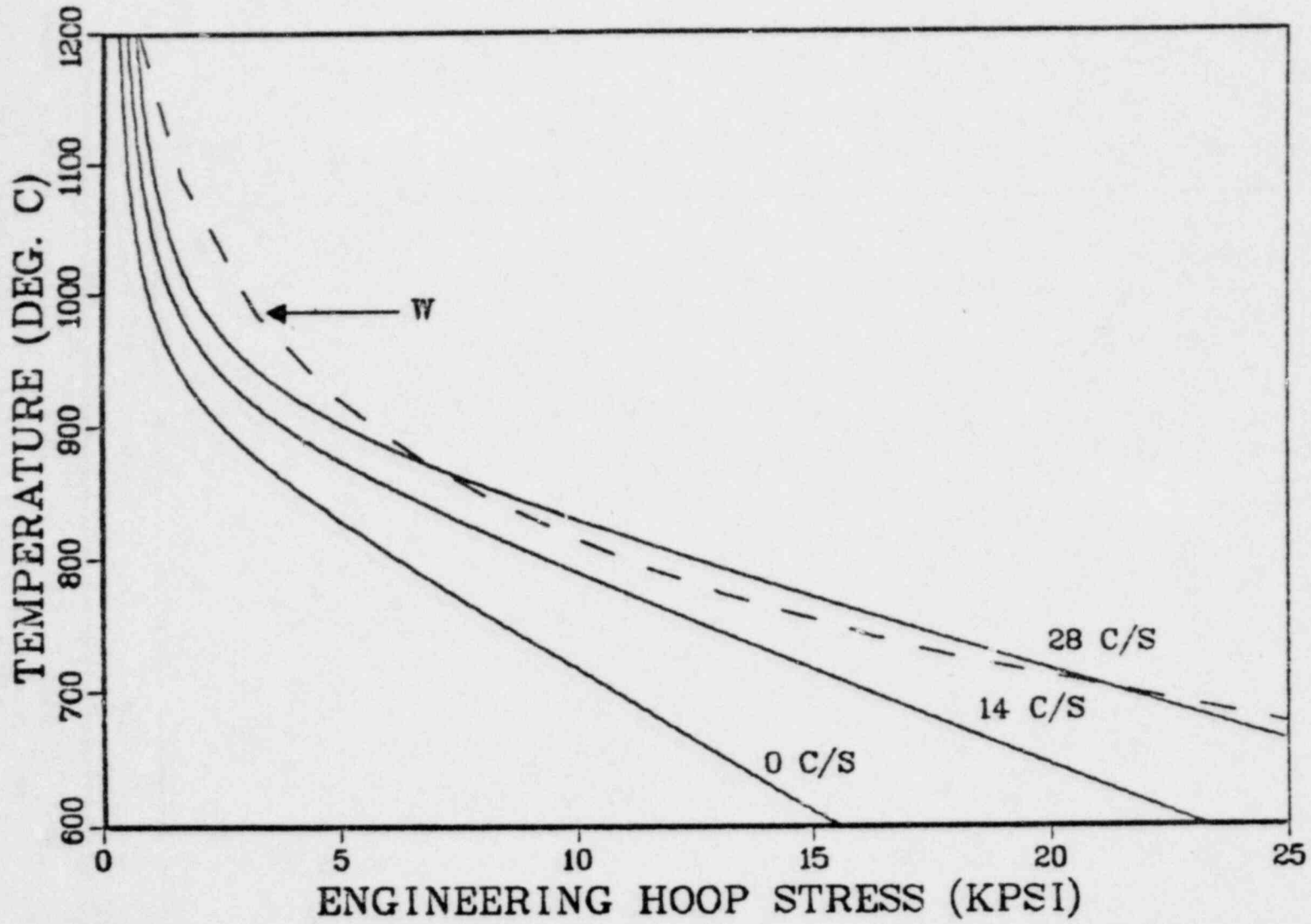


Fig. 39 W large-break model and ORNL correlation of rupture temperature as a function of engineering hoop stress and ramp rate.

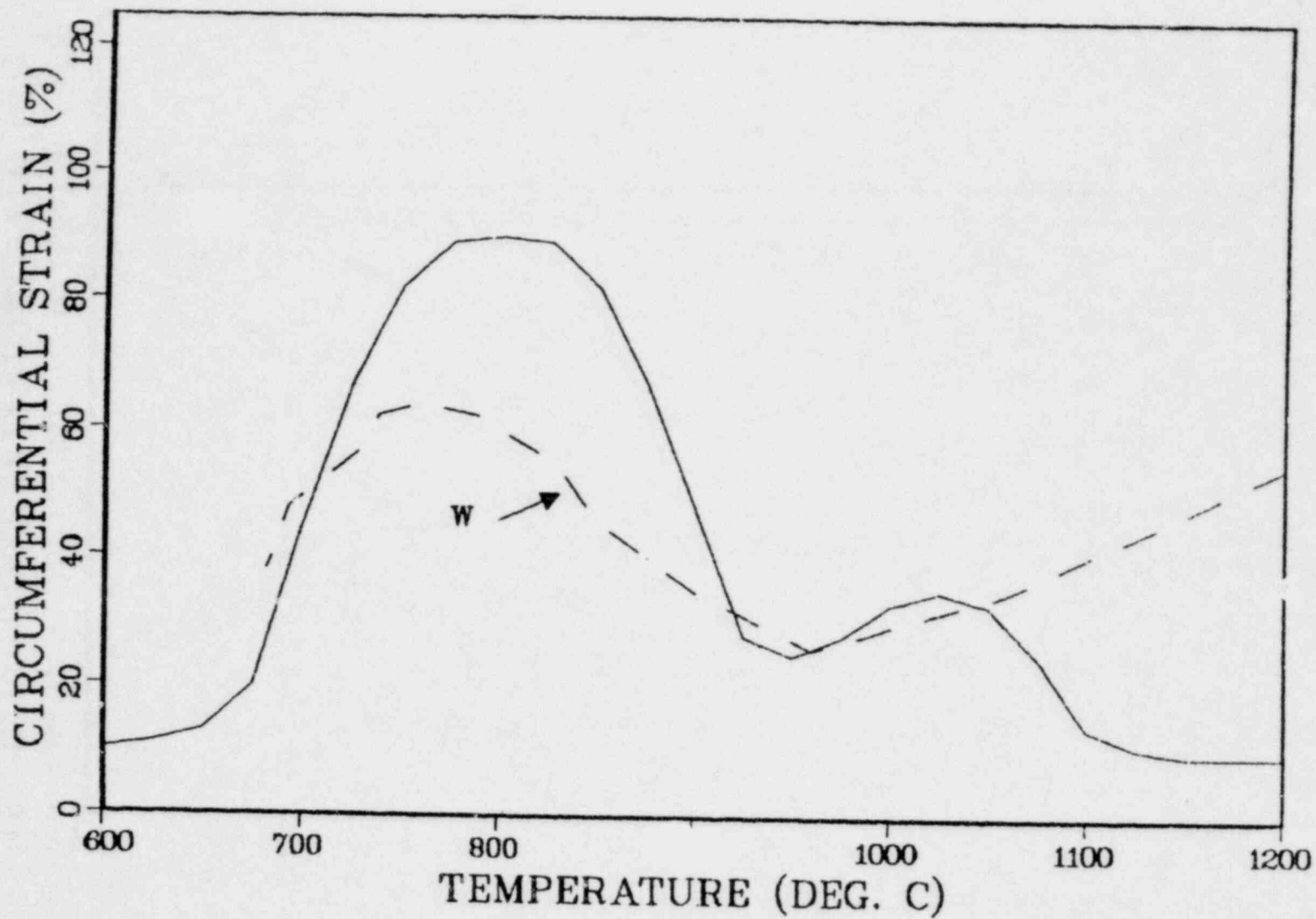


Fig. 40 W model and slow-ramp correlation of circumferential burst strain as a function of rupture temperature.

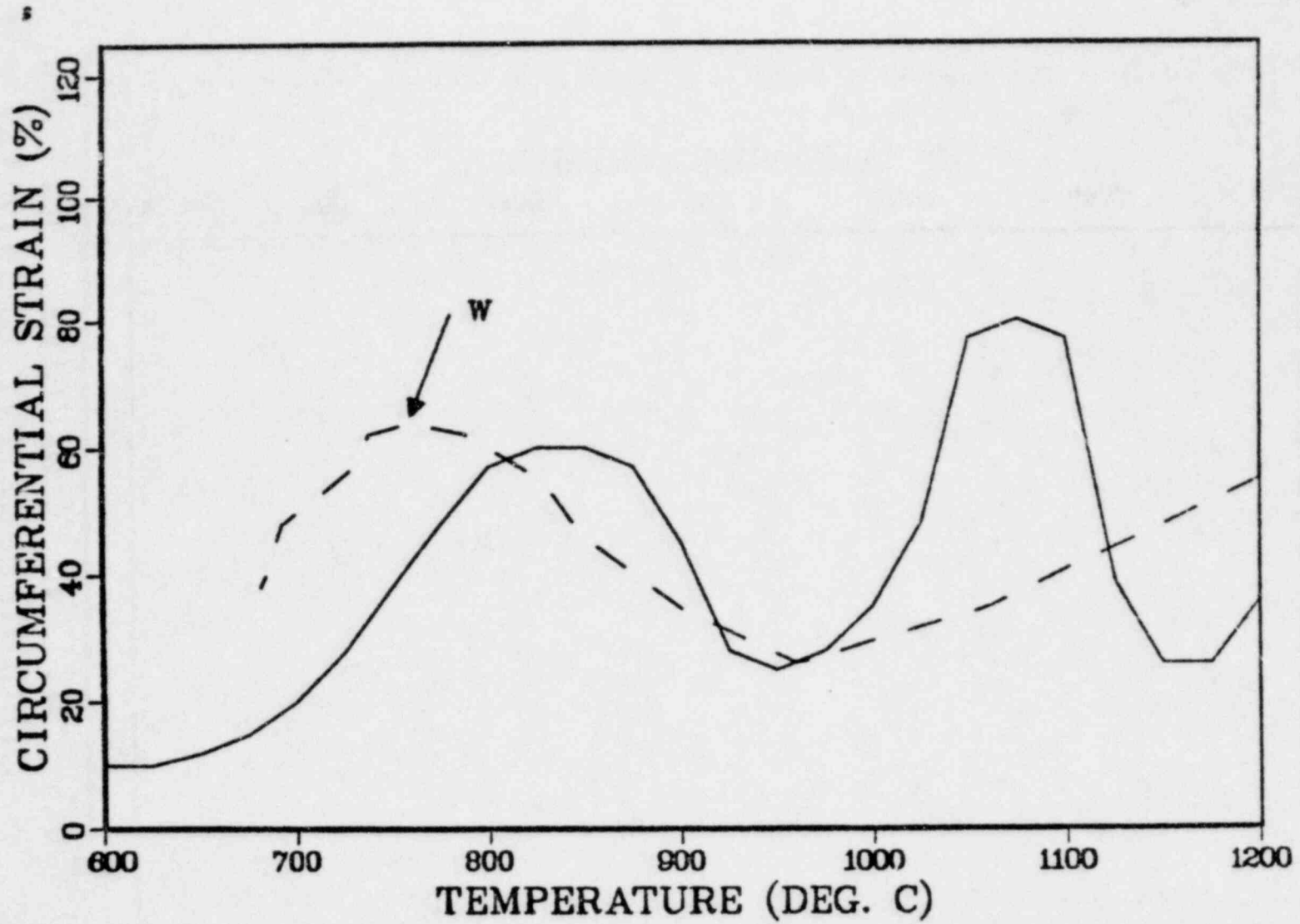


Fig. 41 W model and fast-ramp correlation of circumferential burst strain as a function of rupture temperature.

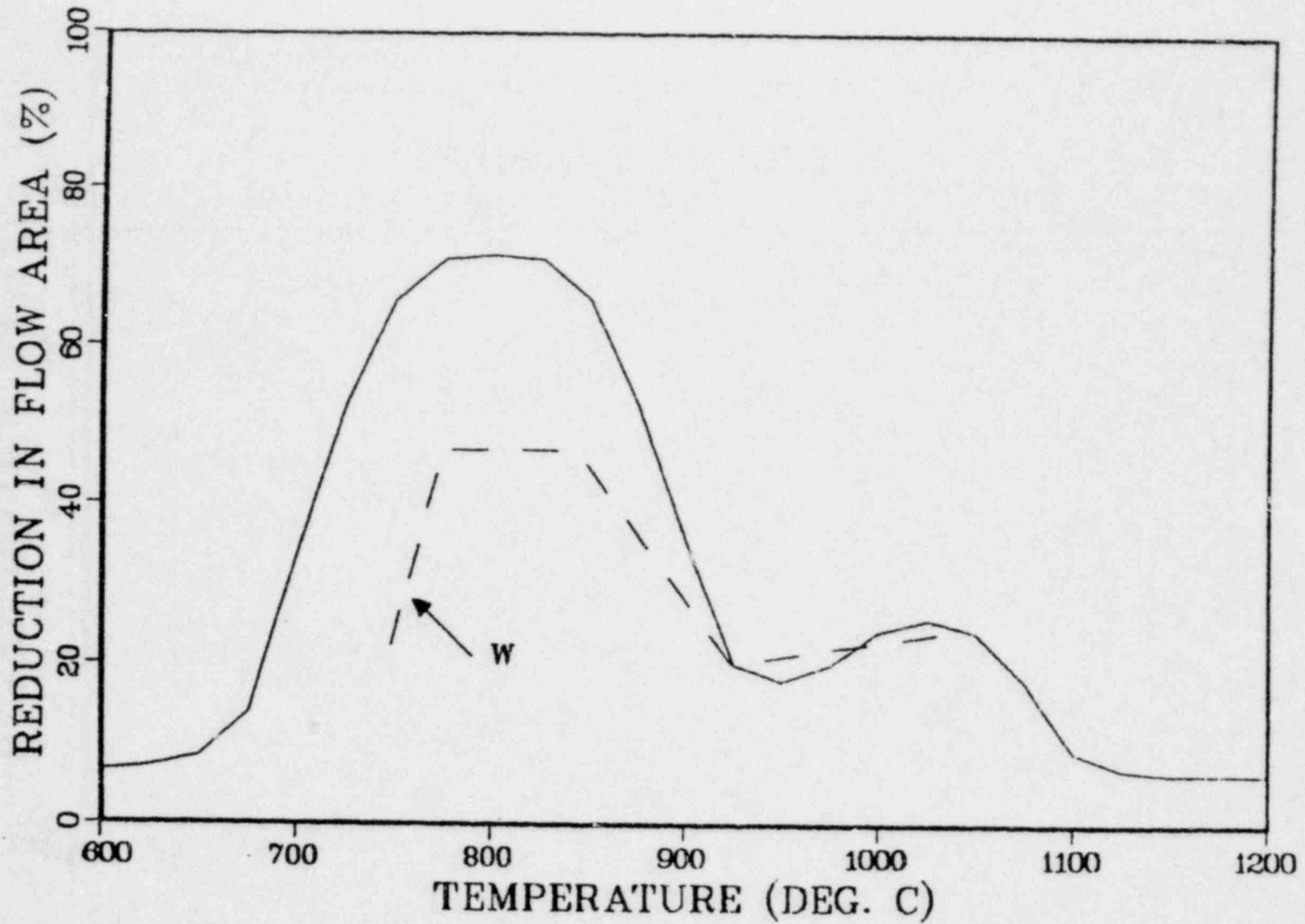


Fig. 42 W model and slow-ramp correlation of reduction in assembly flow area as a function of rupture temperature.



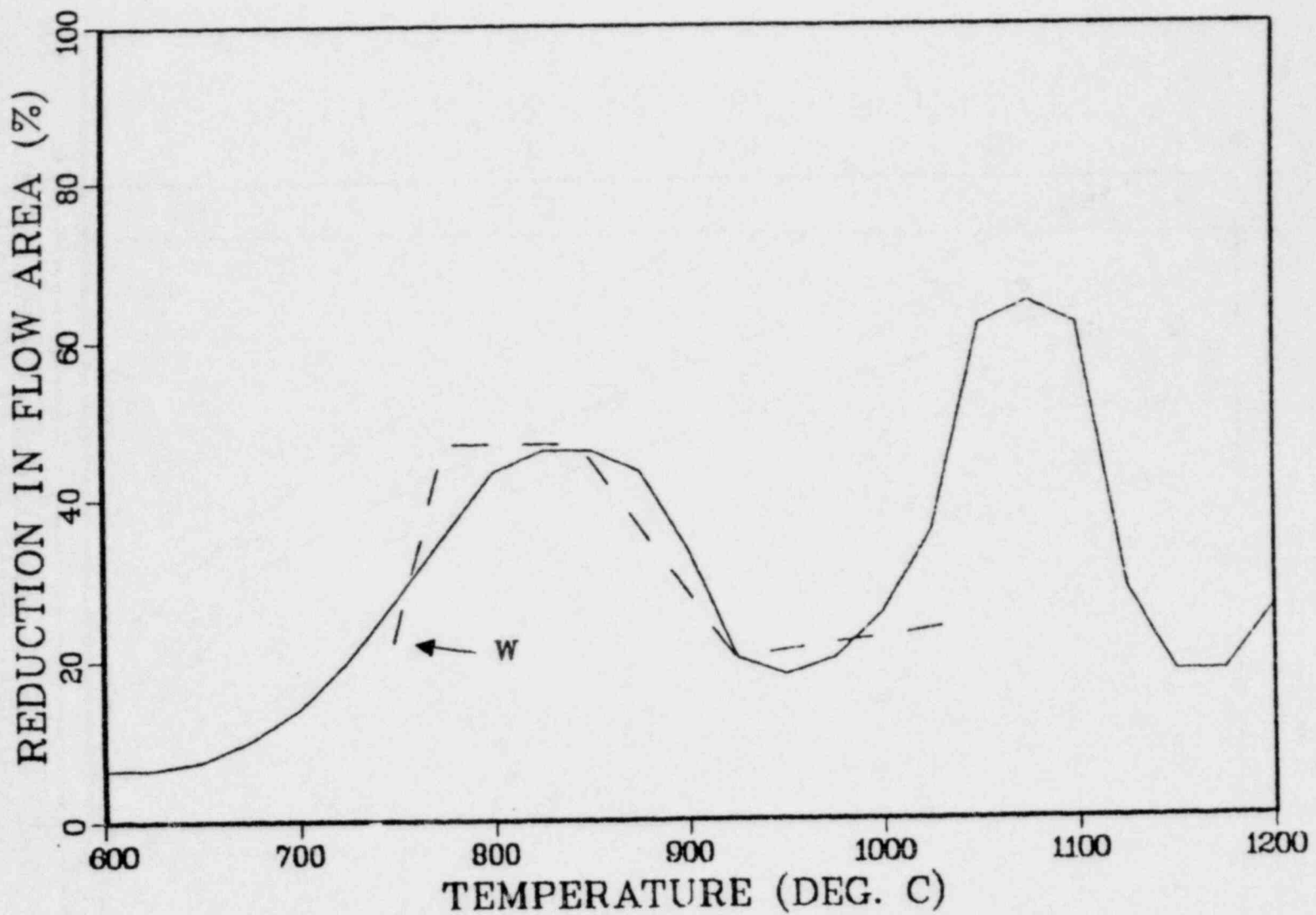


Fig. 43 W model and fast-ramp correlation of reduction in assembly flow area as a function of rupture temperature.

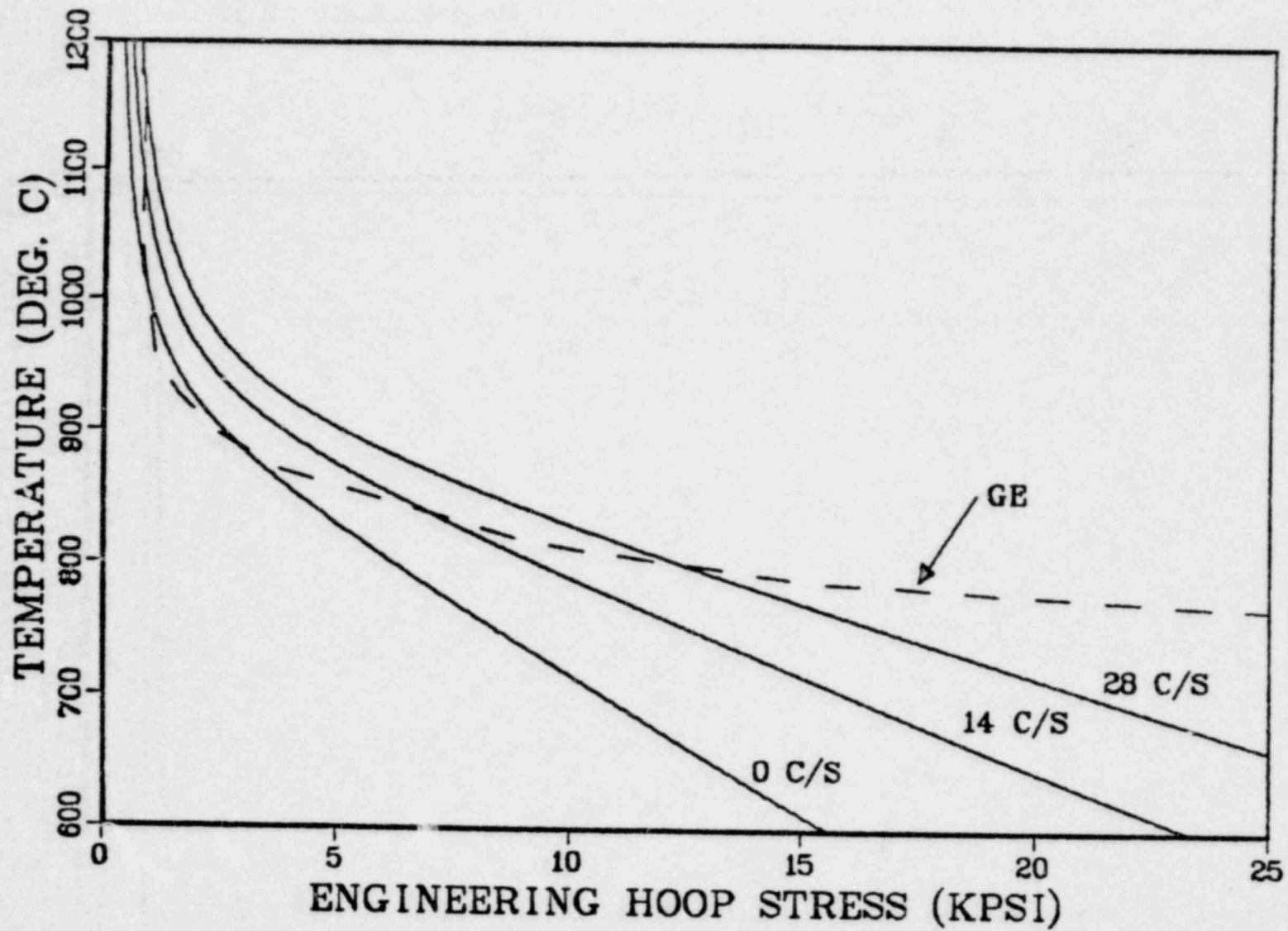


Fig. 44 GE model and ORNL correlation of rupture temperature as a function of engineering hoop stress and ramp rate.

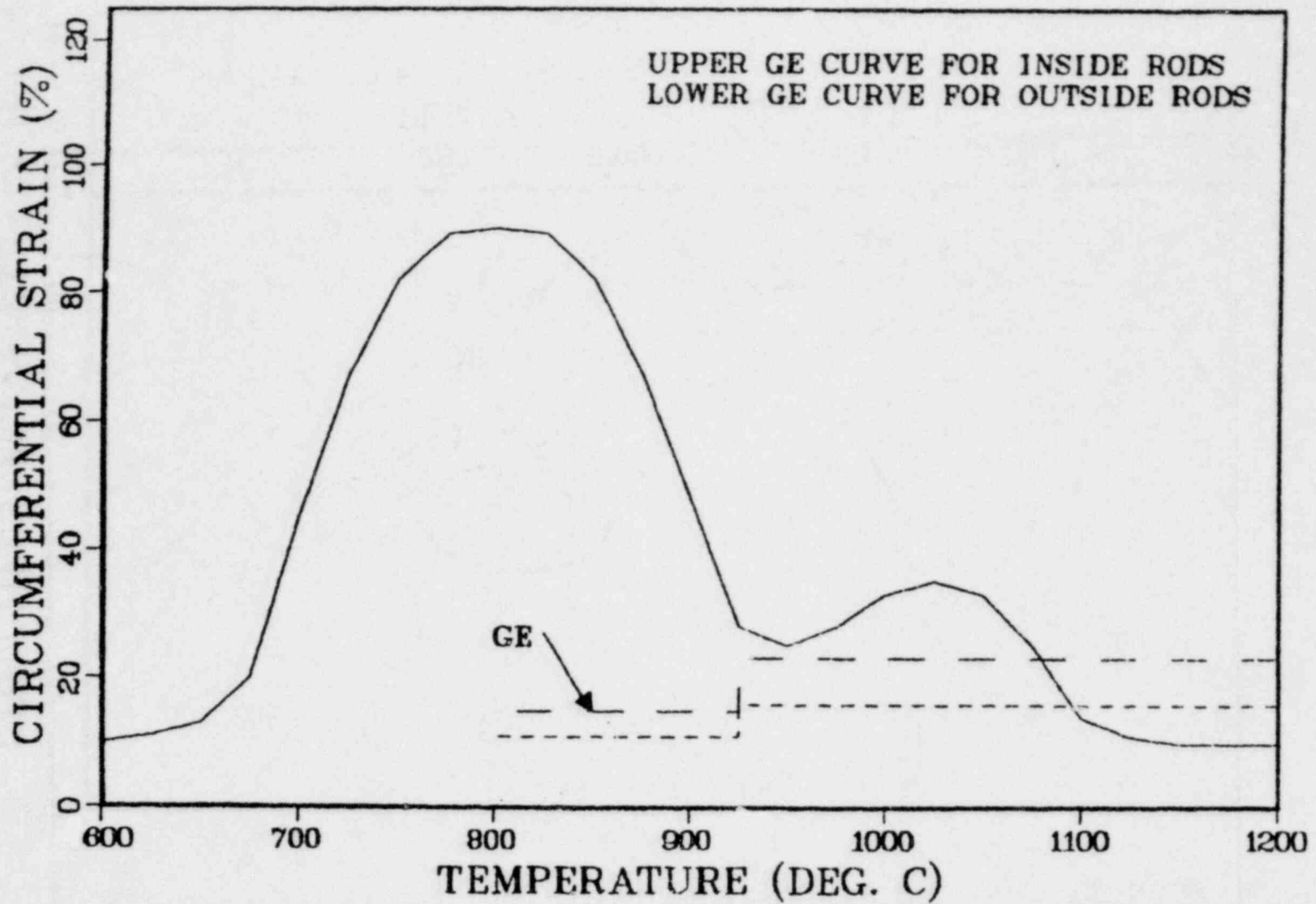


Fig. 45 GE model and slow-ramp correlation of circumferential burst strain as a function of rupture temperature.

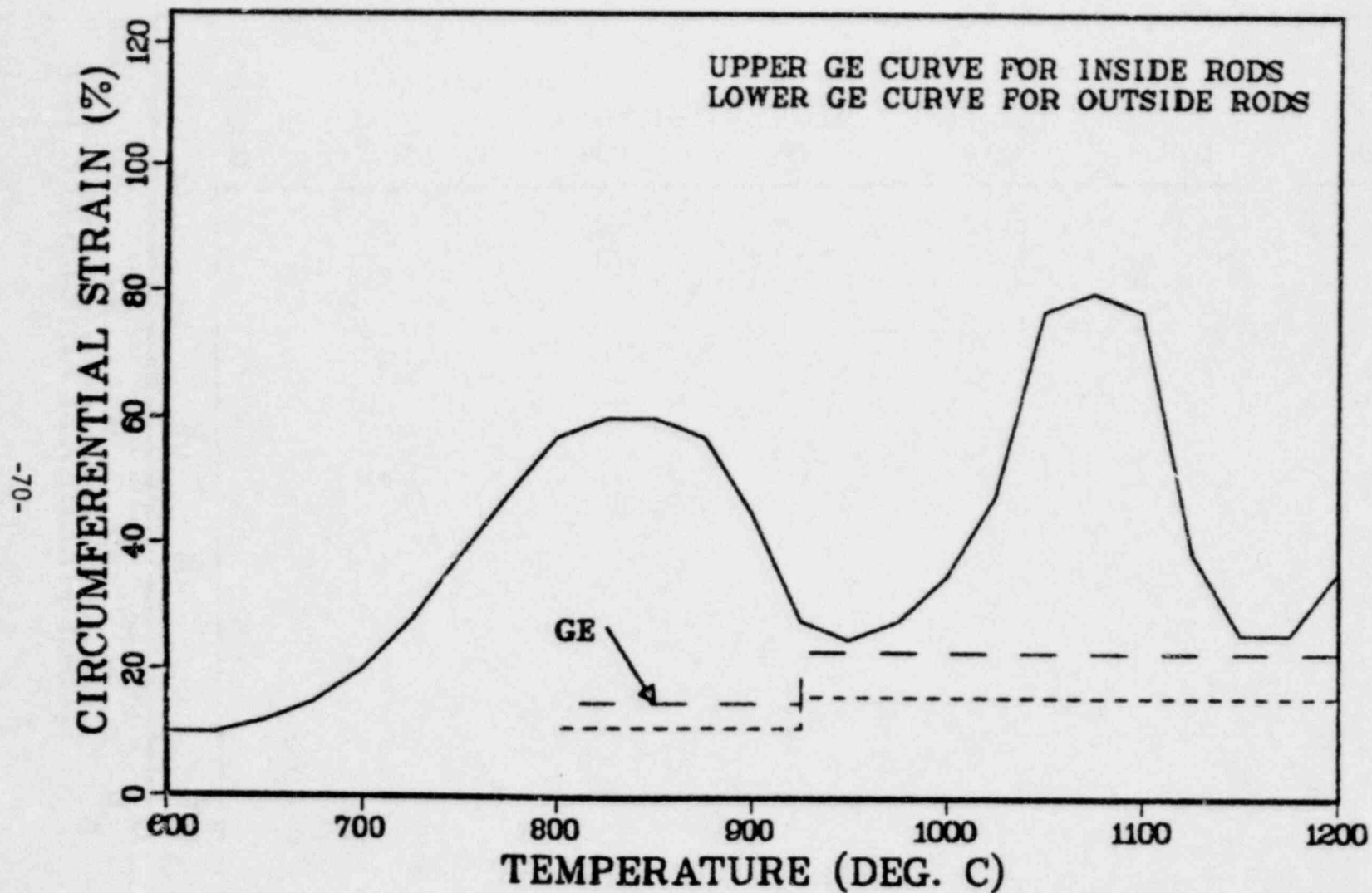


Fig. 46 GE model and fast-ramp correlation of circumferential burst strain as a function of rupture temperature.

Because of BWR spray cooling and a large amount of heat transfer by radiation (to the massive channel boxes), partial flow blockage is less important in BWRs than in PWRs, and GE does not employ a flow-blockage model in their ECCS analysis.

#### 4.6 Exxon

Exxon has different models for PWR and BWR applications. The PWR models are shown in Figs. 47-51.

The rupture temperature model is, like WREM, in good agreement with the present fast-ramp correlation. Although the Exxon PWR strain model exhibits a distinct alpha-plus-beta-phase valley, it differs substantially with the present correlations over a wide range of temperatures (Figs. 48-49). The Exxon PWR blockage model predicts blockages in several temperature ranges that are far larger than any predicted by the correlations presented in this report (Figs. 50-51).

The Exxon BWR models (Fig. 52-54) are similar to the GE models.

#### 4.7 Yankee Atomic Electric

The Yankee Atomic Electric Company performs the ECCS analysis for the Maine Yankee and Yankee Rowe plants. The cladding models employed in the Maine Yankee analysis are identical to the ENC PWR models displayed in Figs. 47-51.

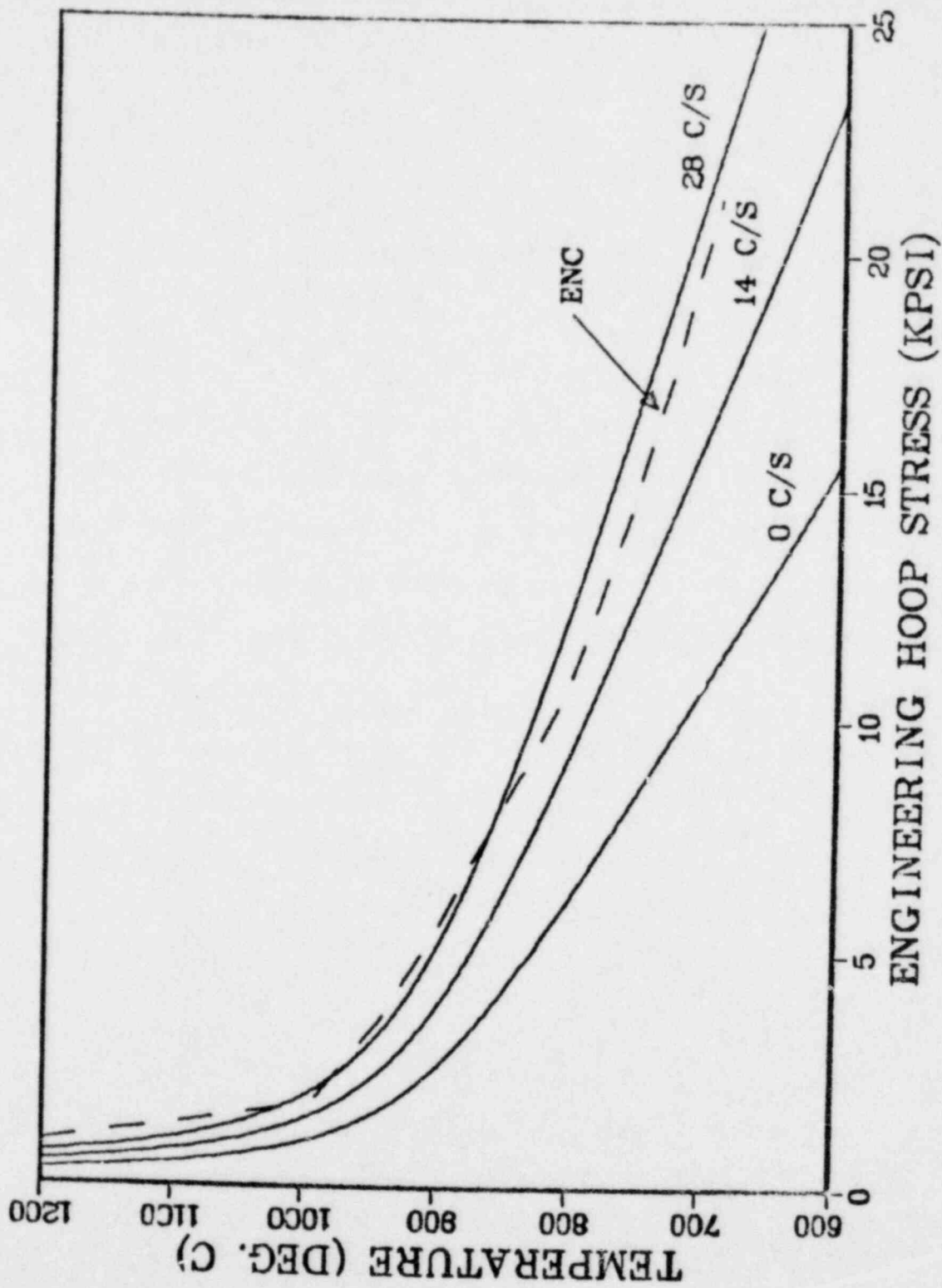


Fig. 47 ENC PWR model and ORNL correlation of rupture temperature as a function of engineering hoop stress and ramp rate.

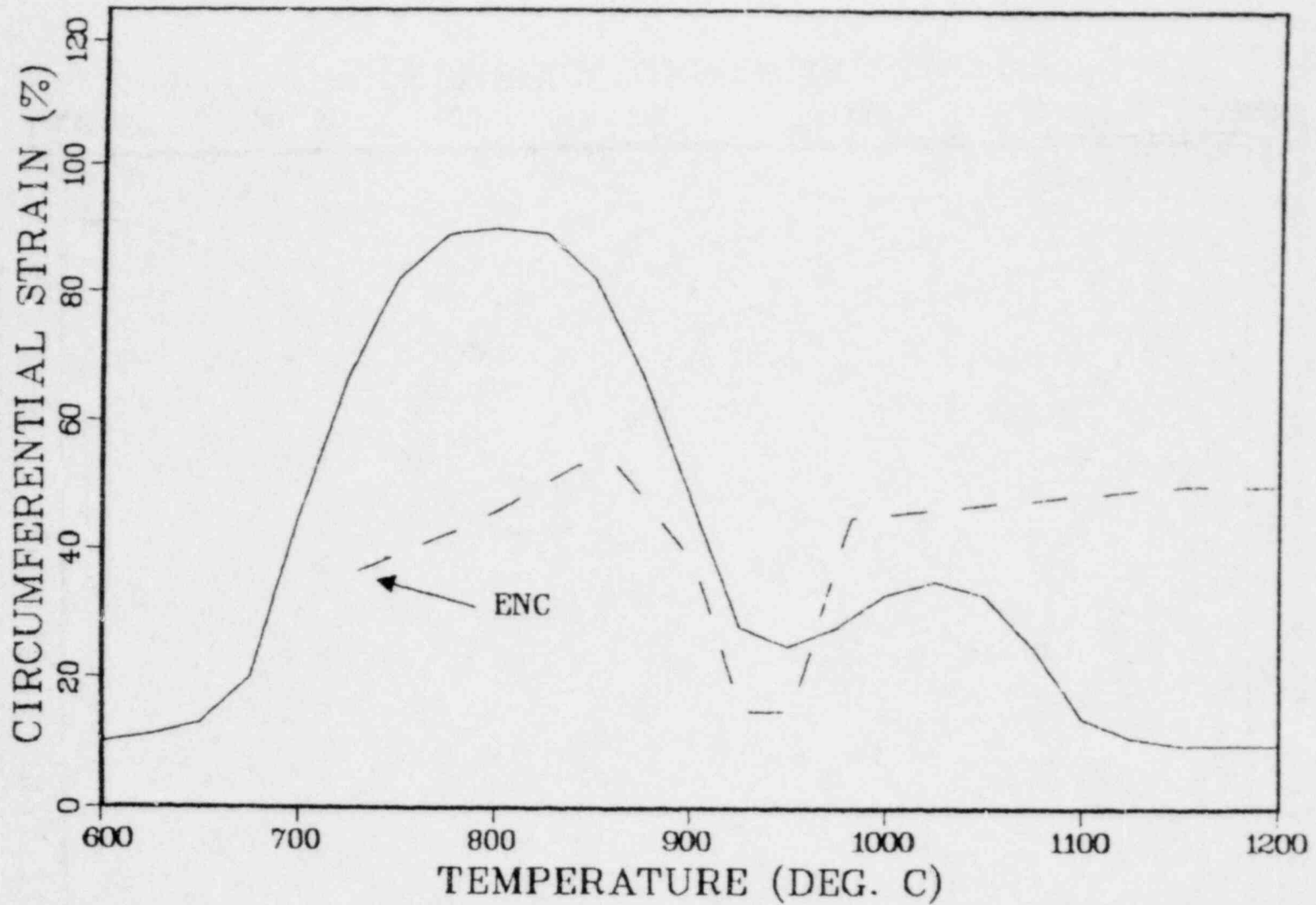


Fig. 48 ENC PWR model and slow-ramp correlation of circumferential burst strain as a function of rupture temperature.

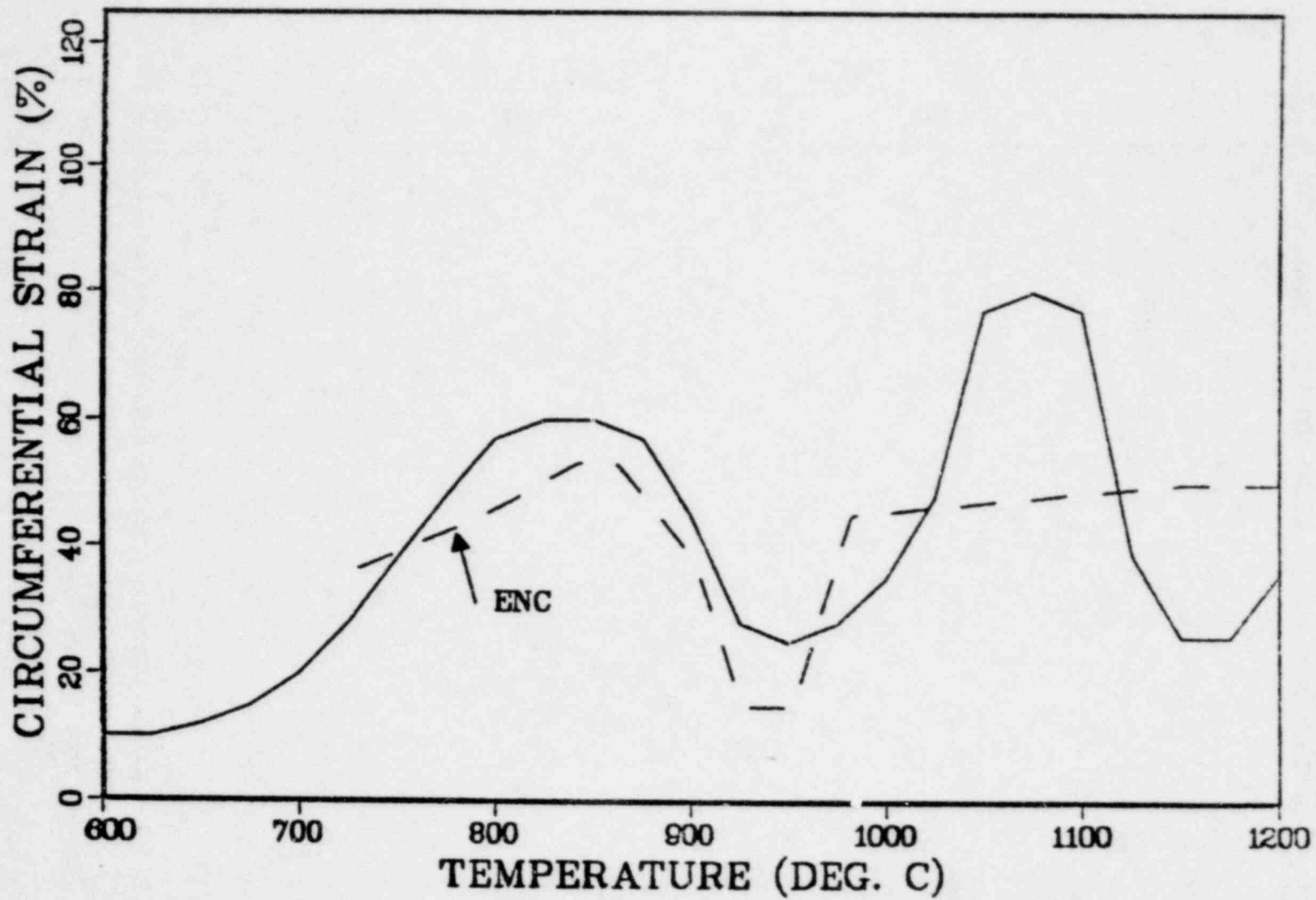


Fig. 49 ENC PWR model and fast-ramp correlation of circumferential burst strain as a function of rupture temperature.



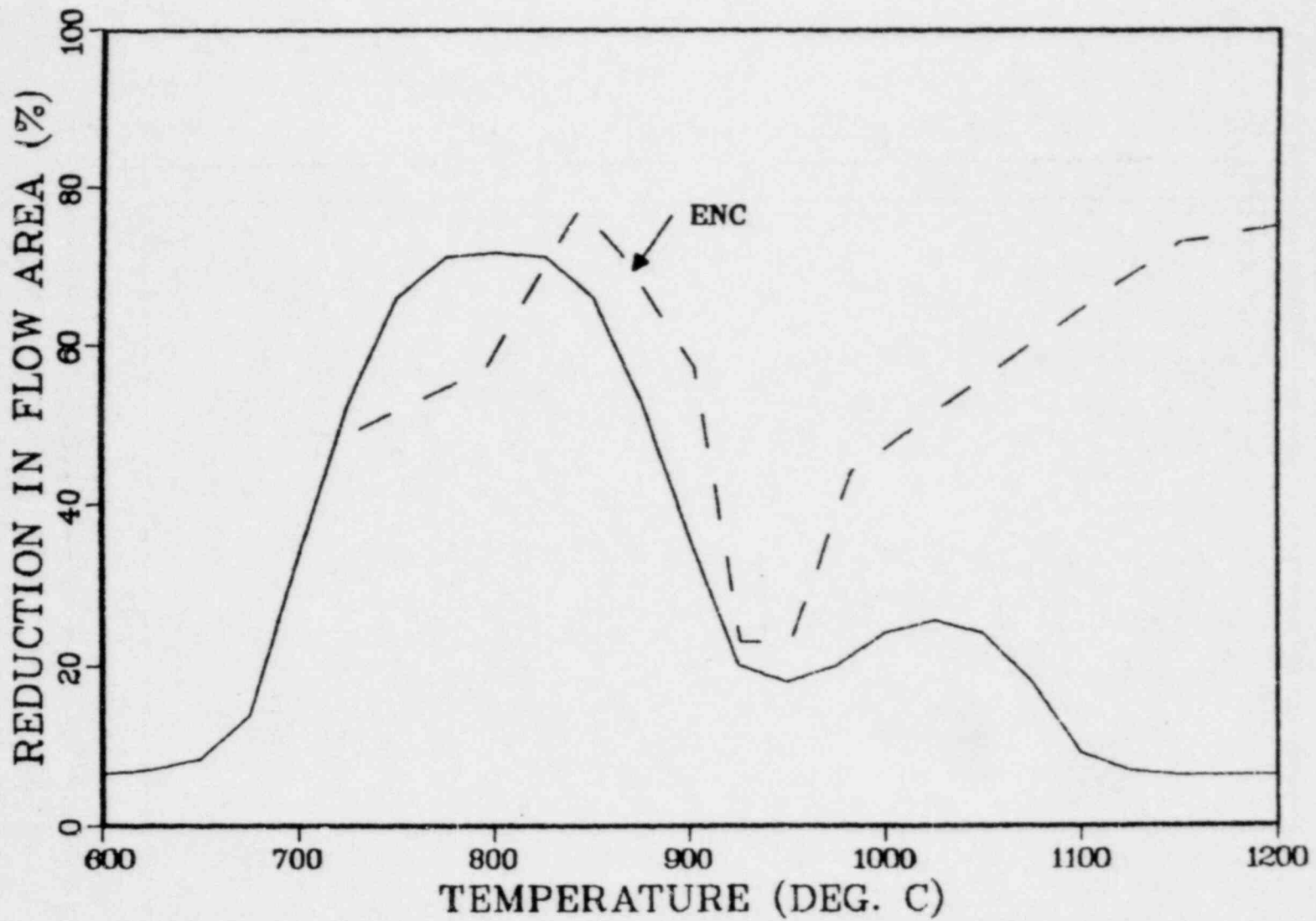


Fig. 50 ENC model and slow-ramp correlation of reduction in assembly flow area as a function of rupture temperature.

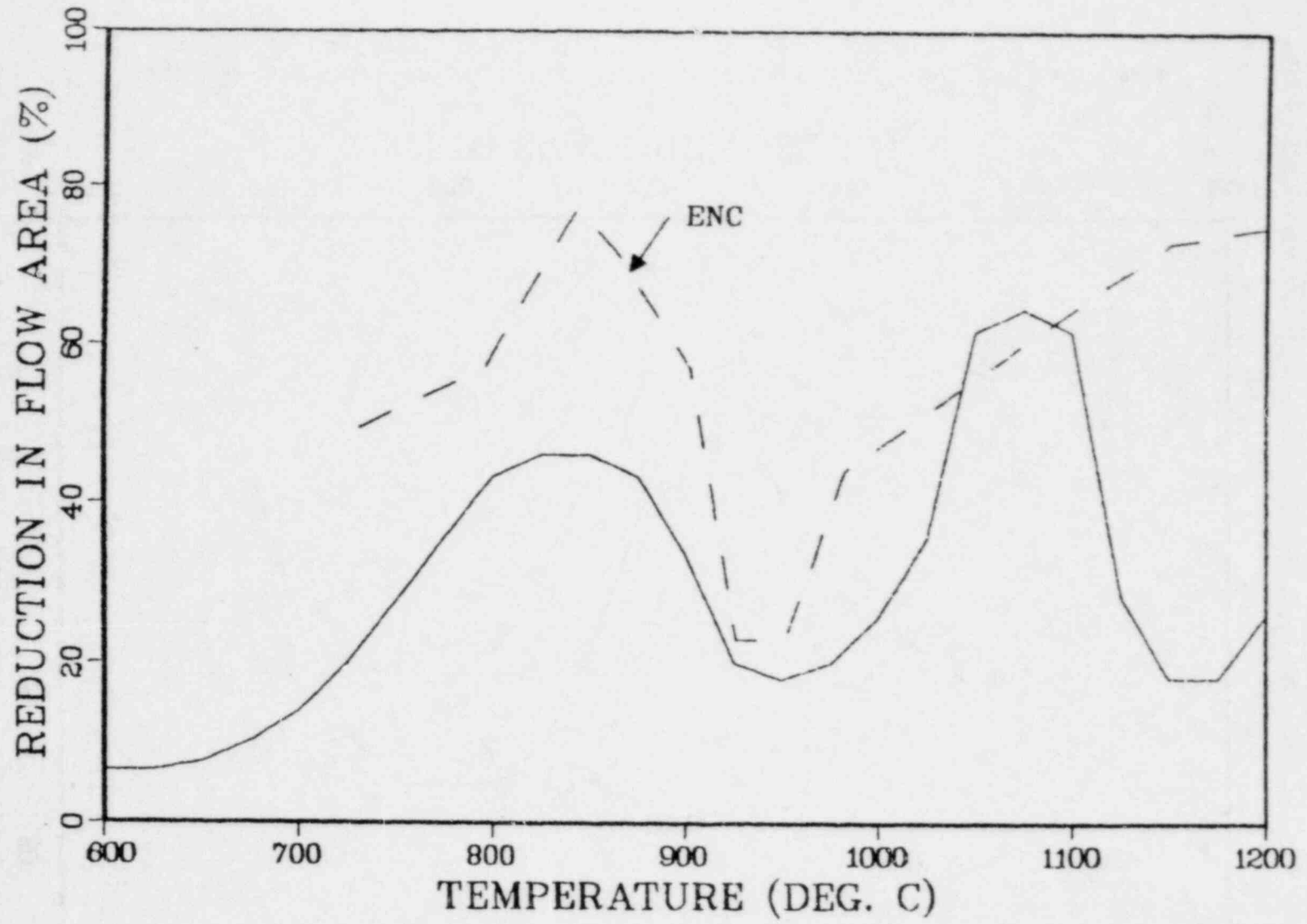


Fig. 51 ENC model and fast-ramp correlation of reduction in assembly flow area as a function of rupture temperature.

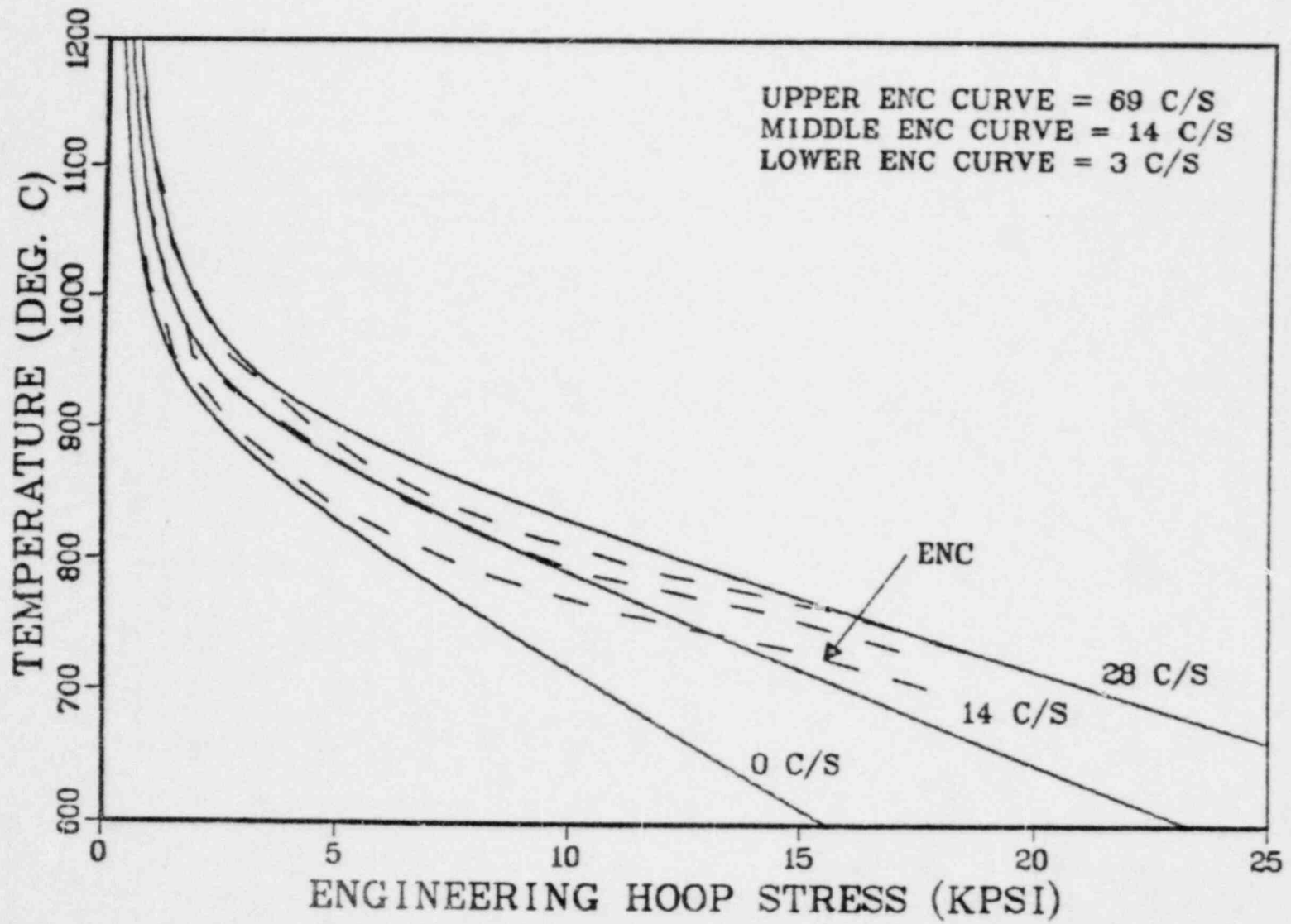


Fig. 52 ENC BWR model and ORNL correlation of rupture temperature as a function of engineering hoop stress and ramp rate.

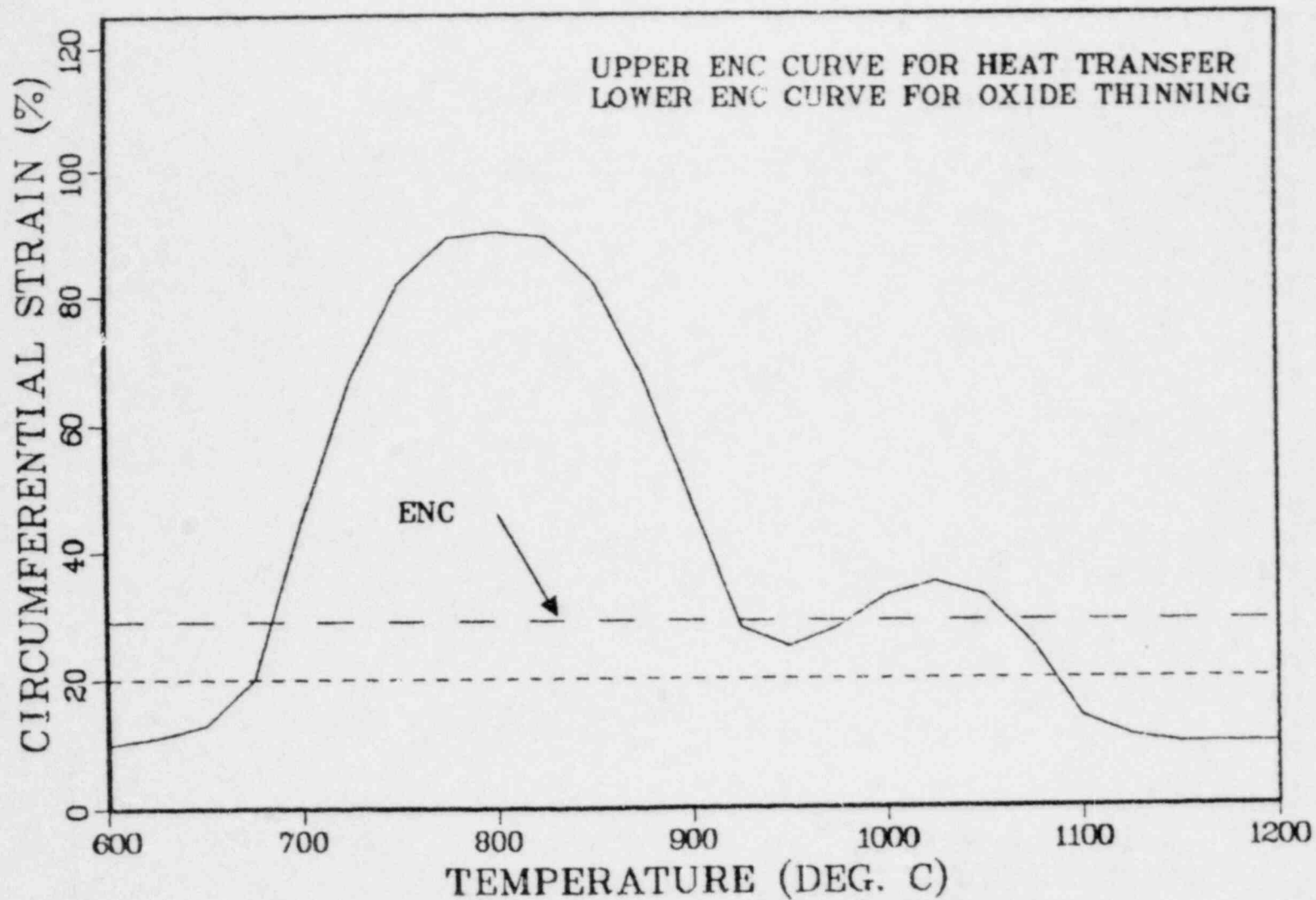


Fig. 53 ENC BWR model and slow-ramp correlation of circumferential burst strain as a function of rupture temperature.

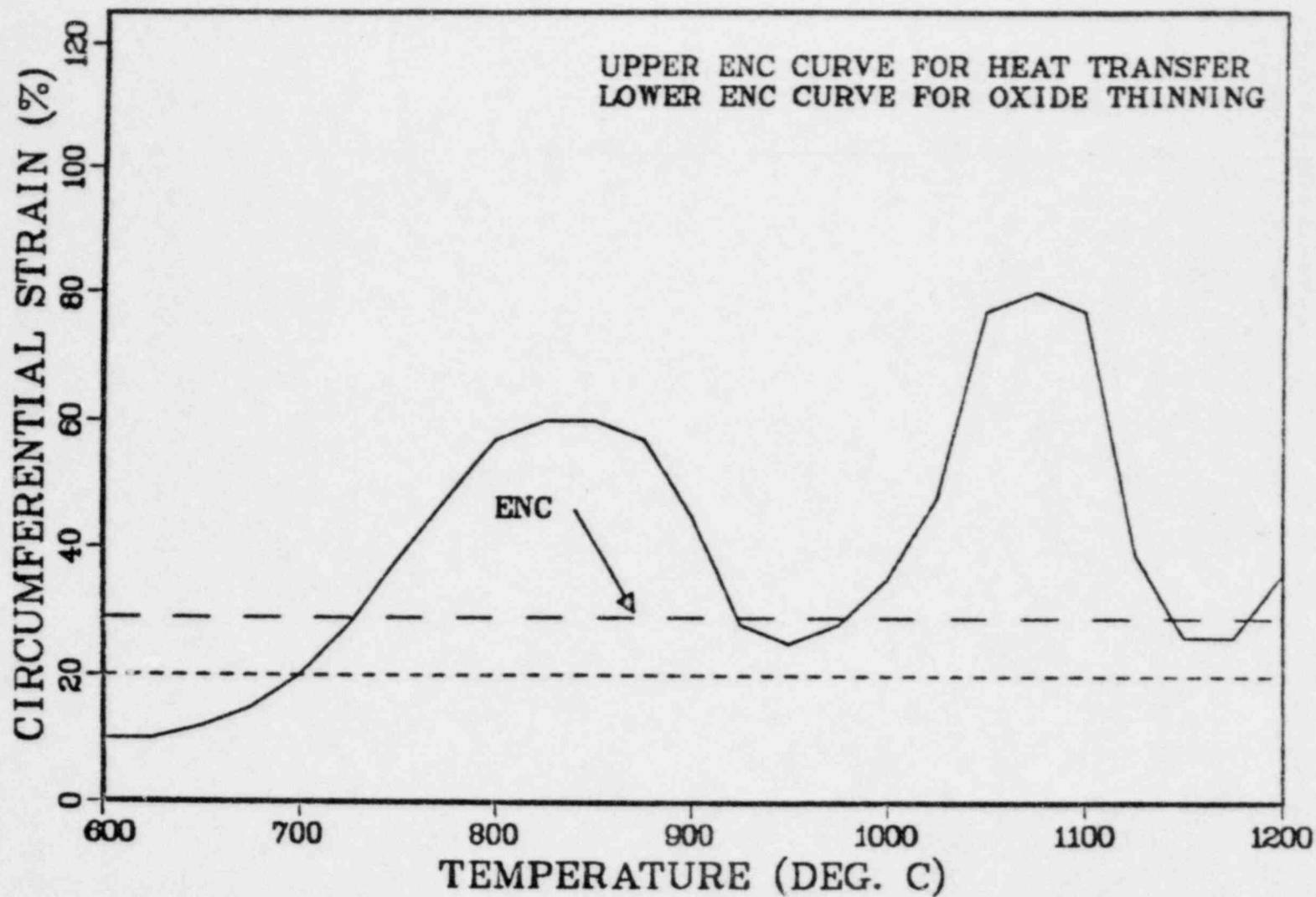


Fig. 54 ENC BWR model and fast-ramp correlation of circumferential burst strain as a function of rupture temperature.

Figures 55-59 show the models used for the Yankee Rowe Cycle 4 analysis. Figure 55 shows the rupture temperature model, which is like WREM and is in good agreement with the present fast-ramp correlation. Figures 56-57 show the burst strain model, which predicts far greater single rod deformation than any of the other licensing models. The flow blockage model exhibits smaller blockages than the present correlation over a large temperature range for slow ramps (Fig. 58) and over a narrow temperature range for fast ramps (Fig. 59).

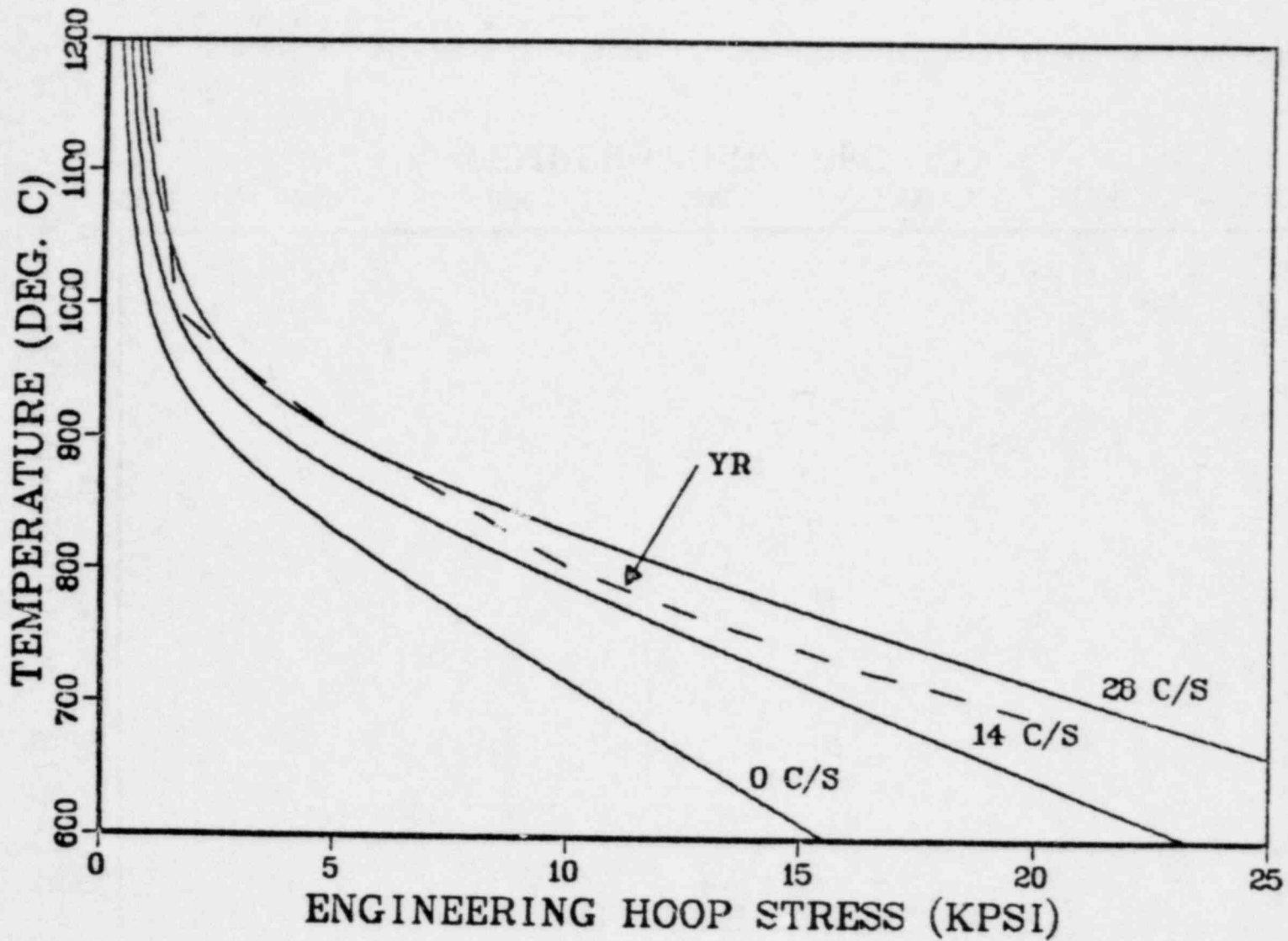


Fig. 55 YR model and ORNL correlation of rupture temperature as a function of engineering hoop stress and ramp rate.

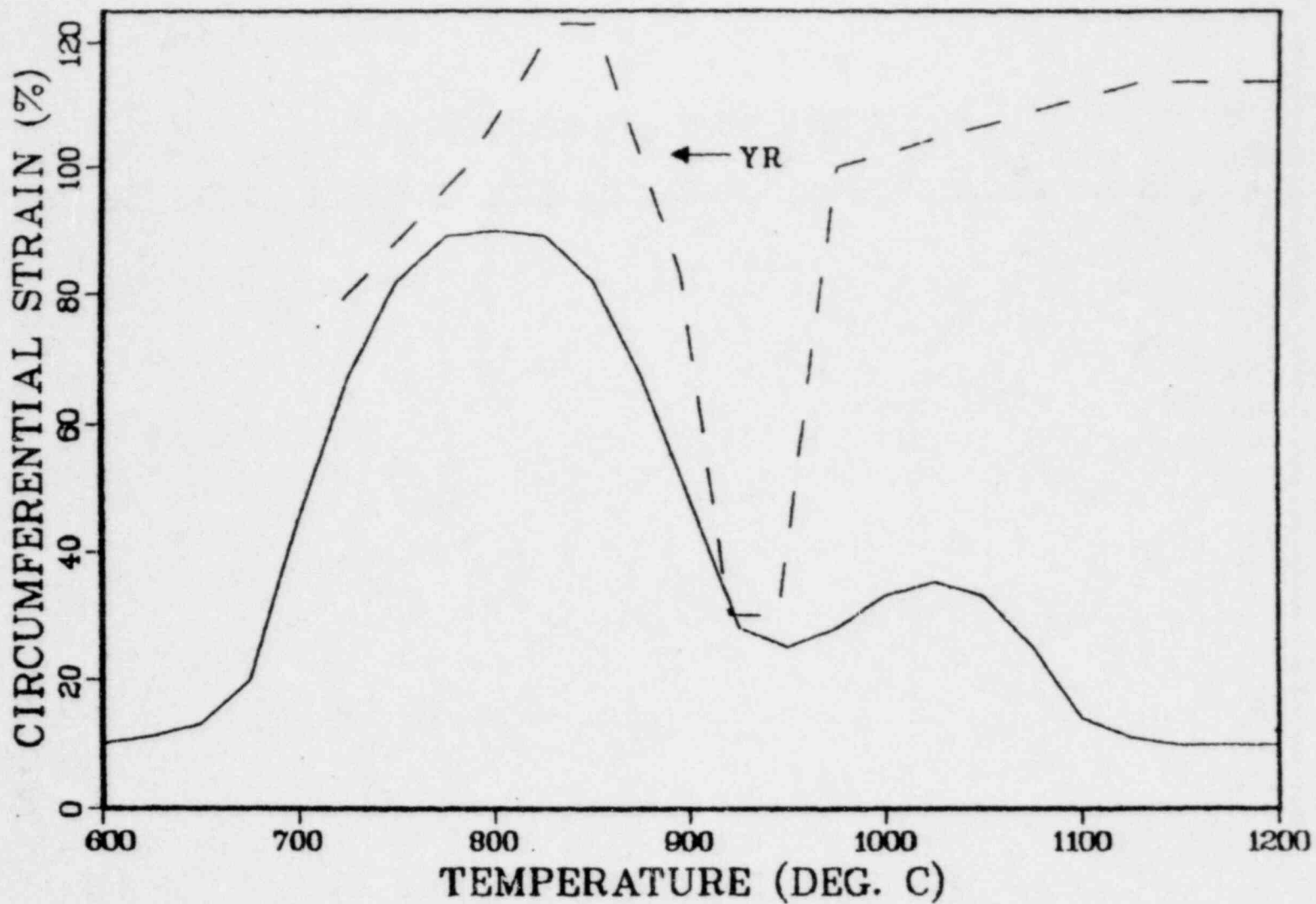


Fig. 56 YR model and slow-ramp correlation of circumferential burst strain as a function of rupture temperature.



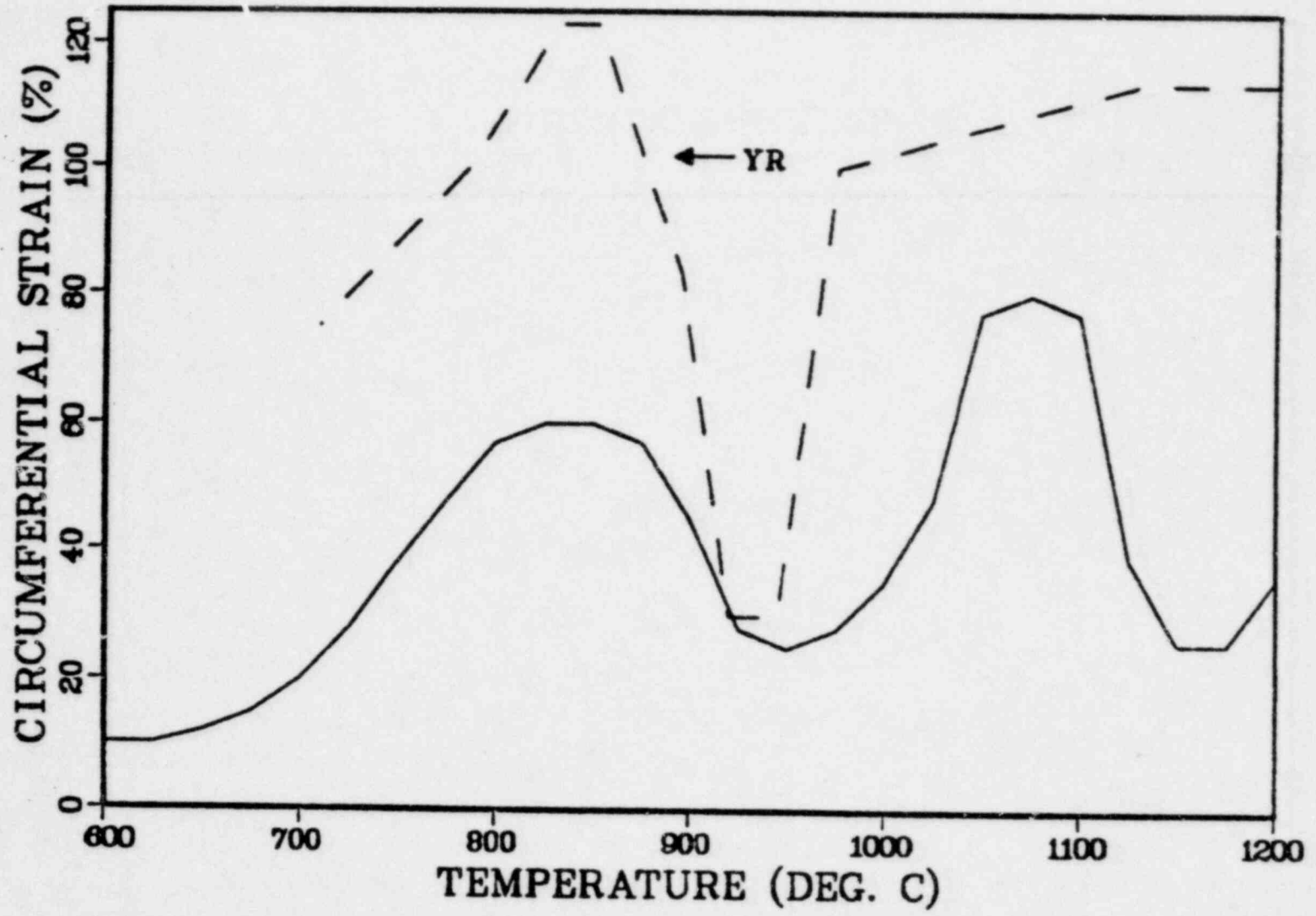


Fig. 57 YR model and fast-ramp correlation of circumferential burst strain as a function of rupture temperature.

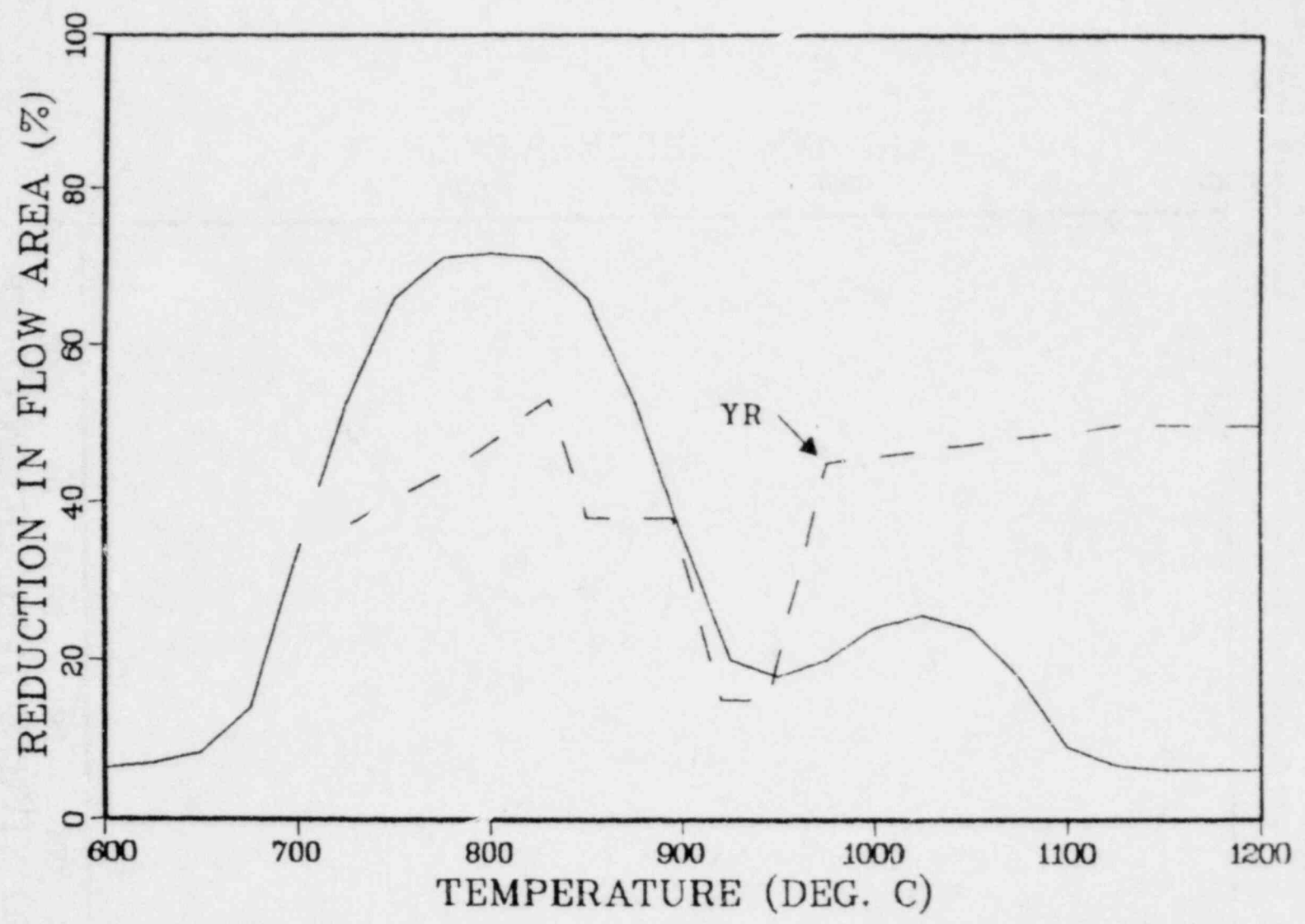


Fig. 58 YR model and slow-ramp correlation of reduction in assembly flow area as a function of rupture temperature.

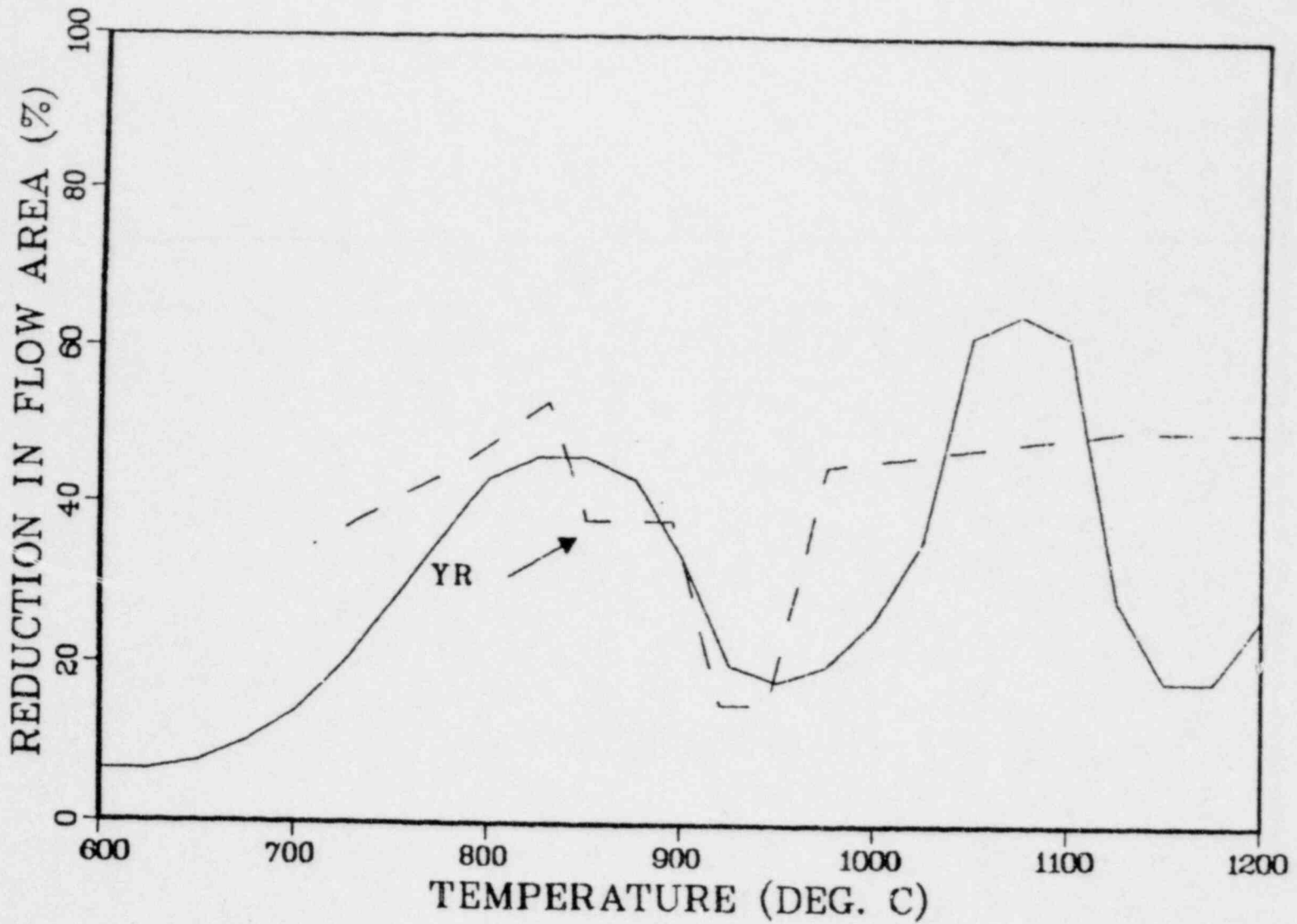


Fig. 59 YR model and fast-ramp correlation of reduction in assembly flow area as a function of rupture temperature.

## 5. CONCLUSIONS

Empirical fuel cladding models that describe the incidence of rupture, the degree of swelling, and the extent of coolant flow blockage have been the subject of extensive confirmatory research during the past five years. During that time, however, the cladding models that are used in the ECCS licensing analyses have not changed. Although the research programs are not finished, we are at a plateau of understanding that suggests that improvements should be made in these licensing models.

We have reviewed all of the available data to date and have selected the most prototypical data from which to derive new cladding correlations. This selection gave most weight to experiments performed in aqueous environments and utilizing internal heaters (either fuel pellets or electrically heated fuel pellet simulators). The data base is not complete, and we have had to make certain assumptions to bridge the gaps. In particular, the number of available bundle measurements of flow blockage is so small that assembly blockages have of necessity been derived from single rod burst strains on the basis of three carefully analyzed bundle tests.

Heating rate effects were found to be important, so all of the cladding correlations were derived as functions of temperature-ramp rate. Most present licensing models do not include ramp-rate effects.

The new cladding correlations differ substantially from the present licensing models. In fact, the present licensing models for each fuel vendor differ substantially from each other. Based on the applicable data, we believe that the new cladding correlations presented in this report and displayed in Figs. 3, 6, 7, and 16 provide the best means available today of predicting swelling and rupture without underestimating the degree of swelling or the incidence of rupture.

There is still uncertainty in these correlations, and further research is needed to confirm or further modify these correlations. Nevertheless, in the interim, we recommend that all industry ECCS models be revised to adopt the new cladding correlations presented in this report.

## 6. REFERENCES

1. U.S. Government Printing Office, "Acceptance Criteria for Emergency Core Cooling Systems for Light Water Nuclear Power Reactors," Part 50.46, Title 10 Energy, Code of Federal Regulations, January 1, 1979. Available from the Superintendent of Documents, U.S. Government Printing Office, Washington, D. C. 20402.
2. U.S. Government Printing Office, "ECCS Evaluation Models," Part 50, Appendix K, Title 10 Energy, Code of Federal Regulations, January 1, 1979. Available from the Superintendent of Documents, U.S. Government Printing Office, Washington, D. C. 20402.
3. Babcock & Wilcox Company, "CRAFT 2--FORTRAN Program for Digital Simulation of a Multinode Reactor Plant During Loss of Coolant," BAW-10092, Revision 2, April 1975.
4. Babcock & Wilcox Company, "B&W's ECCS Evaluation Model," BAW-10104A, Revision 1, March 1976.
5. Combustion Engineering Corporation, "High Temperature Properties of Zircaloy and  $UO_2$  for Use in LOCA Evaluation Models," CENPD-136, July 1974 (Proprietary).
6. Combustion Engineering Corporation, "Calculational Methods for the C-E Large Break LOCA Evaluation Model," CENPD-132P, August 1974 (Proprietary)
7. Combustion Engineering Corporation, "Calculational Methods for the C-E Large Break LOCA Evaluation Model," CENPD-132P, Supplement 1, February 1975 (Proprietary).
8. Combustion Engineering Corporation, "Calculational Methods for the C-E Large Break LOCA Evaluation Model," CENPD-132P, Supplement 2, July 1975 (Proprietary).
9. Westinghouse Electric Corporation, "Westinghouse Emergency Core Cooling System Small Break October 1975 Model," WCAP-8970-P-A, January 1979 (Proprietary).
10. Westinghouse Electric Corporation, "Westinghouse ECCS Evaluation Model October 1975 Version," WCAP-8622, December 1975 (Proprietary). Staff modifications per letter from D. B. Vassallo, U.S. Nuclear Regulatory Commission, to C. Eicheldinger, Westinghouse Electric Corporation, dated May 13, 1976.
11. Westinghouse Electric Corporation, "LOCTA-IV Program: Loss-of-Coolant Transient Analysis," WCAP-8301, June 1974 (Proprietary).
12. Westinghouse Electric Corporation, "SATAN VI PROGRAM: Comprehensive Space-Time Dependent Analysis of Loss-of-Coolant," WCAP-8302, June 1974 (Proprietary).

13. General Electric Company, "General Electric Company Analytical Model for Loss-of-Coolant Analysis in Accordance with 10 CFR 50 Appendix K," NEDO-20566, Volume 1, January 1976.
14. Exxon Nuclear Company, "Exxon Nuclear Company WREM-Based Generic PWR ECCS Evaluation Model," XN-75-41, Volume 1, July 25, 1975.
15. Exxon Nuclear Company, "BULGEX: A Computer Code to Determine the Deformation and the Onset of Bulging of Zircaloy Fuel Rod Cladding (Applicable for Loss of Coolant Accident Conditions)," XN-74-27(A), Revision 2, December 1974.
16. Exxon Nuclear Company, "Supplementary Information Related to Blowdown Analysis and Back Pressure During Reflood," XN-75-41, Supplement 2, August 14, 1975.
17. Exxon Nuclear Company, "HUXY: A Generalized Multirod Heatup Code with 10 CFR 50 Appendix K Heatup Option User's Manual," XN-CC-33(A), Revision 1, November 1975.
18. Yankee Atomic Electric Company, "Appendix C: Yankee Rowe Example Problem, Exxon Nuclear Company WREMBased Generic PWR ECCS Evaluation Model," Exxon Nuclear Company Report XN-75-41, Vol. II, Appendix C, Docket 50-029, June 1976.
19. U.S. Atomic Energy Commission, "In the Matter of Rulemaking Hearing: Acceptance Criteria for Emergency Core Cooling Systems for Light-Water-Cooled-Nuclear Power Reactors," Docket No. RM-50-1, December 28, 1973. Available in NRC PDR for inspection and copying for a fee.
20. D. A. Powers and R. O. Meyer, "Evaluation of Simulated-LOCA Tests that Produced Large Fuel Cladding Ballooning," USNRC Report NUREG-0536, March 1979. Available for purchase from the National Technical Information Service (NTIS), Springfield, Virginia 22161.
21. H. M. Chung and T. F. Kassner, Argonne National Laboratory, "Deformation Characteristics of Zircaloy Cladding In Vacuum and Steam Under Transient-Heating Conditions: Summary Report," USNRC Report NUREG/CR-0344, July 1978. Available in public technical libraries. Also available for purchase from the National Technical Information Service (NTIS), Springfield, Virginia 22161.
22. R. H. Chapman, Oak Ridge National Laboratory, "Multirod Burst Test Program Progress Report for January-March 1978," USNRC Report NUREG/CR-0225, August 1978. Available in public technical libraries. Also available for purchase from the National Technical Information Service (NTIS), Springfield, Virginia 22161.
23. R. H. Chapman, Oak Ridge National Laboratory, "Multirod Burst Test Program Progress Report for April-June 1977," USNRC Report ORNL/NUREG/TM-135, June 1977. Available in public technical libraries. Also available for purchase from the National Technical Information Service (NTIS), Springfield, Virginia 22161.

24. R. H. Chapman, Oak Ridge National Laboratory, "Multirod Burst Test Program Progress Report for April-June, 1979," USNRC Report NUREG/CR-1023, November, 1979. Available in public technical libraries. Also available for purchase from the National Technical Information Service (NTIS), Springfield, Virginia 22161.
25. R. A. Lorenz, D. O. Hobson, and G. W. Parker, Oak Ridge National Laboratory, "Final Report on the First Fuel Rod Failure Transient Test of a Zircaloy-Clad Fuel Rod Cluster in TREAT," Oak Ridge National Laboratory Report ORNL-4635, March 1971. Available in public technical libraries. Also available for purchase from the National Technical Information Service (NTIS), Springfield, Virginia 22161.
26. R. A. Lorenz, D. O. Hobson, and G. W. Parker, "Fuel Rod Failure Under Loss-of-Coolant Conditions in TREAT," Nuclear Technology, II, 502-520 (August 1971). Available in public technical libraries.
27. R. H. Chapman, J. L. Crowley, A. W. Longest, and E. G. Sewell, Oak Ridge National Laboratory, "Effects of Creep Time and Heating Rate on Deformation of Zircaloy-4 Tubes Tested in Steam with Internal Heaters," USNRC Report NUREG/CR-0343, October 1978. Available in public technical libraries. Also available for purchase from the National Technical Information Service (NTIS), Springfield, Virginia 22161.
28. A. M. Garde, H. M. Chung, and T. F. Kassner, Argonne National Laboratories, "Uniaxial Tensile Properties of Zircaloy Containing Oxygen: Summary Report," ANL Report ANL-77-30, June 1977. Available in public technical libraries. Also available for purchase from the National Technical Information Service (NTIS), Springfield, Virginia 22161.
29. D. Lee and W. A. Backofen, "Superplasticity in Some Titanium and Zirconium Alloys," Transactions of the Metallurgical Society of AIME, 239, 1034-1040 (July 1967). Available in public technical libraries.
30. Letter from R. H. Chapman, Oak Ridge National Laboratory, to K. Kniel, U.S. Nuclear Regulatory Commission, dated January 14, 1980. Available in NRC PDR for inspection and copying for a fee.
31. Letter from F. J. Erbacher, Kernforschungszentrum Karlsruhe, to R. H. Chapman, Oak Ridge National Laboratory, dated October 16, 1979. Available in NRC PDR for inspection and copying for a fee.
32. Letter from F. J. Erbacher, Kernforschungszentrum Karlsruhe, to D. A. Powers, U.S. Nuclear Regulatory Commission, dated February 13, 1980. Available in NRC PDR for inspection and copying for a fee.



33. Letter from R. H. Chapman, Oak Ridge National Laboratory, to D. A. Powers, U.S. Nuclear Regulatory Commission, dated February 21, 1980. Available in NRC PDR for inspection and copying for a fee.
34. R. H. Chapman, Oak Ridge National Laboratory, "Multirod Burst Test Program Progress Report for July-December 1977," USNRC Report NUREG/CR-0103, June 1978. Available in public technical libraries. Also available for purchase from the National Technical Information Service (NTIS), Springfield, Virginia 22161.
35. R. H. Chapman, Oak Ridge National Laboratory, "Preliminary Multirod Burst Test Program Results and Implications of Interest to Reactor Safety Evaluation," paper presented at the 6th NRC Water Reactor Safety Research Information Meeting, Gaithersburg, Md., November 7, 1978. Available in NRC PDR for inspection and copying for a fee.
36. Letter from Thomas F. Kassner and Hee M. Chung, Argonne National Laboratory, to Karl Kniel, U.S. Nuclear Regulatory Commission, Subject: Review of CPB Report on ECCS Cladding Models, dated January 3, 1980. Available in NRC PDR for inspection and copying for a fee.
37. R. A. Lorenz, D. O. Hobson, and G. W. Parker, Oak Ridge National Laboratory, "Final Report on the Second Fuel Rod Failure Transient Test of a Zircaloy-Clad Fuel Rod Cluster in TREAT," Oak Ridge National Laboratory Report ORNL-4710, January 1972. Available in public technical libraries. Also available for purchase from the National Technical Information Service (NTIS), Springfield, Virginia 22161.
38. U.S. Nuclear Regulatory Commission, "WREM: Water Reactor Evaluation Model," USNRC Report NUREG-75/056, Revision 1, May 1975. Available from National Technical Information Service (NTIS), Springfield, Virginia 22161.
39. Letter from D. F. Ross, U.S. Nuclear Regulatory Commission, to A. E. Scherer, Combustion Engineering Corporation, dated March 22, 1978. Available in NRC PDR for inspection and copying for a fee.
40. Letter from A. E. Scherer, Combustion Engineering Corporation, (LD-78-069) to D. F. Ross, U.S. Nuclear Regulatory Commission, Subject: C-E ECCS Evaluation Model Flow Blockage Analysis, dated September 18, 1978 (Proprietary).

APPENDIX A

FUEL CLADDING BURST DATA

DATA REFERENCE A (Upright Triangle)

FRF-1

R. A. Lorenz, D. O. Hobson, and G. W. Parker, Oak Ridge National Laboratory, "Final Report on the First Fuel Rod Failure Transient Test of a Zircaloy-Clad Fuel Rod Cluster in TRFAT," Oak Ridge National Laboratory Report ORNL-4635, March 1971. Available in public technical libraries. Also available for purchase from the National Technical Information Service (NTIS), Springfield, Virginia 22161.

R. A. Lorenz, D. O. Hobson, and G. W. Parker, "Fuel Rod Failure Under Loss-of-Coolant Conditions in TREAT," Nuclear Technology, II, 502-520 (August 1971). Available in public technical libraries.

Inpile, 7-rod bundle, steam atmosphere.

Maximum reduction in bundle flow area = 48%.

Mean rod burst strain = 36%.

Mean rod rupture temperature = 889°C.

Mean rod engineering burst stress = 1.71 kpsi.

<u>ROD #</u>	<u>RAMP RATE (°C/S)</u>	<u>PRESSURE AT RUPTURE (PSIG)</u>	<u>RUPTURE TEMPERATURE (°C)</u>	<u>BURST STRAIN (%)</u>	<u>ENGINEERING BURST STRESS (KPSI)</u>
H	25-36	172	966	26	1.39
4-1	25-36	250	799	35	2.02
R	25-36	205	743	36	1.66
4-2	25-36	290	816	42	2.34
L	25-36	162	915	36	1.31
I	25-36	190	827	35	1.54
C	25-36	215	810	40	1.74

DATA REFERENCE A (Upright Triangle)

FRF-2

R. A. Lorenz, D. O. Hobson, and G. W. Parker, Oak Ridge National Laboratory, "Final Report on the Second Fuel Rod Failure Transient Test of a Zircaloy-Clad Fuel Rod Cluster in TREAT," Oak Ridge National Laboratory Report ORNL-4710, January 1972. Available in public technical libraries. Also available for purchase from the National Technical Information Service (NTIS), Springfield, Virginia 22161.

R. A. Lorenz, D. O. Hobson, and G. W. Parker, "Fuel Rod Failure Under Loss-of-Coolant Conditions in TREAT," Nuclear Technology, II, 502-520 (August 1971). Available in public technical libraries.

Inpile, 7-rod bundle, steam atmosphere.

Maximum reduction in bundle flow area = 91%.

Mean rod burst strain = 57%.

Mean rod rupture temperature = 1254°C.

Mean rod engineering burst stress = 0.69 kpsi.

<u>ROD #</u>	<u>RAMP RATE (°C/S)</u>	<u>PRESSURE AT RUPTURE (PSIG)</u>	<u>RUPTURE TEMPERATURE (°C)</u>	<u>BURST STRAIN (%)</u>	<u>ENGINEERING BURST STRESS (KPSI)</u>
58-3	44	85	1260	50	0.69
11	44	85	1216	46	0.69
12	44	85	1260	64	0.69
13	44	85	1260	58	0.69
16	44	85	1260	70	0.69
17	44	85	1260	47	0.69
18	44	85	1260	61	0.69

DATA REFERENCE B (Cross)

R. H. Chapman, Oak Ridge National Laboratory, "Multirod Burst Test Program Progress Report for April-June 1977," USNRC Report ORNL/NUREG/TM-135, June 1977. Available in public technical libraries. Also available for purchase from the National Technical Information Service (NTIS), Springfield, Virginia 22161.

R. H. Chapman, J. L. Crowley, A. W. Longest, and E. G. Sewell, Oak Ridge National Laboratory, "Effects of Creep Time and Heating Rate on Deformation of Zircaloy-4 Tubes Test in Steam with Internal Heaters," USNRC Report NUREG/CR-0343, October 1978. Available in public technical libraries. Also available for purchase from the National Technical Information Service (NTIS), Springfield, Virginia 22161.

Out-of-pile, single rod, steam atmosphere.

<u>ROD #</u>	<u>RAMP RATE (°C/S)</u>	<u>PRESSURE AT RUPTURE (PSIG)</u>	<u>RUPTURE TEMPERATURE (°C)</u>	<u>BURST STRAIN (%)</u>	<u>ENGINEERING BURST STRESS (KPSI)</u>
PS-1	28	922	893	18	7.47
PS-3	28	809	873	29	6.56
PS-4	28	850	871	21	6.88
PS-5	28	830	882	26	6.72
PS-10	28	870	901	20	7.05
PS-12	28	891	898	18	7.21
PS-14	28	844	883	25	6.84
PS-15	28	893	885	17	7.24
PS-17	28	1760	778	25	14.2
SR-1	28	116	1166	26	0.94
SR-2	28	146	1082	44	1.19
SR-3	28	249	1011	43	2.02
SR-4	28	650	921	17	5.26
SR-5	28	1380	810	26	11.2
SR-7	28	2090	736	20	17.0
SR-8	28	178	1020	43	1.44
SR-13	28	155	1079	79	1.26
SR-15	28	2780	714	14	22.5
SR-17	28	154	1049	53	1.25
SR-19	28	2760	688	16	22.4
SR-20	28	154	1049	55	1.25
SR-21	28	162	1023	48	1.32
SR-22	28	129	1081	50	1.05
SR-23	28	139	1077	35	1.13
SR-24	28	144	1057	67	1.16
SR-25	28	139	1092	78	1.13
SR-26	28	120	1130	34	0.98
SR-27	28	133	1084	41	1.08
SR-28	28	1220	835	27	9.87
SR-29	28	1170	843	27	9.45
SR-37	28	1967	760	23	15.9
SR-38	28	1998	770	20	16.2

DATA REFERENCE C (Plus)

MRBT B-1

R. H. Chapman, Oak Ridge National Laboratory, "Multirod Burst Test Program Progress Report for July-December 1977," USNRC Report NUREG/CR-0103, June 1978. Available in public technical libraries. Also available for purchase from the National Technical Information Service (NTIS), Springfield, Virginia 22161.

R. H. Chapman, Oak Ridge National Laboratory, "Preliminary Multirod Burst Test Program Results and Implications of Interest to Reactor Safety Evaluation," paper presented at the 6th NRC Water Reactor Safety Research Information Meeting, Gaithersburg, Md., November 7, 1978. Available in NRC PDR for inspection and copying for a fee.

R. H. Chapman and others, "Bundle B-1 Test Data Multirod Burst Test Program," Interim Report ORNL/NUREG/TM-322, prepared for NRC by Oak Ridge National Laboratory, June 1979. Available in NRC PDR for inspection and copying for a fee.

Out-of-pile, 16-rod bundle, heated shroud, steam atmosphere.

Maximum reduction in bundle flow area = 49%.

Mean rod burst strain = 42%.

Mean rod strain in plane of maximum blockage = 27%.

Mean rod rupture temperature = 868°C.

Mean rod engineering burst stress = 8.72 kpsi.

<u>ROD #</u>	<u>RAMP RATE (°C/S)</u>	<u>PRESSURE AT RUPTURE (PSIG)</u>	<u>RUPTURE TEMPERATURE (°C)</u>	<u>BURST STRAIN (%)</u>	<u>ENGINEERING BURST STRESS (KPSI)</u>
1	29	1124	852	36	9.10
2	29	1075	867	32	8.71
3	29	----	---	--	----
4	29	1052	860	36	9.33
5	29	1005	872	45	8.14
6	29	1104	872	43	8.94
7	29	1052	869	36	8.52
8	29	1074	872	42	8.70
9	29	1030	870	47	8.34
10	29	1059	873	45	8.58
11	29	1054	847	53	8.54
12	29	1114	863	37	9.02
13	29	1091	878	59	8.84
14	29	1066	875	42	8.63
15	29	1062	865	42	8.60
16	29	1092	848	39	8.85

DATA REFERENCE C (Plus)

MRBT B-2

R. H. Chapman, Oak Ridge National Laboratory, "Multirod Burst Test Program Progress Report for July-December 1977," USNRC Report NUREG/CR-0103, June 1978. Available in public technical libraries. Also available for purchase from the National Technical Information Service (NTIS), Springfield, Virginia 22161.

R. H. Chapman, Oak Ridge National Laboratory, "Multirod Burst Test Program Report for July-December 1978," USNRC Report NUREG/CR-0655, June 1979 Available in public technical libraries. Also available for purchase from the National Technical Information Service (NTIS), Springfield, Virginia 22161.

R. H. Chapman and others, "Bundle B-2 Test Data Multirod Burst Test Program," Interim Report ORNL/NUREG/TM-337, prepared for NRC by Oak Ridge National Laboratory, August 1979. Available in NRC PDR for inspection and copying for a fee.

Out-of-pile, 16-rod bundle, steam atmosphere.

Maximum reduction in bundle flow area = 53%.  
 Mean rod burst strain = 42%.  
 Mean rod strain in plane of maximum blockage = 28%.  
 Mean rod rupture temperature = 858°C.  
 Mean rod engineering burst stress = 8.88 kpsi.

ROD #	RAMP RATE (°C/S)	PRESSURE AT RUPTURE (PSIG)	RUPTURE TEMPERATURE (°C)	BURST STRAIN (%)	ENGINEERING BURST STRESS (KPSI)
1	29	1117	870	35	9.05
2	29	1114	846	39	9.02
3	29	1096	853	40	8.88
4	29	1100	872	42	8.91
5	29	1127	866	35	9.13
6	29	1004	857	58	8.13
7	29	1067	861	56	8.64
8	29	1097	856	38	8.89
9	29	----	---	--	----
10	29	1065	856	43	8.63
11	29	1112	853	40	9.01
12	29	1094	851	40	8.86
13	29	1134	883	41	9.19
14	29	1048	858	42	8.49
15	29	1152	836	35	9.33
16	29	1117	848	42	9.05

DATA REFERENCE C (Plus)

MRBT B-3

R. H. Chapman, Oak Ridge National Laboratory, "Preliminary Multirod Burst Test Program Results and Implications of Interest to Reactor Safety Evaluation," paper presented at the 6th NRC Water Reactor Safety Research Information Meeting, Gaithersburg, Md., November 7, 1978. Available in NRC PDR for inspection and copying for a fee.

R. H. Chapman, Oak Ridge National Laboratory, "Multirod Burst Test Program Progress Report for April-June 1979," USNRC Report NUREG/CR-1023, November 1979. Available in public technical libraries. Also available for purchase from the National Technical Information Service (NTIS), Springfield, Virginia 22161.

R. H. Chapman and others, "Bundle B-3 Test Data Multirod Burst Test Program," Interim Report ORNL/NUREG/TM-360, prepared for NRC by Oak Ridge National Laboratory, January 1980. Available in NRC PDR for inspection and copying for a fee.

Out-of-pile, 16-rod bundle, heated shroud, steam atmosphere.

Maximum reduction in bundle flow area = 75%.

Mean rod burst strain = 57%.

Mean rod strain in plane of maximum blockage = 40%.

Mean rod rupture temperature = 764°C.

Mean rod engineering burst stress = 11.07 kpsi.

ROD #	RAMP RATE (°C/S)	PRESSURE AT RUPTURE (PSIG)	RUPTURE TEMPERATURE (°C)	BURST STRAIN (%)	ENGINEERING BURST STRESS (KPSI)
1	10	1393	771	48	11.28
2	10	1280	779	76	10.39
3	10	----	---	--	-----
4	10	1318	767	55	10.68
5	10	1375	764	63	11.14
6	10	1327	770	61	10.75
7	10	----	---	--	-----
8	10	1320	756	78	10.69
9	10	1320	754	59	10.69
10	10	1362	774	50	11.03
11	10	1396	775	57	11.31
12	10	1414	761	47	11.45
13	10	1486	760	49	12.04
14	10	1405	769	42	11.38
15	10	1335	753	53	10.81
16	10	1407	747	59	11.40

DATA REFERENCE D (Closed Circle)

F. Erbacher, H. J. Neitzel, and K. Wiehr, Kernforschungszentrum Karlsruhe, "Interaction Between Thermohydraulics and Fuel Clad Ballooning in a LOCA, Results of REBEKA Multirod Burst Tests with Flooding," paper presented at the 6th NRC Water Reactor Safety Research Information Meeting, Gaithersburg, Md, November 7, 1978. Available in file for USNRC Report NUREG-0536.

F. Erbacher, H. J. Neitzel, M. Reimann, and K. Wiehr, Kernforschungszentrum Karlsruhe, "Fuel Rod Behavior in the Refilling and Reflooding Phase of a LOCA-Burst Test with Indirectly Heated Fuel Rod Simulators," paper presented at the NRC Zircaloy Cladding Review Group Meeting, Idaho Falls, May 23, 1977. Available in file for USNRC Report NUREG-0536.

K. Wiehr and H. Schmidt, Kernforschungszentrum Karlsruhe, "Out-of-Pile Experiments on Ballooning of Zircaloy Fuel Rod Claddings Test Results with Shortened Fuel Rod Simulators," KfK Report 2345, October 1977. Available in file for USNRC Report NUREG-0536.

F. Erbacher, H. J. Neitzel, M. Reimann, and K. Wiehr, "Out-of-Pile Experiments on Ballooning in Zircaloy Fuel Rod Claddings in the Low Pressure Phase of a Loss-of-Coolant Accident," p. 56 in Specialists' Meeting on the Behavior of Water Reactor Fuel Elements Under Accident Conditions, CSNI Conference Proceeding, Spatind, Norway, September 13-16, 1976, published in 1976. Available in public technical libraries.

F. Erbacher, H. J. Neitzel, and K. Wiehr, "Studies on Zircaloy Fuel Clad Ballooning in a Loss-of-Coolant Accident -- Results of Burst Tests with Indirectly Heated Fuel Rod Simulators," p. 429 in Proceedings of the Fourth International Conference: Zirconium in the Nuclear Industry, ASTM Committee B-10, Stratford-upon-Avon, England, June 27-29, 1978, published in 1979. Available in public technical libraries.

Out-of-pile, single rod, air and steam atmosphere.

ROD #	RAMP RATE (°C/S)	PRESSURE AT RUPTURE (PSIG)	RUPTURE TEMPERATURE (°C)	BURST STRAIN (%)	ENGINEERING BURST STRESS (KPSI)
?	11	?	880	27	?
?	11	856	880	51	5.91
?	11	?	865	33	?
?	11	?	860	44	?
?	11	?	840	32	?
?	11	?	840	36	?
?	11	?	840	43	?
?	11	?	840	54	?
?	11	?	830	47	?
?	11	?	825	27	?
?	11	?	825	33	?
18	11	1420	823	33	9.81



DATA REFERENCE D (Continued)

<u>ROD #</u>	<u>RAMP RATE (°C/S)</u>	<u>PRESSURE AT RUPTURE (PSIG)</u>	<u>RUPTURE TEMPERATURE (°C)</u>	<u>BURST STRAIN (%)</u>	<u>ENGINEERING BURST STRESS (KPSI)</u>
?	11	?	820	28	?
?	14	?	820	38	?
14	11	1420	810	38	9.81
?	11	?	810	42	?
?	11	?	810	44	?
35	11	1380	794	27	9.54
?	11	?	780	27	?
?	11	?	780	30	?
?	11	?	780	52	?
?	11	?	770	26	?
?	11	?	770	32	?
?	11	?	760	24	?
?	11	?	755	23	?
?	11	?	755	52	?

DATA REFERENCE E (Open Circle)

E. Karb, Kernforschungszentrum Karlsruhe, "In-Pile Experiments in the FR-2 DK-LOOP on Fuel Rod Behavior During a LOCA," paper presented at the US/FRG Workshop on Fuel Rod Behavior, Karlsruhe, June 1978. Available in file for USNRC Report NUREG-0536.

E. H. Karb, Kernforschungszentrum Karlsruhe, "Results of the FR-2 Nuclear Tests on the Behavior of Zircaloy Clad Fuel Rods," paper presented at the 6th NRC Water Reactor Safety Research Information Meeting, Gaithersburg, Md, November 7, 1978. Available in file for USNRC Report NUREG-0536.

E. H. Karb, Kernforschungszentrum Karlsruhe, "Results of FR-2 In-Pile Tests on LWR Fuel Rod Behavior," paper presented at the 4th JAERI-FRG-NRC Annual Fuel Behavior Information Exchange, Idaho Falls, Idaho, June 22-29, 1979. Available in NRC PDR for inspection and copying for a fee.

Inpile, single rod, steam atmosphere.

ROD #	RAMP RATE (°C/S)	PRESSURE AT RUPTURE (PSIG)	RUPTURE TEMPERATURE (°C)	BURST STRAIN (%)	ENGINEERING BURST STRESS (KPSI)
A1.1	7.1	725	810	64	5.01
A2.1	20	1276	820	36	8.82
B1.6	8.2	1160	825	38	8.02
B3.1	10	1146	825	37	7.92
B1.3	12.7	885	845	34	6.12
A2.2	12.1	841	860	56	5.81
B1.1	17.5	754	900	30	5.21
B1.5	9	653	910	60	4.51
B1.2	8.7	653	915	25	4.51
B3.2	12.1	725	915	50	5.01

DATA REFERENCE F (Open Square)

R. H. Chapman, J. L. Crowley, A. W. Longest, and E. G. Sewell, Oak Ridge National Laboratory, "Effects of Creep Time and Heating Rate on Deformation of Zircaloy-4 Tubes Tested in Steam with Internal Heaters," URNRC Report NUREG/CR-0343, October 1978. Available in public technical libraries. Also available for purchase from the National Technical Information Service (NTIS), Springfield, Virginia 22161.

Out-of-pile, single rod, steam atmosphere.

<u>ROD</u> <u>#</u>	<u>RAMP</u> <u>RATE</u> <u>(°C/S)</u>	<u>PRESSURE</u> <u>AT RUPTURE</u> <u>(PSIG)</u>	<u>RUPTURE</u> <u>TEMPERATURE</u> <u>(°C)</u>	<u>BURST</u> <u>STRAIN</u> <u>(%)</u>	<u>ENGINEERING</u> <u>BURST STRESS</u> <u>(KPSI)</u>
SR-33	0	825	762	23	6.68
SR-34	0	844	766	32	6.84
SR-35	0	648	775	29	5.25
SR-36	0	660	821	29	5.35
SR-43	4	1105	773	29	8.95
SR-44	5	1060	777	30	8.59
SR-41	9	1416	757	27	11.5
SR-42	10	1373	761	28	11.1

DATA REFERENCE G (Asterisk)

REBEKA-1, 2, 3

F. Erbacher, H. J. Neitzel, and K. Wiehr, Kernforschungszentrum Karlsruhe, "Interaction Between Thermohydraulic and Fuel Clad Ballooning in a LOCA, Results of REBEKA Multirod Burst Tests with Flooding," paper presented at the 6th NRC Water Reactor Safety Research Information Meeting, Gaithersburg, Md., November 7, 1978. Available in file for USNRC Report NUREG-0536.

K. Wiehr, Kernforschungszentrum Karlsruhe, "Results of REBEKA Test 3," paper presented at the 4th JAERI-FRG-NRC Annual Fuel Behavior Information Exchange, Idaho Falls, Idaho, June 22-29, 1979. Available in NRC PDR for inspection and copying for a fee.

Out-of-pile, 9-rod bundles, steam and water atmosphere.

TEST #	INITIAL RAMP RATE (°C/S)	MEAN PRESSURE AT RUPTURE (PSIG)	MEAN RUPTURE TEMPERATURE (°C)	MEAN BURST STRAIN (%)	MEAN ENGINEERING BURST STRESS (KPSI)	REDUCTION IN FLOW AREA (%)
1	7	870	815	29	6.01	25
2	7	800	870	53	5.53	50
3	7	725	830	44	5.05	52

DATA REFERENCE H (Inverted Triangle)

M. Bocek, Kernforschungszentrum Karlsruhe, "FABIOLA," paper presented at the 4th JAERI-FRG-NRC Annual Fuel Behavior Information Exchange, Idaho Falls, Idaho, June 22-29, 1979. Available in NRC PDR for inspection and copying for a fee.

Out-of-pile, single rod, heated shroud, steam atmosphere.

<u>ROD</u> <u>#</u>	<u>RAMP</u> <u>RATE</u> <u>(°C/S)</u>	<u>PRESSURE</u> <u>AT RUPTURE</u> <u>(PSIG)</u>	<u>RUPTURE</u> <u>TEMPERATURE</u> <u>(°C)</u>	<u>BURST</u> <u>STRAIN</u> <u>(%)</u>	<u>ENGINEERING</u> <u>BURST STRESS</u> <u>(KPSI)</u>
1	3	563	860	66	3.92
4	11	1375	790	8	9.58
8	7.8	1375	780	35	9.58
10	10	2013	750	33	14.03
12	9	563	890	29	3.92
13	10	1810	765	10	12.62

DATA REFERENCE I (Diamond)

R. H. Chapman, Oak Ridge National Laboratory, "Multirod Burst Test Program Progress Report for July-December 1979," to be published about July 1980.

Letter from R. H. Chapman, Oak Ridge National Laboratory, to D. A. Powers, U.S. Nuclear Regulatory Commission, dated February 21, 1980. Available in NRC PDR for inspection and copying for a fee.

Out-of-pile, single rod, heated shroud, steam atmosphere.

<u>ROD #</u>	<u>RAMP RATE (°C/S)</u>	<u>PRESSURE AT RUPTURE (PSIG)</u>	<u>RUPTURE TEMPERATURE (°C)</u>	<u>MAXIMUM ROD STRAIN (%)</u>	<u>ENGINEERING BURST STRESS (KPSI)</u>
SR-47	10	1436	775	78	12.35
SR-49	5	1107	783	95	9.52
SR-51	0	1030	790	93	8.86
SR-53	0	846	762	83	7.28
SR-57	0	725	775	110	6.23
SR-50	10	666	897	56	5.73
SR-52	10	1437	761	49	12.36
SR-60	28	1036	879	24	8.91
SR-61	28	2073	762	31	17.83
SR-62	28	608	937	31	5.23
SR-63	0	822	760	99	7.07
SR-64	5	1231	766	110	10.59
SR-65	5	1307	748	74	11.24
SR-67	1	645	824	107	5.55
SR-69	1	579	854	116	4.98

DATA REFERENCE J (Closed Square)

Letter from F. J. Erbacher, Kernforschungszentrum Karlsruhe, to R. H. Chapman, Oak Ridge National Laboratory, dated October 16, 1979.  
Available in NRC PDR for inspection and copying for a fee.

Out-of-pile, single rod, heated shroud, steam atmosphere.

<u>ROD #</u>	<u>RAMP RATE (°C/S)</u>	<u>PRESSURE AT RUPTURE (PSIG)</u>	<u>ROD-TIP TEMPERATURE (°C)</u>	<u>BURST STRAIN (%)</u>	<u>ENGINEERING BURST STRESS (KPSI)</u>
100	10.4	1975	765	72.0	13.77
101	10.1	1920	755	72.6	13.38
102	10.5	1678	795	81.8	11.69
103	10.6	1393	825	92.5	9.71
104	10.4	1131	855	75.0	7.88
105	9.5	858	894	45.7	5.98
106	9.7	581	938	50.7	4.05
107	10.7	1122	864	86.0	7.82
108	10.1	1124	852	85.1	7.83
109	1.4	1976	723	76.2	13.78
110	1.9	1708	748	82.1	11.91
111	1.9	1428	779	81.2	9.95
112	1.7	1137	819	103.7	7.92
113	1.7	854	866	72.6	5.95
114	28.9	1971	794	36.8	13.73
115	29.3	1944	793	62.9	13.55
116	27.8	1721	802	43.6	12.00
117	29.2	1420	844	60.2	9.89
118	33.7	1106	916	36.8	7.71
119	35.0	1150	904	37.4	8.01
120	37.9	1427	883	50.4	9.94
121	8.9	1717	781	71.7	11.97
122	9.6	1434	810	57.2	10.00
123	9.0	1150	834	71.7	8.01
124	9.0	1148	837	66.1	8.00
125	8.9	876	885	72.6	6.10
126	9.9	2095	763	57.2	14.60
127	31.5	1991	827	45.1	13.88
128	25.2	1708	803	48.1	11.91
129	29.5	1711	817	57.2	11.93
130	31.5	1436	898	53.7	10.01
131	24.1	1147	870	51.9	7.99
132	25.4	1427	847	59.6	9.94
133	0.8	1438	737	75.0	10.03
134	1.6	1724	746	86.3	12.02
135	0.8	2001	701	79.1	13.95
136	0.9	1151	786	116.2	8.02
137	0.9	867	824	112.9	6.05
138	0.8	580	870	78.0	4.04

DATA REFERENCE K (Upright Triangle in Square)

L. M. Lowry, J. S. Perrin, A. J. Markworth, and W. J. Gallagher, Battelle Columbus Laboratories, "Evaluating Strength and Ductility of Irradiated Zircaloy, Task 5," USNRC Report NUREG/CR-0582, November 1978. Available for purchase from the National Technical Information Service, Springfield, Virginia 22161.

L. M. Lowry, J. S. Perrin, A. J. Markworth, and M. P. Landow, Battelle Columbus Laboratories, "Evaluating Strength and Ductility of Irradiated Zircaloy, Task 5," USNRC Report NUREG/CR-0982, November 1979. Available for purchase from the National Technical Information Service, Springfield, Virginia 22161.

Out-of-pile, single rod, steam atmosphere.

<u>ROD</u> <u>#</u>	<u>RAMP</u> <u>RATE</u> <u>(°C/S)</u>	<u>PRESSURE</u> <u>AT RUPTURE</u> <u>(PSIG)</u>	<u>RUPTURE</u> <u>TEMPERATURE</u> <u>(°C)</u>	<u>BURST</u> <u>STRAIN</u> <u>(%)</u>	<u>ENGINEERING</u> <u>BURST STRESS</u> <u>(KPSI)</u>
N8/9-29	28	140	1135	39	1.14
N8/30-50	28	125	1071	25	1.02
N8/71-91	28	198	1008	46	1.62
NS/112-132	34	254	978	43	2.08
N8/50-70	28	290	927	23	2.37
O14/42-62	28	360	948	16	2.94
G8/70-89	34	478	925	12	3.91
F8/70-90	15	696	863	21	5.69
A1/35-55	18	945	786	23	7.73
A8/42-62	28	925	849	33	7.56
M12/33-55	28	938	782	18	7.67
M12/70-90	28	954	804	13	7.80
F8/35-55	28	954	814	17	7.80
A1/79-99	34	958	788	16	7.83
K8/35-55	28	1265	825	16	10.35
K8/14-34	28	1488	741	22	12.17
K8/70-90	28	1550	792	30	12.68
N8/91-111	28	1815	734	17	14.84
K10/105-125	6	1162	746	34	9.51
K10/71-91	6	218	897	16	1.78
K10/35-55	15	139	999	16	1.14
K10/14-34	18	150	931	17	1.23
47103-4	28	143	1066	37.5	1.09
47118-12	28	180	967	35.6	1.37
47104-3	28	242	934	29.9	1.84
47010-17	28	341	924	37.8	2.59
47110-4	28	650	854	15.9	4.95
47110-7	28	991	831	31.4	7.54
47110-14	28	1100	799	58.9	8.37
47111-12	28	1268	745	36.7	9.65
47110-20	28	1463	762	25.3	11.13
47111-6	5.6	833	778	74.7	6.34
47101-16	28	1200	788	17.1	91.3



DATA REFERENCE K (Continued)

<u>ROD #</u>	<u>RAMP RATE (°C/S)</u>	<u>PRESSURE AT RUPTURE (PSIG)</u>	<u>RUPTURE TEMPERATURE (°C)</u>	<u>BURST STRAIN (%)</u>	<u>ENGINEERING BURST STRESS (KPSI)</u>
47101-11	28	1237	783	18.3	9.42
47101-6	28	649	803	10.8	4.94
47101-3	28	500	892	9.9	3.80
Archive 1	28	704	936	18.2	5.36
Archive 2	28	1250	830	22.9	9.51
32211A-13	28	180	1043	12.3	1.37
32211A-20	28	248	877	19.1	1.89
31778A-13	28	419	860	17.8	3.19
31917A-16	28	674	850	11.9	5.13
31965A-12	28	918	827	31.0	6.98
31983A-15	28	1069	857	19.1	8.13
31785A-5	28	1273	782	20.2	9.69
31785A-9	28	1573	777	12.7	11.97

DATA REFERENCE L (Cross in Circle)

Bundles-7805, 7806, 7807, and 7808

S. Kawasaki, "Multirod Burst Tests at JAERI," paper presented at the 4th JAERI-FRG-NRC Annual Fuel Behavior Information Exchange, Idaho Falls, Idaho, June 22-29, 1979. Available in NRC PDR for inspection and copying for a fee.

Letter from S. Kawasaki, Japan Atomic Energy Research Institute, to R. O. Meyer, U.S. Nuclear Regulatory Commission, dated December 24, 1979. Available in NRC PDR for inspection and copying for a fee.

Out-of-pile, 49-rod bundles, heated shroud, steam atmosphere.

TEST #	INITIAL RAMP RATE (°C/S)	MEAN PRESSURE AT RUPTURE (PSIG)	MEAN RUPTURE TEMPERATURE (°C)	MEAN BURST STRAIN (%)	MEAN ENGINEERING BURST STRESS (KPSI)	REDUCTION IN FLOW AREA (%)
7805	6.1-7.7	818	825	?	6.56	85.3
7806	6.0-7.3	359	885	?	2.88	35.6
7807	5.9-7.2	1111	765	?	8.91	77.8
7808	7	578	855	?	4.64	46.9

## APPENDIX B

TABULATION OF CLADDING CORRELATIONS

## Slow-Ramp Correlations

Rupture Temperature (°C)	<10°C/s Burst Strain (%)	<10°C/s Flow Blockage (%)
600	10	6.5
625	11	7.0
650	13	8.4
675	20	13.8
700	45	33.5
725	67	52.5
750	82	65.8
775	89	71.0
800	90	71.5
825	89	71.0
850	82	65.8
875	67	52.5
900	48	35.7
925	28	20.0
950	25	18.0
975	28	20.0
1000	33	24.1
1025	35	25.7
1050	33	24.1
1075	25	18.0
1100	14	9.2
1125	11	7.0
1150	10	6.5
1175	10	6.5
1200	10	6.5

### Fast-Ramp Correlations

Rupture Temperature (°C)	>25°C/s Burst Strain (%)	>25°C/s Flow Blockage (%)
600	10	6.5
625	10	6.5
650	12	7.5
675	15	10.0
700	20	13.8
725	28	20.0
750	38	27.5
775	48	35.7
800	57	43.3
825	60	46.0
850	60	46.0
875	57	43.3
900	45	33.5
925	28	20.0
950	25	18.0
975	28	20.0
1000	35	25.7
1025	48	35.7
1050	77	61.6
1075	80	64.5
1100	77	61.6
1125	39	28.5
1150	26	18.3
1175	26	18.3
1200	36	26.2

APPENDIX C

FORMAL COMMENTS ON DRAFT NUREG-0630

Listed below are the formal comments that have been received on draft NUREG-0630, which was issued in November 1979 for a critique by the technical community. These comments have been placed in the NRC PDR (Memorandum from D. A. Powers, NRC, to Public Document Room, "Formal Comments on Draft NUREG-0630," accession number 8002280641, March 14, 1980. Available in NRC PDR for inspection and copying for a fee.)

1. Memorandum from D. A. Hoatson, NRC, to K. Kniel, "Review of NUREG-0630 In ECCS Cladding Models," December 5, 1979.
2. Letter from R. H. Buchholz, General Electric Company, to R. P. Denise, NRC, Subject: Comments on The Draft Report "Cladding Swelling and Rupture Models for LOCA Analysis," NUREG-0630 Dated November 8, 1979, dated December 7, 1979.
3. Letter from D. O. Hobson, Oak Ridge National Laboratory, to K. Kniel, NRC, dated December 10, 1979.
4. Telex from J. Hannaford, United Kingdom Nuclear Installations Inspectorate, to R. O. Meyer, NRC, Subject: Comments on NUREG-0630 "Cladding Swelling and Rupture Models for LOCA Analysis," dated December 10, 1979.
5. Letter from J. H. Taylor, Babcock & Wilcox Company, to R. P. Denise, NRC, dated December 10, 1979.
6. Letter from G. F. Owsley, Exxon Nuclear Company, to R. P. Denise, NRC, dated December 10, 1979.
7. Letter from D. E. Vandeburgh, Yankee Atomic Electric Company, to R. P. Denise, NRC, Subject: Technical Review of Draft NUREG-0630 dated December 10, 1979.
8. Letter from T. M. Anderson, Westinghouse Electric Corporation, to R. P. Denise, NRC, dated December 10, 1979.
9. Memorandum from R. O. Meyer, NRC, to R. P. Denise, "Evaluation of Westinghouse Comments on Draft NUREG-0630," January 5, 1980.
10. Letter from A. E. Scherer, Combustion Engineering Company, to R. P. Denise, NRC, Subject: Review of Draft Report NUREG-0630, "Cladding Swelling and Rupture Models for LOCA Analysis," dated December 11, 1979.

11. Letter from P. L. Rittenhouse, Oak Ridge National Laboratory, to D. A. Powers, NRC, Subject: NUREG-0630, dated December 20, 1979.
12. Letter from T. F. Kassner and H. M. Chung, Argonne National Laboratory, to K. Kniel, NRC, Subject: Review of CPB Report on ECCS Cladding Models, dated January 3, 1980.
13. Letter from W. B. Loewenstein, Electric Power Research Institute, to R. Budnitz, NRC, dated January 9, 1980.
14. Letter from R. O. Meyer, NRC, to W. B. Loewenstein, Electric Power Research Institute, dated February 5, 1980.
15. Letter from R. H. Chapman, Oak Ridge National Laboratory, to K. Kniel, NRC, dated January 14, 1980.
16. Letter from R. H. Chapman, Oak Ridge National Laboratory, to D. A. Powers, NRC, Subject: Additional Comments on NUREG-0630, dated February 21, 1980.
17. Letter from F. J. Erbacher, Kernforschungszentrum Karlsruhe, to D. A. Powers, NRC, dated February 13, 1980.
18. Telex from R. O. Meyer, NRC, to R. Van Houten, NRC, dated February 19, 1980.
19. Telex from R. Van Houten, NRC, to R. Meyer, NRC, dated February 21, 1980.
20. Telex from D. Powers, NRC, to A. Fiege, Kernforschungszentrum Karlsruhe, dated February 27, 1980.
21. Telex from A. Fiege, Kernforschungszentrum Karlsruhe, to D. Powers, NRC, dated March 4, 1980.
22. Letter from R. H. Chapman, Oak Ridge National Laboratory, to D. A. Powers, NRC, Subject: Revised Figure 1 for Additional Comments on NUREG-0630 dated 2-21-80, dated March 6, 1980.

NRC FORM 335 (7-77)		U.S. NUCLEAR REGULATORY COMMISSION <b>BIBLIOGRAPHIC DATA SHEET</b>		1. REPORT NUMBER (Assigned by DDC) NUREG-0630	
4. TITLE AND SUBTITLE (Add Volume No., if appropriate) CLADDING SWELLING AND RUPTURE MODELS FOR LOCA ANALYSIS				2. (Leave blank)	
7. AUTHOR(S) DALE A. POWERS AND RALPH O. MEYER				5. DATE REPORT COMPLETED MONTH: March   YEAR: 1980	
9. PERFORMING ORGANIZATION NAME AND MAILING ADDRESS (Include Zip Code) CORE PERFORMANCE BRANCH DIVISION OF SYSTEMS SAFETY OFFICE OF NUCLEAR REACTOR REGULATION U.S. NUCLEAR REGULATORY COMMISSION WASHINGTON, D. C. 20555				DATE REPORT ISSUED MONTH: April   YEAR: 1980	
12. SPONSORING ORGANIZATION NAME AND MAILING ADDRESS (Include Zip Code) CORE PERFORMANCE BRANCH DIVISION OF SYSTEMS SAFETY OFFICE OF NUCLEAR REACTOR REGULATION U.S. NUCLEAR REGULATORY COMMISSION WASHINGTON, D. C. 20555				6. (Leave blank)	
13. TYPE OF REPORT TECHNICAL REPORT				PERIOD COVERED (Inclusive dates) N/A	
15. SUPPLEMENTARY NOTES				10. PROJECT/TASK/WORK UNIT NO.	
16. ABSTRACT (200 words or less) <p>A DESCRIPTION IS GIVEN OF FUEL CLADDING BEHAVIOR AS IT IS MODELED FOR EMERGENCY-CORE-COOLING-SYSTEM (ECCS) EVALUATIONS IN THE SAFETY ANALYSIS OF LOSS-OF-COOLANT ACCIDENTS (LOCAS). DATA ARE TABULATED FROM EXPERIMENTS THAT EMPLOYED INTERNALLY HEATED ZIRCALOY CLADDING THAT WAS RUPTURED IN AQUEOUS ATMOSPHERES, AND NEW CORRELATIONS BASED ON THESE DATA ARE GIVEN FOR CLADDING RUPTURE TEMPERATURE, CLADDING BURST STRAIN, AND FUEL ASSEMBLY FLOW BLOCKAGE. COMPARISONS OF THESE CORRELATIONS WITH INDUSTRY MODELS THAT ARE USED IN CURRENT LICENSING ANALYSES FOR COMMERCIAL NUCLEAR POWER PLANTS REVEAL SUBSTANTIAL DIFFERENCES. THE CORRELATIONS IN THIS REPORT ARE INTENDED TO BE USED AS LICENSING STANDARDS FOR FUTURE LOCA ANALYSES UNTIL SUCH TIME THAT THE CONTINUING RESEARCH PROGRAM WOULD DEMONSTRATE A NEED FOR FURTHER REVISIONS.</p>				11. CONTRACT NO.	
17. KEY WORDS AND DOCUMENT ANALYSIS FUEL ROD LOCA FLOW BLOCKAGE ECCS ZIRCALOY				17. DESCRIPTORS METAL CYLINDER OF UO <sub>2</sub> PELLETS LOSS-OF-COOLANT ACCIDENT REDUCTION-IN-FLOW-AREA EMERGENCY-CORE-COOLING SYSTEM FUEL ROD CLADDING MATERIAL	
17b. IDENTIFIERS/OPEN-ENDED TERMS NONE				19. SECURITY CLASS (This report) UNCLASSIFIED	
18. AVAILABILITY STATEMENT UNLIMITED				21. NO. OF PAGES 132	
19. SECURITY CLASS (This page) UNCLASSIFIED				22. PRICE \$	

UNITED STATES  
NUCLEAR REGULATORY COMMISSION  
WASHINGTON, D. C. 20555

OFFICIAL BUSINESS  
PENALTY FOR PRIVATE USE, \$300

POSTAGE AND FEES PAID  
U.S. NUCLEAR REGULATORY  
COMMISSION

